

POLITECNICO DI TORINO

Corso di Laurea Magistrale in Ingegneria Energetica e Nucleare



TESI DI LAUREA MAGISTRALE

Experimental assessment of the performance of liquids solvent for carbon capture

Relatore:

Prof. Massimo Santarelli

Correlatore:

Salvatore Cannone

Candidato:

Giuseppe Picerno

Luglio 2021

Summary

The human influence on the climate system is evident, the atmospheric concentration of greenhouse gases (GHG), such as carbon dioxide, methane and nitrous oxide, from anthropogenic source is the largest ever. Recent climate change has caused impacts on both the human and natural systems, resulting in atmospheric and ocean's surface warming, reducing the amount of ice and rising sea levels ¹.

As shown in *Figure 1.1*, annual total CO₂ emissions have been increasing continuously since the pre-industrial era, due to economic development and population growth. By reaching unprecedented concentrations in recent decades ².

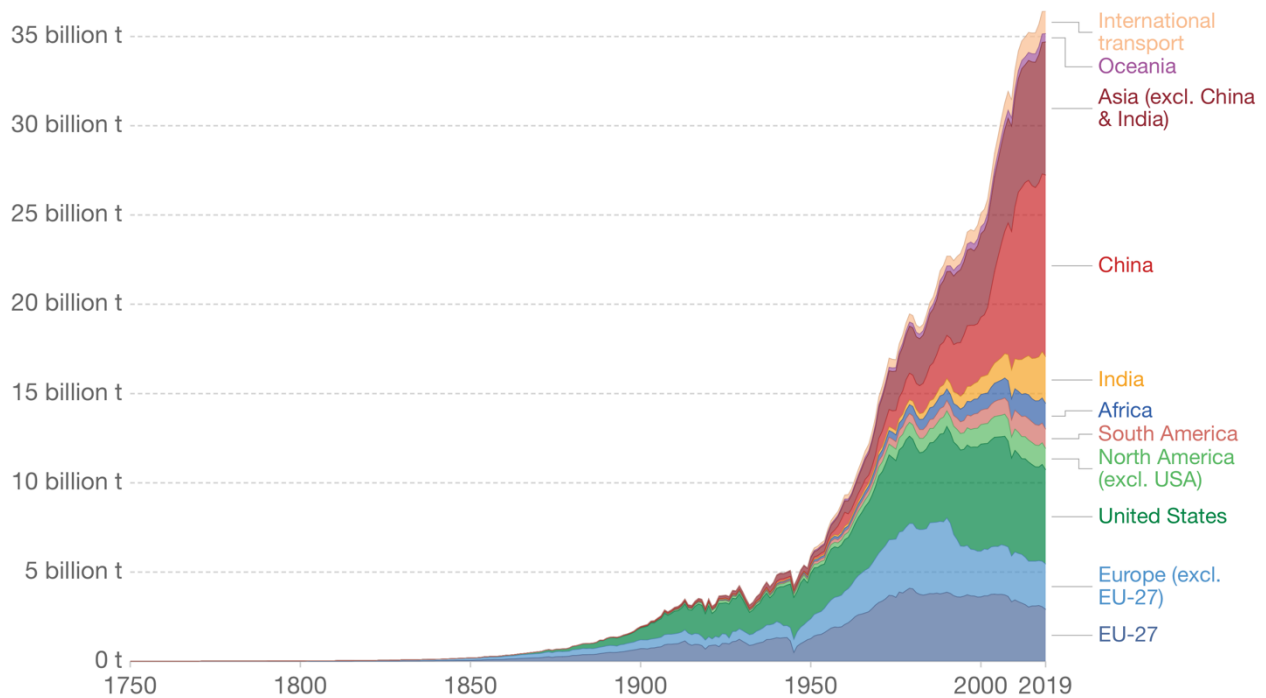


Figure 1.1 Annual total CO₂ emission (expressed in gigatonnes of CO₂ per year, Gtco₂/yr) by world region ²

Indeed, carbon dioxide represented the main contribution to greenhouse gas emissions, which accounted for as much as 78% of anthropogenic emissions since 1970. The overall increase in emissions can be attributed more to the use of fossil fuels in the energy sector (47%), followed by industry (30%), transport (11%) and construction (3%). The latter contribution would increase if indirect emissions were also taken into account ¹.

To stabilize concentrations of CO₂ in the atmosphere, the world needs to reach net-zero emissions. This requires large and fast reductions in emissions ².

With the Paris Agreement for the first time, all nations come together for a common cause and make efforts to combat climate change and adapt to its effects, with greater support for developing countries; so, it tracks a new course in global climate effort. The main objective of the Paris Agreement is to strengthen the global response to the threat of climate change, maintaining an increase in global temperature well below 2 °C compared to pre-industrial levels and pursuing efforts to limit the increase in temperature to 1.5 °C ⁶.

According to the remain carbon budget (i.e., the remaining CO₂ that can be emitted over a given timeframe, in order to achieve a particular temperature target with a given probability) obtained from the IPCC projection of non-CO₂ emission to 2100, *ETP 2017* ⁵ present different pathways for the future transformation of energy sector. They differ in their level of ambition towards stated climate target but represent a significant departure from a historical business-as-usual approach.

On the basis of the stringent target states in the Paris Agreements, the ETP has analysed to what extent the development of current technologies can keep the temperature rise well below 2 °C. According to the scenario "*Beyond 2 °C*" (*B2DS*), the technological improvement of the energy sector is pushed to its maximum practicable to reach zero emissions for 2060 and negative emissions for 2100, (*Figure 1.3*), without the need for scientific discoveries. This approach limits cumulative CO₂ emissions to below about 750 GtCO₂ by the end of the century, which is consistent with a 50% probability of keeping the increase in global temperatures below 1.75 °C, compared to pre-industrial levels.

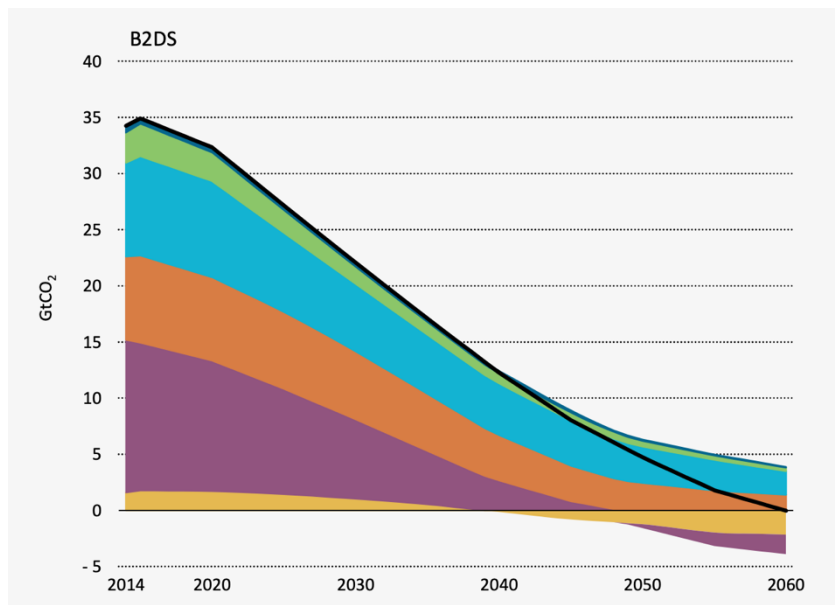


Figure 1.2 CO₂ reductions in B2SD ⁵

As highlighted in the *Figure 1.3*, the energy sector will be a source of negative emissions, necessary to balance the transport and industry sectors and to achieve total zero emissions for 2060. Achieving

negative emissions will require the development of carbon capture technologies (CCS) in combination with bioenergy (BECCS).

Indeed, this cumulative reduction in emissions requires the exploitation of several technologies, in which the main contribution is made by the CCS technologies (32%) together with energy efficiency (34%), as shown in *Figure 1.4*.

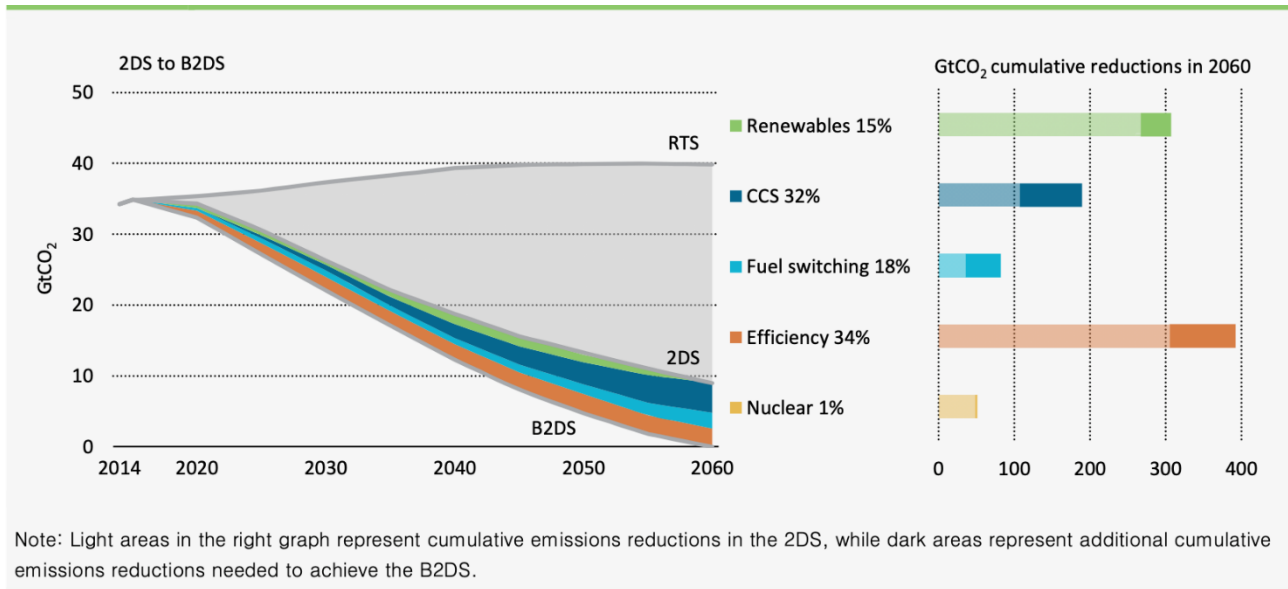


Figure 1.3 Global CO₂ emission reductions by technology and scenario ⁵

Where *the Technological Reference Scenario (RTS)* takes into account environmental policies and commitments made by various countries. Providing a "baseline-scenario" according to which CO₂ emissions from industrial processes will be continuously growing until about 2050, with a global temperature increase estimated to have reach 2.7 °C for 2100, and an increasing trend in the following years ⁵. Whereas *the 2DS* reflected the commitments made during the Copenhagen agreement in 2009, consistent with a 50% probability of limiting the global average temperature increase to below 2 °C by 2100, compared to pre-industrial levels.

CCS is often referred to as one of the key technologies for mitigating greenhouse gas emissions, the technology can be used to reduce emissions from power plants, installations for hydrogen production and industrial processes and therefore considered as a viable alternative to the use of renewable and nuclear sources, also thanks to its various advantages ⁸. First of all, the CCS, in particular for the post-combustion technologies, allows the exploitation of existing energy plants, through an integration with a few adjustments to the plant itself; besides, the CCS is a viable option for the decarbonisation of industrial processes with high emissions. Finally, it is possible to combine CCS with low-carbon bioenergy (BECCS) for the generation of negative emissions: if the use of biomass allows sequestering as much CO₂ as is emitted in the production process (bioenergy or biofuel), with the

addition of CCS technology, an additional capture would be achieved which would allow CO₂ to be withdrawn from the atmosphere.

CO₂ capture and storage (CCS) is a process based on the separation of CO₂ at a given stage of energy conversion or industrial processes, followed by its compression, transportation and then storage, typically in geological sites suitable for retaining it. Depending on the process or application of the installation, there are three main approaches to the capture of CO₂ from fossil fuels: *post-combustion capture (PCC)*, *pre-combustion capture* and *oxyfuel combustion*.

In particular, post-combustion capture is the most mature and already widely available technology on the market ²³, for this process the CO₂ is removed from the flue gas before they can be expelled into the atmosphere ¹⁵. The conventional process of PCC, based on an aqueous solution of amine, exploits a selective chemical absorption that affects only acidic gases, thus exploiting the different nature of CO₂ from the remaining gases present in the mixture. This process must be reversible, being able to exploit in this way the absorbing species in a continuous cycle of absorption and desorption. This cyclic process is based on a temperature variation: CO₂ is absorbed into an aqueous amine solution at a relatively low temperatures (40-60 °C), so it has a high affinity with CO₂. The rich solution is then brought to high temperatures (100-140 °C) to shift the chemical equilibrium and reduce affinity with CO₂, thus allowing the regeneration of the absorbing species and the separation of the previously captured CO₂ ²³.

The basic configuration of the PCC post-combustion capture process is shown in Figure 2.9.

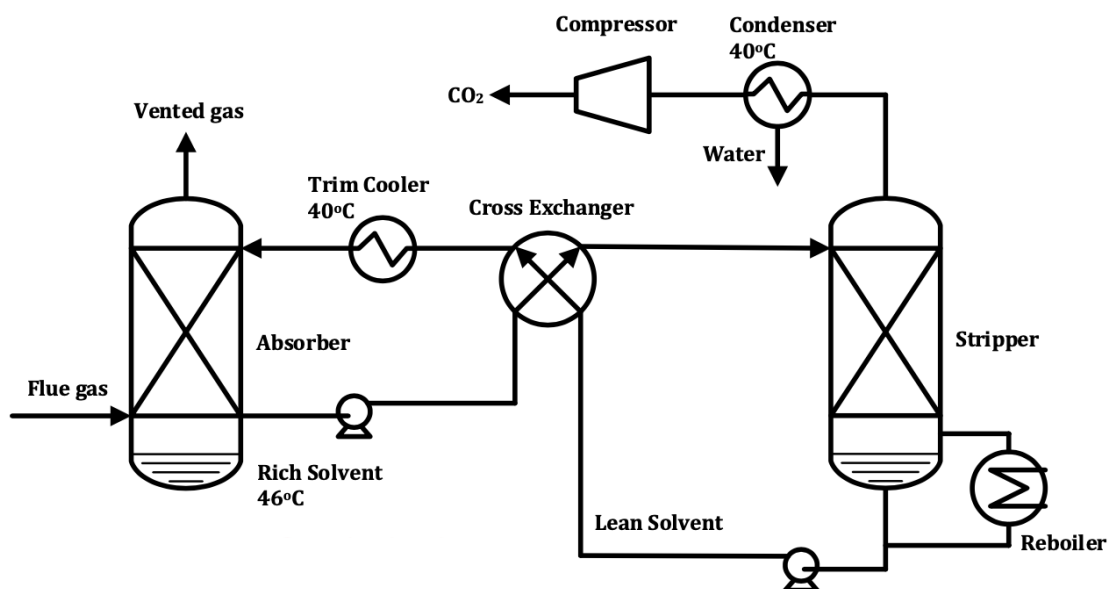


Figure 2.1 Scrubbing di ammine con simple stripper ³³

The mixture of CO₂-containing gas and the absorbent comes into contact within a packed column, that is, a column filled with grossly porous packaging material. The fresh absorbent is inserted into the upper part of the column and flows downwards by gravity along the solid surface of the packaging material. The flue gasses are introduced from the bottom of the column and pumped upwards. This is a typical counter-current process that generates a large contact surface between the gases and the liquid. As the absorber moves along the column it absorbs increasing amounts of CO₂, until it reaches saturation. Once the absorbent reaches the base of the column, it is collected, pumped into the stripping column, and heated by means of a heat exchanger. The stripping column is quite similar to the absorption column, and again, the CO₂-rich absorbent is introduced from the top. For conventional process, steam is produced at the base of the stripping column, used both to transport heat along the column and to dilute the CO₂ released. The absorbent flowing downwards releases CO₂, which flows upwards along with the steam produced at the bottom of the column. Steam dilutes CO₂ and releases heat by condensation. The pure solvent at high temperature at the outlet from the stripping column is sent to the heat exchanger and then further cooled to be able to return inside the absorber at a temperature of around 40 °C. Therefore, this process allows obtaining free combustion gases of CO₂ at the exit of the absorber, and the production of almost pure CO₂ at the exit of the stripping column ²³.

The separation of CO₂ from a gas mixture, using reactive chemical absorption, is based on a combination of physical and chemical processes. These processes occur as a result of the direct counter between the liquid and gaseous phases and are favoured by providing or removing heat.

Figure 2.2 shows the absorption of CO₂ gas by a liquid:

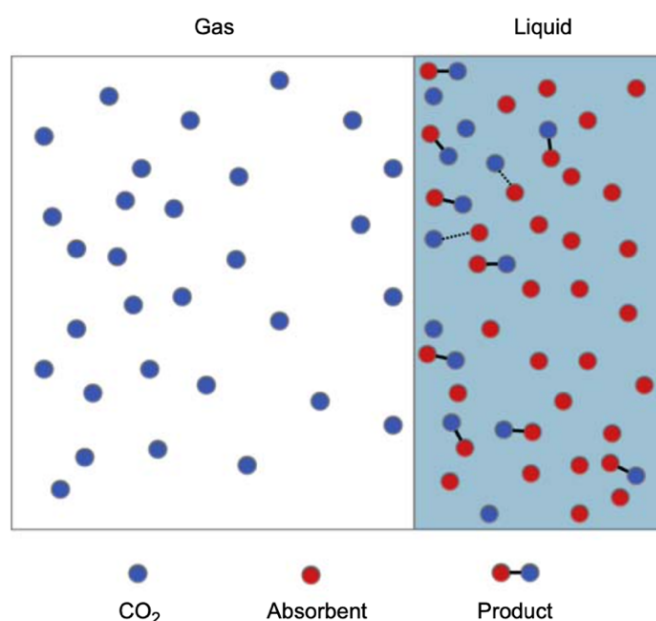


Figure 2.2 Graphical representation of gaseous CO₂ passing through the gas-liquid interface and undergoing chemical reactions with the absorbent ²³

The gaseous CO₂ at the interface dissolves within the liquid phase, in this way, coming into contact with a molecule of the absorbing species, reacts chemically to give rise to a distinct chemical product. This reduces the concentration of dissolved CO₂ in the liquid phase and encourages more migration of gaseous CO₂ to the gas-liquid interface. This migration is driven by the diffusion process, that is, a spontaneous movement of molecules from a region with a higher concentration to one with a lower concentration ²³. This process continues until an equilibrium is reached between the two phases, where the liquid is saturated under gas conditions. The concentration gradient is called the *driving force* (DF), and can be quantified as follows:

$$DF = P_{CO_2} - P_{CO_2}^* \quad (2.1)$$

Where P_{CO_2} is the concentration of CO_{2(g)} defined as partial pressure (kPa) and $P_{CO_2}^*$ is the concentration of dissolved CO₂ defined as partial equilibrium pressure (kPa), or the resulting partial pressure for a certain concentration at the equilibrium of CO₂, $[CO_2]^*$ (mol/m³) ²⁴.

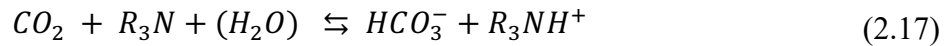
As far as a conventional aqueous ammine solution is concerning, when a primary or secondary amine that react rapidly with CO₂ is present at large concentration, this reaction can be considered dominant, and reactions with water and hydroxide can be neglected ²³. In this situation, it's possible to consider the following overall reactions, based on the kind of ammine present in solution:

- For *primary amines*, the overall reaction that occurs is as follows:



In which two amine molecules are needed for each absorbed CO₂ molecule: the carbamide acid initially formed deprotonates for high pH values, and the proton released is then captured by the second amine.

- *Tertiary amines and sterically hindered amines* do not present such disadvantage:



The overall reaction involves the use of a single molecule of amine per molecule of CO₂. Allowing, theoretically, to absorb twice as much CO₂ as reactive amines. However, tertiary amines and sterically hindered amines have a slower reaction rate, for this reason, all practical processes based on the use of tertiary amines include a certain amount of promoter, a rapid reactive amine added at lower concentrations ²³.

The scrubbing of amines is based on temperature variation to promote solvent regeneration. This process is optimized by working the absorber at low temperatures and the stripper at high temperatures. Typically the flue gas and the poor solvent are cooled up to 30-40 °C with cooling water or ambient air; while the high temperatures of the stripper are limited by the thermal degradation of the solvent or by the temperature that can be reached with condensation vapour or other heat sources ²⁸. The energy consumption of the adsorption/desorption process is currently considered to be still too high. In particular, the energy demand for solvent regeneration, for a basic pilot plant and considering the use of an aqueous solution at the 0,3 g/g MEA (the solvent conventionally used), is estimated at 3.6-3.8 GJ/t_{CO2}, for which a thermal efficiency loss is estimated at 11-15%. Approximately 70-80% of total energy demand, including the CO₂ compression stage, is considered to be due to solvent regeneration alone; for this reason, research only focused on the reduction of such energy consumption ²⁹.

It has been suggested that the use of ionic liquids (IL) as alternative solvents would have many advantages over convention amine-based CO₂ absorption. In addition to the lower energy demand for solvent regeneration, ILs have lower volatility, lower vapour pressure, are non-flammable, are more thermal stable, and are easier to recycle ¹⁸. Indeed, the non-volatility of ILs allows separation of CO₂ from the rich solvent more facilitated, with a reduced energy consumption compared to CO₂ capture methods based on the scrubbing of amines. Moreover, the use of ILs, compared to conventional volatile solvents, allows avoiding the loss of solvent by preventing air pollution caused by organic substances.

However, a key property for absorption performance is the viscosity. In general, IL viscosity is relatively high and increase further as a result of CO₂ absorption due to chemical reactions. High viscosity values will reduce the heat transfer coefficient as well as hinder the CO₂ diffusion process. Therefore, the reduction of the viscosity of the IL is at the center of significant and continuous research efforts ⁴².

The most important property of ionic liquids is considered to be the tunability, as it allows the design of activity-specific ionic liquids (TSIL) ⁴¹. Millions of possible combinations of different cations, anions and functional groups, provide the IL with specific physicochemical properties and influence their CO₂ capture performance ⁴³. Most ILs absorb CO₂ through a physical mechanism, through the physical interaction between cations, anions and CO₂. Although ILs represent a different option for CO₂ capture, the physical mechanism of absorption of ILs cannot yet compete with the solvents currently on the market, due to the lower CO₂ absorption capacity found for post-combustion capture, interacting with flue gas at atmospheric pressure and low CO₂ concentration ⁴³. Indeed, the aqueous solutions of MEA, while presenting problems associated with degradation, corrosion and volatility, are characterized by high CO₂ capture capacity. As a result, ILs need to incorporate reactive sites in their structures, functionalizing cation and anion with amine groups to increase the CO₂ absorption capacity at the low pressures found in PCC processes, thus constituting a viable alternative to

conventional solvents ⁴². However, functionalization often leads to greater intermolecular interactions, resulting in increased viscosity as a result of CO₂ absorption. To solve this problem, ILs are used in solution with liquids at high boiling point, to counterbalance the high viscosity of ILs. Moreover, these blends have the advantage of reducing the costs associated with the use of ILs, which are typically very high ⁴⁷.

The most common cations (such as imidazolium and pyridinium) and anions (often fluorine) of ILs are produced from non-renewable material, showing weak biocompatibility and biodegradability, and high toxicity. For this reason, in recent years studies have focused on the synthesis of IL from renewable materials and low toxicity. Amino acids are one of the most abundant biomaterials in nature and are recognized as non-toxic, biodegradable and biocompatible. As a result, they can be considered as an excellent raw material for the synthesis of ILs, also thanks to their moderate costs ⁵². Moreover, each AA contains functionalized amines, so IL based on AA (AAILs) can be considered as task-specific anions optimal for the synthesis of IL in CO₂ capture processes ⁵⁴. In 2005, the group of *Fukumoto* ⁵³ synthesized for the first time liquid ions based on amino acids (AAILs), and since then many of the anions used for the production of IL have a natural origin. Also, recently IL-based choline, an essential micronutrient of natural origin, have been synthesized and characterized, showing a high biodegradability and low toxicity. Less attention, however, has been paid to Choline-based AAILs, which show promising physicochemical and thermal properties.

In my thesis, the performance of conventional aqueous monoethanolamine solution is compared with a Choline-based AAIL. In particular, the [Cho][Pro] was selected for the study of the process of CO₂ absorption/desorption by IL due to the presence of the heterocyclic ring of proline (a secondary amine), which would favour a 1:1 mechanism, in which carbamate acid is produced through a direct reaction between a single molecule of [Cho][Pro] and CO₂ ⁵⁴. Indeed, for [Cho][Pro], the CO₂ is absorbed and fixed by the formation of two different species, carbamate and carbamate acid, by means of two different reactions, as shown in *Figure 3.10*.

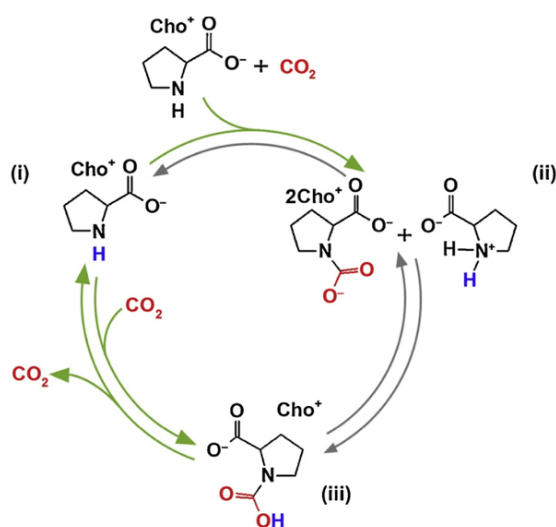


Figure 3.1 Path of reactions between [Cho][Pro] and CO₂. Observed reactions indicated in green; possible unobserved reactions indicated in grey ⁵⁴

Carbamate along with ammonium is formed by the reaction of two amine molecules and one CO₂ molecule (2:1 mechanism), while carbamide is produced by a 1:1 stoichiometric reaction mechanism⁵⁵.

To overcome the issues deriving from their extremely high viscosity, [Cho][Pro] was diluted in dimethyl sulfoxide (DMSO, supplied by Merck, purity $\geq 99\%$). DMSO is an aprotic solvent but exhibits properties like water, and it is completely miscible with the ILs utilized. It is non-toxic, and it has a high boiling point. The DMSO allows performing a process of absorption/desorption of CO₂ by a simple change of pressure or temperature, without the need to produce steam inside the desorption column. This allows reducing the energy required for CO₂ desorption in comparison with aqueous amines systems⁵⁴.

As shown in *Figure 4.1*, the bench consists of two stainless steel packed columns used to investigate the CO₂ absorption and stripping process. The first column ($V = 2$ l, $p < 25$ bar, $T < 65$ °C) act as an absorption section where CO₂ is removed from the simulated flue gas stream by a solvent, and the second one ($V = 4$ l, $p < 4.5$ bar; $T < 125$ °C) is a regeneration section where the absorption capability of the rich solvent is restored. The feed gas mixture was prepared by mixing pure gas with a typical composition of the post-combustion process.

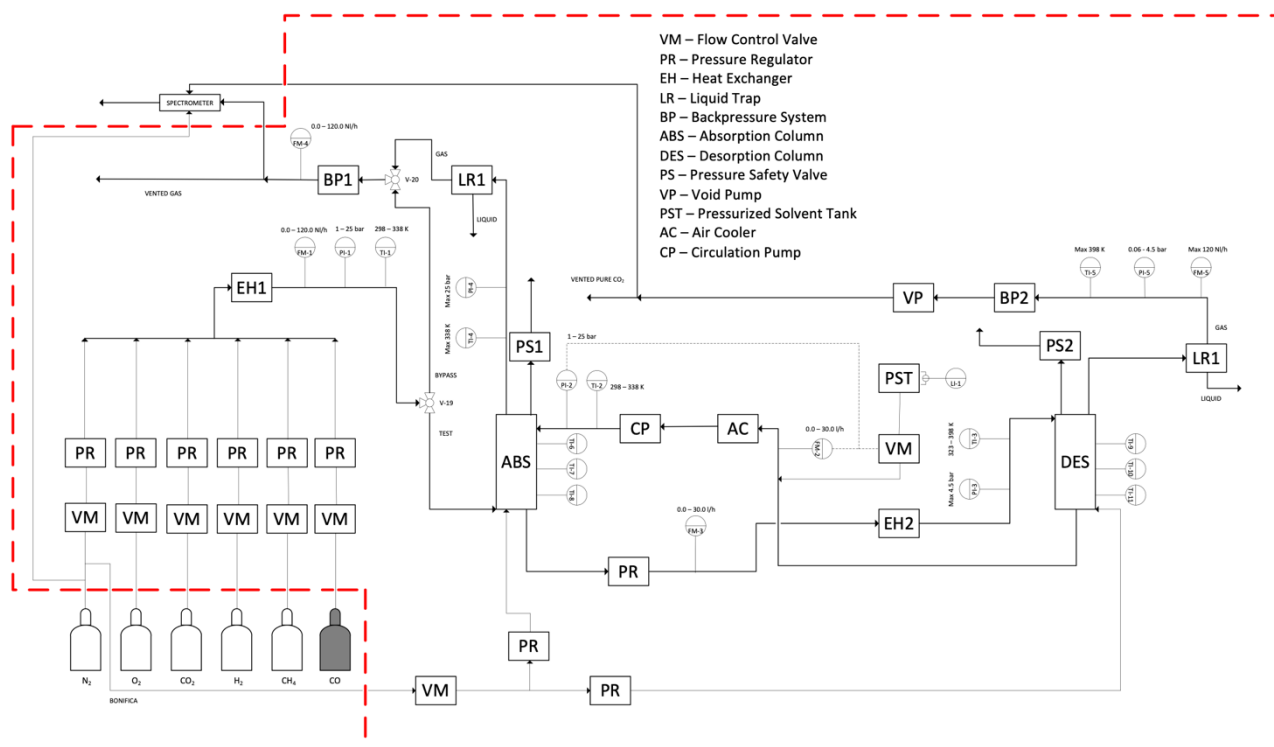


Figure 4.1 Schematic diagram of the experimental setup

The individual gas flows necessary to simulate the mixture of interest shall be introduced. Pressure regulators (PR) shall be capable of modulating the gas pressure between a value close to the maximum operating and storage value (25 bar) and a minimum of 1 bar, controlled by a pressure gauge with a transmitter placed downstream of mixing.

The resulting mixture is heated by an electric heater to the inlet temperature in the absorber for the test. A three-way valve system bypasses the absorption reactor: part of the mixture is analysed by the mass spectrometer. The flow rates of the individual gases in the mixture are varied until the desired composition is reached. In the meantime, the intended solvent flow rate for the correct conduct of the test is circulated in the closed circuit between the two reactors, thanks to the pump (CP). Then reach the operating temperature of the reactors, thanks to the activation of the electric heater (EH2) in the inlet to the stripper and the air cooler (AC) in the inlet to the absorber.

The electric heater (EH1) that conditions the gaseous mixture has a heating cable that brings the absorber to the operating temperature foreseen for the test (controlled by the indicator with transmitter TI7). The electric solvent heater performs the same operation on the stripper (controlled by the indicator with transmitter TI10). The vacuum pump ensures a possible depression of the stripper.

The bench can work in the "continuous" configuration or the "batch" configuration. In continuous, it has a poor solvent recirculation from the stripper to the absorber. For batch configuration, the absorption and desorption process are performed by means of a single column, varying the operating conditions of temperature and pressure. For this configuration, there is no counter-flow between solvent and gas mixture. In fact, the solvent is introduced inside the absorption column, forming a flat surface of heat exchange between the gaseous and liquid phase. The gas mixture is continuously introduced from the bottom of the column, coming directly into contact with the liquid solvent.

In order to assess the objectives of the thesis, it has been evaluated that the batch configuration is the best choice. The initial purpose of this work was to evaluate the reliability of the bench, performing absorption tests with an aqueous monoethanolamine solution (MEA, 30% by weight) and comparing the results with the literature. Furthermore, the alternative of chemical absorption with Choline-based AAILs solution, [Cho][Pro], in DMSO (12.5% wt/wt), which shows promising physicochemical and thermal properties, has been investigated. The task is to verify how the 1:1 reaction mechanism is actually favored for the [Cho][Pro], and investigate the regeneration of the solvent, assessing the conditions for which a complete desorption of CO₂ can be achieved. Finally, provide qualitative information on the possible energy saving of the process.

To measure the experimental loading capacity of the MEA, pure CO₂ was flowed through 1,00 dm³, until no more CO₂ was absorbed. In order to facilitate the reaction, a relatively low temperature has been set, around 30 °C. The experiment was carried out at atmospheric pressure, the load capacity, expressed in *mol CO₂/mol MEA* , is reported as a function of time in *Figure 5.1*.

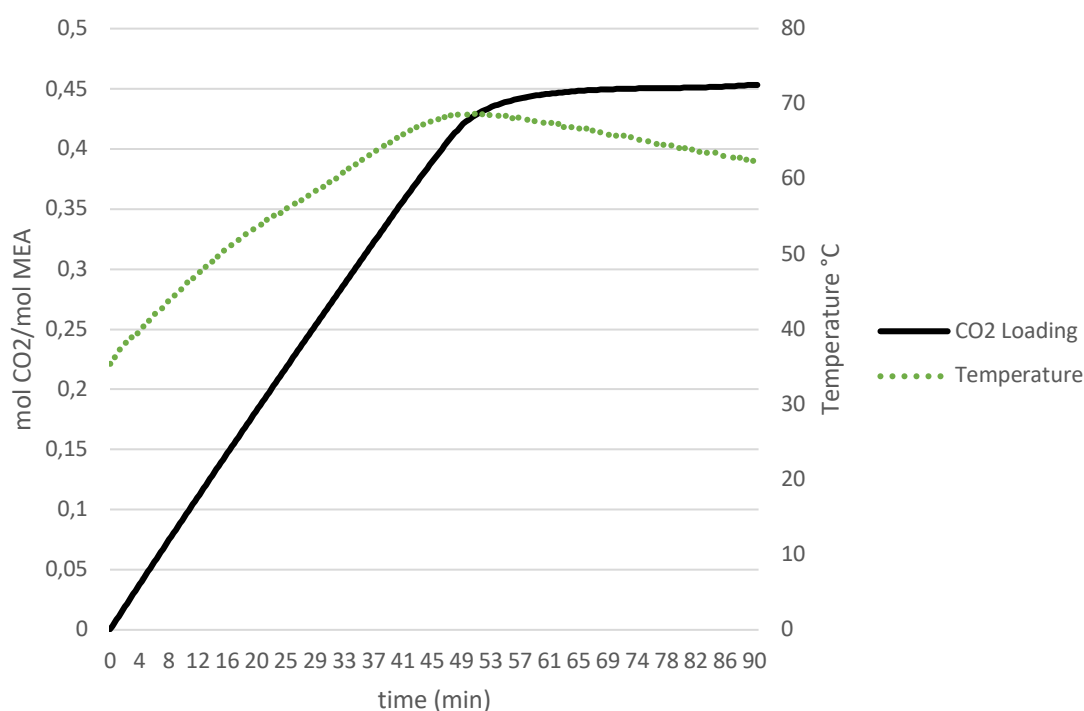


Figure 5.1 The CO₂ loading in the pure solution of 30% wt/wt MEA in function of time (starting absorption temperature: 303 K, gas flow: 78 Nl/h, CO₂ concentration: 100%, solution volume: 1,00 l).

After 90 minutes, no more CO₂ is absorbed by the solution. The result is in good agreement with the literature ⁶³, approaching the theoretical value of 0,5 *mol CO₂/mol MEA*. It is important to consider how the test bench does not present a heat sink at the absorption column, such as to remove excess heat. Therefore, due to the exothermic nature of the reaction, the temperature inside the absorption column has increased reaching a peak around 70 °C, then decrease then decrease when the absorption rate goes down.

In order to assess the influence of temperature on the CO₂ loading capacity, the test was repeated for three different initial temperatures, and the results are presented in *Figure 5.3*. Although the absence of a heat sink prevents testing at a constant temperature, the effect of temperature on the absorption performance of the aqueous solution of MEA is evident

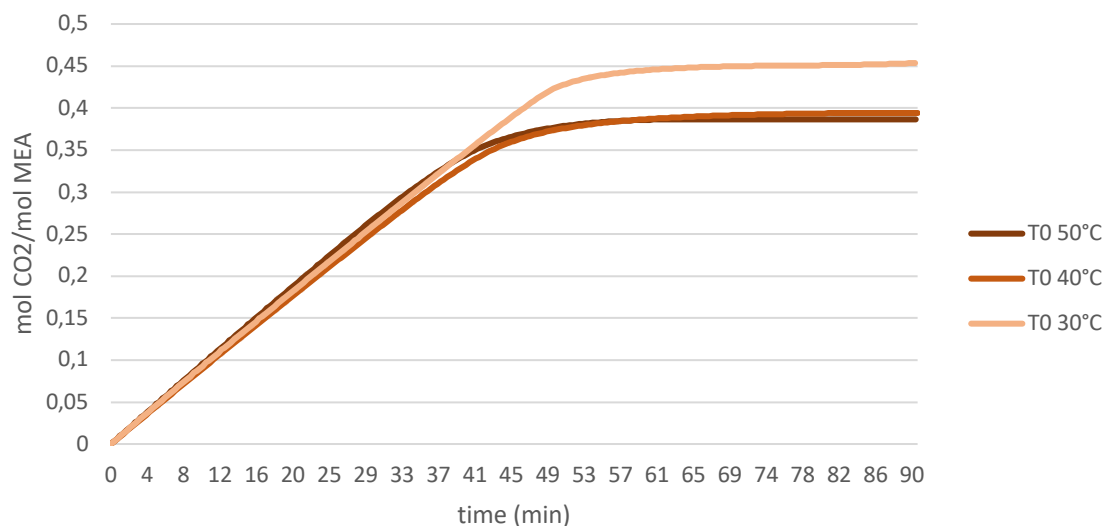


Figure 5.2 CO₂ loading into an aqueous solution of MEA at different temperatures (absorption pressure: 1 bar, gas flow: 78 NL/h, CO₂ concentration: 100%, solution volume: 1,00 l)

The absorption capacity of the CO₂ for a fresh [Cho][Pro] solution in DMSO (12.5% wt/wt) is measured for 90 minutes, bubbling a constant gas flow rate (9 NL/h) of pure CO₂ at atmospheric pressure. To compare the absorption performance with that of MEA and have a match to the results in the literature, was chosen the temperature of 30 °C. The results are presented in *Figure 5.4*.

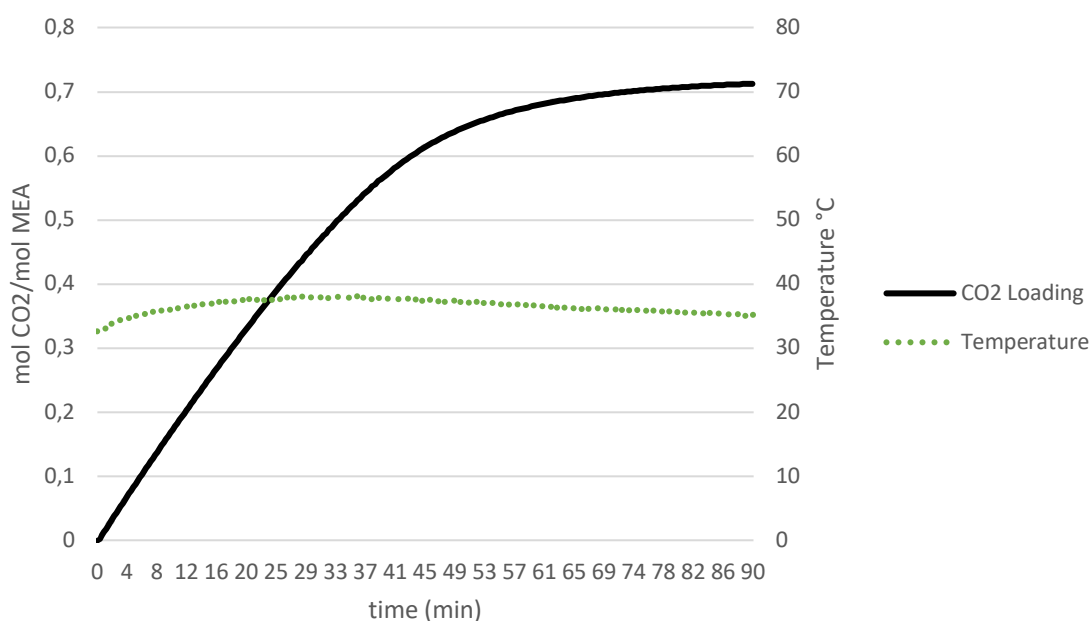


Figure 5.3 The CO₂ loading in the fresh solution of 12,5% wt/wt [Cho][Pro] in DMSO in function of time (starting absorption temperature: 303 K, gas flow: 9 NL/h, CO₂ concentration: 100%, solution volume: 0,50 l).

In contrast to the MEA, the operating temperature during the test remained almost constant, despite the lack of a heat sink. This provides a clear indication of the lower exothermicity of IL, which results in lower consumption due to the need for heat removal in order to improve the CO₂ absorption performance.

In addition, the figure shows how the loading capacity of [Cho][Pro] exceeds the value of $0,5 \text{ mol CO}_2/\text{mol IL}$. The heterocyclic ring of proline seems actually favour the stoichiometric reaction 1:1, compared to the reaction mechanism 1:2, with the formation of carbamic acid.

The CO_2 absorption capacity for [Cho][Pro] was compared to the results obtained by *Shengjuan Yuan et al.*⁶⁴, for the same [AA] in a 5 to 30% wt/wt solution in water. Such results showed a good agreement with respect to the same IL solution in water ($\approx 10\%$ wt/wt) at a temperature of 30°C . In addition, the results indicate that it is possible to approximate and exceed the theoretical value of $1 \text{ mol CO}_2/\text{mol IL}$, but using greater concentrations of IL and operating pressures of up to 15 bar. Indeed, the increase in the partial pressure of CO_2 corresponds to an increase in the driving force that regulates the concentration gradient of CO_2 between the gaseous and liquid phases. This favours the process of diffusion of the molecules of CO_2 inside of the bulk of the liquid phase, favouring the chemical reaction.

Besides the absorption performance, the feasibility of solvent regeneration is also an important factor in practical applications. The regeneration of the [Cho][Pro] solution in DMSO was investigated during four cycles of absorption/desorption with a duration of 90 minutes per process. The desorption process was studied by using an inert gas (N_2) with a flow rate of 18 Nl/h . During the process, the system was heated up to 80°C , with a rate of $3,9^\circ\text{C/min}$, at atmospheric pressure. The results of this experiment are presented in *Figure 5.5*, showing CO_2 loading capacity variation during the absorption/desorption cycles.

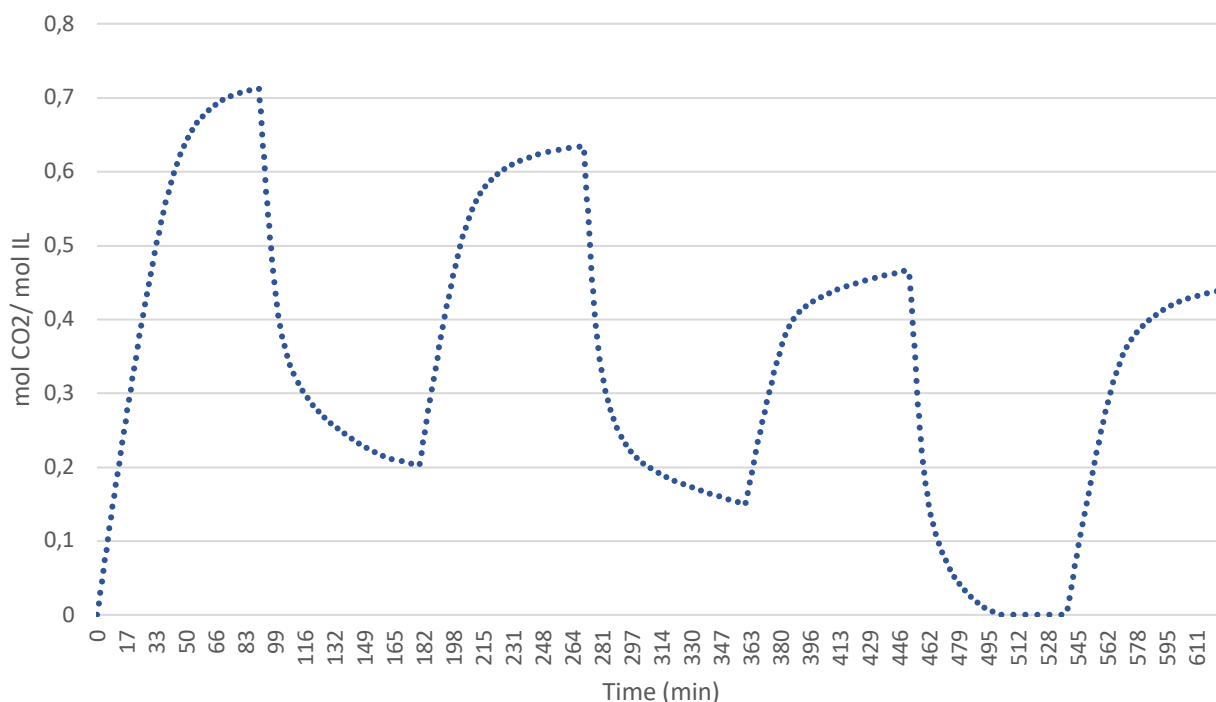


Figure 5.4 Four consecutive cycle of CO_2 absorption (absorption temperature: 30°C , CO_2 flow: 9 Nl/h , N_2 flow: 18 Nl/h , solvent volume: $0,5 \text{ l}$, regeneration temperature: 80°C , absorption time: 90 min , desorption time: 90 min)

The absorption performance of the [Cho][Pro] decreasing progressively from the first cycle, which has a CO₂ loading above 0,7 mol CO₂/mol IL, and then stand at a steady-state value of \approx 0,45 mol CO₂/mol IL for the third and fourth cycles of absorption. The regeneration efficiency, with respect to the first cycle, in turn, was 89,1%, 65,4%, 61,8% for the second, the third and the fourth cycle respectively.

However, this IL-DMSO solution revealed competitive performances as its regeneration efficiency reported a few reductions (<4% variation) during the last two cycles and its absorption capacity was compared to such of the fresh aqueous MEA (i.e., between 0,44 and 0,45 mol CO₂/mol IL), although the aqueous MEA is recognized as very efficient absorbent.

Complete desorption would be possible by increasing the regeneration time or increasing the temperature, allowing the release of the carbamate species, which have high thermal stability. From this point of view, the lack of complete solubility of Proline, at such desorption temperatures, can be considered the cause of the loss of absorption capacity, an effect that can be removed with an increase in temperature.

In order to assess how temperature influences solvent regeneration, the desorption process was carried out by exposing the solution to a constant flow of 18 NL/h of N₂ and divided into several steps. Initially, the solution was heated to a temperature of 70 °C, and left unchanged until no more CO₂ was released, for a total of 80 minutes. Subsequently, the temperature has been increased to 80 °C to assess the desorption performance under these conditions. The process has been repeated several times with a gradual temperature increase of 10 °C per step, up to 110 °C.

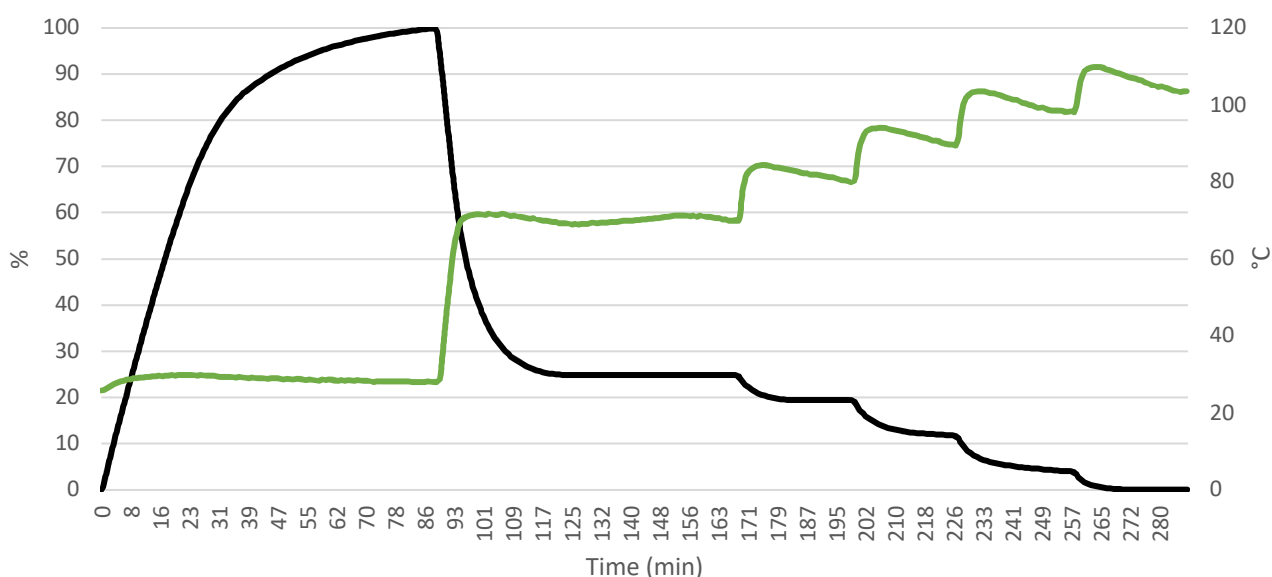


Figure 5.5 Variation of CO₂ concentration into 12,5% wt/wt [Cho][Pro] in DMSO (absorption temperature: 303 K, operating pressure: 1 bar, CO₂ gas flow: 9 NL/h, N₂ gas flow: 18 NL/h, solution volume: 0,50 l).

As can be seen from the figure, in the first minutes of the desorption process the CO₂ is released even at low temperatures, this is due to the reduction of the partial pressure of the CO₂ in the presence of a constant flow of nitrogen. In addition, CO₂ is released by the decomposition of the carbonic acid species, whose formation reaction is reversible at room temperature. Subsequently, the rate of desorption of CO₂ decreases, until it reaches a plateau after about 25-30 minutes from the beginning of the desorption process. Therefore, the desorption process is accelerated again only in the presence of an increase in temperature, such as to allow the release of CO₂ from the carbamate species, which have greater thermal stability. For this experiment, the complete desorption of the released CO₂ occurs in the vicinity of 110 °C.

The process was subsequently repeated to assess the variation of the CO₂ concentration in solution for an initial desorption temperature of 80 and 90 °C (see *Figure 5.9* in chapter five). As expected, an increase in the initial desorption temperature results in a higher regeneration performance. The higher the temperature, the greater the amount of CO₂ released during the first desorption step. The variation in the percentage of CO₂ released as the initial desorption temperature changes is shown in *Figure 5.10*.

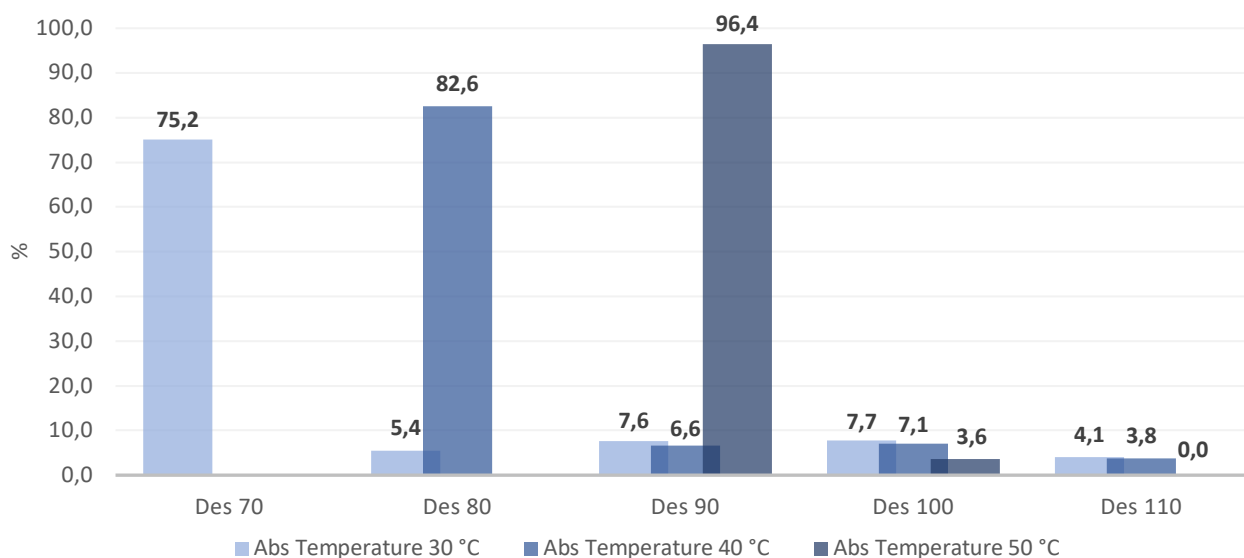


Figure 5.6 Variation in the percentage of desorbed CO₂ for the three desorption tests, as temperature changes

This experiment shows that, even if for total regeneration of the solvent it is necessary to go up to high temperatures (up to 100 °C for an initial desorption temperature of 90 °C), good regeneration performance also occurs at relatively low temperatures (over 75 % of CO₂ released at 70 °C). It is worth that the classic aqueous solutions of amine, such as MEA, require temperatures of around 120 °C to approach regeneration. In addition, tests carried out on the 30% wt/wt aqueous solution of MEA showed that no desorption was detected for temperatures below 100 °C.

Finally, it has been shown that the absorption reaction by [Cho][Pro] is actually reversible, although relatively high temperatures are needed to achieve complete regeneration.

One of the main disadvantages of using the MEA is the presence of water in the solution, which results in a significant increase in the energy consumption of the process compared to using the IL. The energy required for the regeneration of the conventional aqueous solution, which is the main contribution to the overall energy expenditure, includes the demand for sensitive and latent heat, as well as the enthalpic energy necessary to occur the opposite reaction and to decompose the carbamate and carbamic acid moieties. Although the enthalpy of reaction of [Cho][Pro] and MEA has not been evaluated, some qualitative considerations can be made on the remaining two contributions. The demand for sensitive heat is necessary to heat the solvent up to the operating temperature of the desorption step, while latent heat is needed to generate steam within the stripping column such as to dilute the CO₂ released and facilitate the regeneration process. This latter contribution is absent for the [Cho][Pro] since it does not need any steam production for solvent regeneration. Moreover, the sensitive heat decreases as the specific heat of IL-based solvents is lower than the conventional solution at 30% MEA, which is greatly influenced by the high specific heat of the water.

Based on the comparison made between the aqueous solution of MEA and the solution of [Cho][Pro] in DMSO, it can be established that the potential benefits of using IL include: (i) lower consumption due to the need to dissipate heat during the absorption process, linked to the minor exothermicity of IL; (ii) a zero contribution of latent heat on the energy demand for solvent regeneration; (iii) a reduced latent energy demand due to the absence of water in the solution and a reduced temperature difference between the absorption and desorption process. Finally, the use of a TSIL solution from renewable biomaterials provides additional benefits such as low costs, low environmental impacts, low viscosity values respects to more common ILs. These features make the solutions based on [Cho][Pro] an optimal absorbent and competitive at the state-of-the-art for industrial flue gas treatment, which would allow the CO₂ capture or its subsequent use as raw material with high purity.

Abstract

CCS is one of the main processes for mitigating greenhouse gas emissions. CCS can be used to reduce emissions from power plants, installations for hydrogen production, industrial processes and play a key role in biogas upgrading. Therefore, CCS is considered a viable alternative to the use of renewable and nuclear sources.

The thesis aims to evaluate the reliability of the bench by evaluating the absorption performance of an aqueous monoethanolamine solution (MEA, 30% by weight) used as a benchmark and comparing the results with the literature. Furthermore, chemical absorption with task-specific choline-based amino acid, [Cho][Pro], will be investigated. The drawbacks related to the high viscosity and high cost of ILs were reduced by applying DMSO as ILs solvent, using a 12,5% wt/wt [Cho][Pro] solution in DMSO. Proline has been used as an amino acid, as the heterocyclic ring should favour its solubility in DMSO, favouring the regeneration of the solvent.

The absorption experiments were designed to assess the loading capacity, m , of CO₂ by an aqueous solution of MEA, and the liquid ion [Cho][Pro] in DMSO, for different temperatures and CO₂ partial pressure. The tests were performed in batch configuration, thus using a single column to achieve the absorption and desorption of CO₂.

The result of the absorption experiment, performed at 30 °C, for the MEA is in good agreement with the literature, approaching the theoretical value of 0,5 *mol CO₂/mol MEA*. Moreover, the effect of temperature on the absorption performance of the aqueous solution of MEA shows a decrease in loading capacity with the increase in absorption temperature.

In addition, optimal conditions for CO₂ capture by [Cho][Pro] and solvent regeneration have been explored. The results showed that a fresh solution of [Cho][Pro] in DMSO could absorb up to 0,7 mol CO₂ captured/mol IL in solution, at 30 °C and 1 bar. Again, an increase in the absorption temperature corresponds to a decrease in the load capacity. In addition, the regeneration efficiency for the [Cho][Pro] has been evaluated by means of 4 consecutive absorption/desorption cycles, carried out at 30 and 80 °C. The results obtained show a loss of absorption performance, which stabilize from the third cycle (89,1%, 65,4%, 61,8% for the second, third, and fourth cycles, respectively). Studies on the influence of temperature on solvent regeneration have shown that complete desorption can be achieved by bringing the desorption column to higher temperatures. In particular, for a desorption temperature of 90 °C, the release of 96,4 % of the previously captured CO₂. Finally, the absorption and regeneration performance of [Cho][Pro] was compared with the conventional aqueous solvent, showing promising results.

Index

CHAPTER I.....	1
INTRODUCTION TO CARBON CAPTURE & STORAGE	1
1.1 CLIMATE CHANGE AND GREENHOUSE EMISSIONS	1
1.1.1 <i>Factors influencing CO₂ emissions</i>	2
1.1.2 <i>The Representative Concentration Pathways</i>	3
1.1.3 <i>ETP 2017 scenarios</i>	4
1.2 REDUCING EMISSIONS BY CO ₂ CAPTURE AND STORAGE.....	7
1.3 ROLE AND VALUE OF CCS IN MEETING TARGETS	8
1.3.1 <i>Bioenergy with Carbon Capture and Storage (BECCS)</i>	9
1.5 CO ₂ CONVERSION AND UTILIZATION (CCU).....	14
1.6 CO ₂ TRANSPORT AND GEOLOGICAL STORAGE.....	15
1.7 CURRENT STATUS OF CCS DEVELOPMENT	18
1.8 THE CASE FOR POST-COMBUSTION	21
1.9 AMINE-BASED PROCESSES FOR POST-COMBUSTION CO ₂ CAPTURE.....	21
1.10 OBJECTIVE OF MY THESIS	22
CHAPTER II	25
THE POST-COMBUSTION CAPTURE BY LIQUID SOLVENTS.....	25
2.1 INTRODUCTION TO PCC	25
2.2 THE PHYSICS OF ABSORPTION.....	27
2.2.1 <i>Solubility, driving force, and diffusion</i>	28
2.2.2 <i>Mass transfer across the gas-liquid interface</i>	29
2.3 THE CHEMISTRY OF ABSORPTION	30
2.3.1 <i>The kinetics of the reaction of CO₂ in aqueous amine solutions</i>	31
2.3.2 <i>Chemical kinetics and enhanced mass transfer</i>	32
2.5 CONVENTIONAL AQUEOUS AMMINE AND CARBONATE	35
2.6 EQUIVALENT WORK.....	36
2.8 ADVANCED ABSORPTION.....	38
2.9 ADVANCED REGENERATION SYSTEMS	40
2.10 SOLVENT SELECTION FOR ENERGY PERFORMANCE	43
2.10.2 <i>Rate of CO₂ absorption</i>	44
2.10.3 <i>Thermal degradation</i>	46
2.10.4 <i>Heat of absorption</i>	46
2.11 SOLVENT MANAGEMENT	47
2.11.1 <i>Oxidative degradation</i>	47
2.11.2 <i>Flue gas impurities</i>	49
2.11.3 <i>Nitrosamine</i>	49
2.11.4 <i>Amine volatility</i>	50
2.11.5 <i>Amine aerosol emissions</i>	50
CHAPTER III.....	51
IONIC LIQUIDS FOR POST-COMBUSTION CO₂ CAPTURE	51
3.1 IONIC LIQUIDS PROPERTIES.....	51
3.2 CO ₂ SOLUBILITY IN IONIC LIQUIDS	52
3.3 TASK-SPECIFIC IONIC LIQUIDS	53
3.4 AMINE-CO ₂ CHEMICAL INTERACTION.....	54
3.5 IONIC LIQUIDS DEGRADATION	56
3.5.1 <i>Degradation in presence of the microorganism</i>	56
3.5.2 <i>Thermal degradation</i>	57
3.7 CO ₂ ABSORPTION IN CHOLINE-BASED AAILs	59
3.8 [Cho][AA]S-BASED SOLUTIONS.....	62

3.9 SYNTHESIS OF [CHO][PRO]	63
CHAPTER IV	65
EXPERIMENTAL SECTION AND METHODS.....	65
4.1 PLANT DESCRIPTION.....	65
4.1.1 <i>Experimental set-up</i>	66
4.2 CO ₂ ABSORPTION AND DESORPTION MEASUREMENTS TESTS	68
4.2.1 <i>Absorption loading</i>	70
4.2.2 <i>Regeneration efficiency</i>	70
4.2.3 <i>Saturation of the solution</i>	71
4.3 CO ₂ ABSORPTION AND DESORPTION MECHANISMS	71
CHAPTER V	73
RESULTS AND DISCUSSION	73
5.1 ABSORPTION OF CO ₂ WITH AN AQUEOUS SOLUTION OF MEA.....	73
5.2 ABSORPTION OF CO ₂ WITH A SOLUTION OF [CHO][PRO] IN DMSO	76
5.2.1 <i>Effect of absorption/desorption cycle on regeneration efficiency</i>	77
5.2.2 <i>Effect of temperature on the absorption</i>	79
5.3 EFFECT OF TEMPERATURE ON DESORPTION PROCESS.....	79
5.4 COMPARISON WITH 30% AQUEOUS MEA SOLUTION	82
CONCLUSION	85

Index of Figures

Figure 1.1 Annual total CO ₂ emission (expressed in gigatonnes of CO ₂ per year, Gtco ₂ /yr) by world region ²	1
Figure 1.2 Global CO ₂ emissions reductions by technology sector: from RTS to 2SD ⁵	5
Figure 1.3 Remaining CO ₂ reductions in 2SD and B2SD ⁵	6
Figure 1.4 Global CO ₂ emission reductions by technology and scenario ⁵	6
Figure 1.5 CO ₂ captured and stored by a reference installation ⁷	7
Figure 1.6 Biogas production from anaerobic co-digestion at wastewater treatment plant ¹⁴	10
Figure 1.7 Principles of the three main CO ₂ capture options ¹⁵	11
Figure 1.8 Electricity costs for gas and coal plants, with and without CO ₂ capture ¹⁵	13
Figure 1.9 Life-cycle of carbon capture and utilization ⁹	14
Figure 1.10 Methods for storage of CO ₂ in underground geological formations ⁴	16
Figure 1.11 Current progress of Carbon Capture, Storage and Utilization, in terms of TRL. BECCS: bioenergy con CCS; IGCC: integrated gasification combined cycle; EGR: enhanced gas recovery; EOR: enhanced oil recovery; NG: natural gas ⁹	18
Figure 1.12 Large-scale CCS projects for the world. The size of the circles is proportional to the CO ₂ capture capacity of the project to the colour indicates the life-cycle of the project ⁹	20
Figure 2.1 Schematic diagram of the amine-based PCC plant ²³	26
Figure 2.2 Graphical representation of gaseous CO ₂ passing through the gas-liquid interface and undergoing chemical reactions with the absorbent ²³	27
Figure 2.3 Mass transfer across the stagnant film regions of thickness d _G and d _L at the gas-liquid interface ²³	29
Figure 2.4 Set of reactions ²³	31
Figure 2.5 Power consumption with different stripper configurations. AFS, advanced flash stripper; LVC, lean vapour compression; MHI, Mitsubishi Heavy Industries ³⁰	38
Figure 2.6 Design curves for an adiabatic absorption column (dashed curve), in-and-out intercooling (blue curve), and isothermal (black curve) ³³	39
Figure 2.7 Design of an in-and-out intercooling ³³	39
Figure 2.8 Ratio of minimum solvent rate to an adiabatic absorber (no intercooling) and an intercooler absorber ³³	39
Figure 2.9 Scrubbing di ammine con simple stripper ³³	40
Figure 2.10 Advanced Flash Stripper AFS ²⁸	41
Figure 2.11 Interheated stripper, 8 m PZ ²⁸	42
Figure 2.12 Lean vapour compression LVC ²⁸	42
Figure 2.13 Optimal concentration of PZ to maximize energy properties at 40° C ²⁸	45
Figure 2.14 A large absorption heat reduce the equivalent work. MDEA, methyl diethanolamine; MEA, monoethanolamine; PZ, piperazine ²⁸	47
Figure 2.15 Oxidation rates of common amines with cycles from 55 to 120 °C ³⁸	48
Figure 2.16 The nitrosamine cycle ³⁹	49
Figure 3.1 Examples of the most common cations (above) and anions (below) used for ILs ⁴²	51
Figure 3.2 TSIL Davis structure and reaction mechanism for CO ₂ absorption ⁴²	54
Figure 3.3 Reaction mechanism between CO ₂ and [Nh ₂ p-bim] [BF ₄] and DIAL, respectively ⁴³	55
Figure 3.4 Proposed reaction mechanism of CO ₂ with [P66614]- [Pro] ⁴³	55
Figure 3.5 Viscosities η and Densities ρ as a function of temperature: ■, [Ch][Gly]; red ●, [Ch][L-Ala]; green ▲, [Ch][β -Ala]; blue ▼, [Ch][Pro]; pink ◆, [Ch][Ser] ⁴⁷	58
Figure 3.6 Decomposition temperature for several [Cho][AA] ⁴⁷	59
Figure 3.7 Chemical structure of the four [Cho][AA] IL ⁵⁵	59
Figure 3.8 Possible scenarios of reaction between CO ₂ and amines. a) Formation of ammonium carbamate by a 2:1 reaction mechanism; b) formation of carbamide acid by a 1:1 reaction mechanism ⁵⁵	60
Figure 3.9 Path of reactions between [Cho][Gly] and CO ₂ . Observed reactions indicated in green; possible unobserved reactions indicated in grey ⁵⁴	60
Figure 3.10 Path of reactions between [Cho][Pro] and CO ₂ . Observed reactions indicated in green; possible unobserved reactions indicated in grey ⁵⁴	61
Figure 3.11 Synthesis pathways of [Cho][Pro] ⁵⁴	63

Figure 4.1 Schematic diagram of the experimental setup	65
Figure 4.2 Photos of CO ₂ capture bench in the lab A1 of Environment Park, science, and technology park in Turin...	67
Figure 5.1 The CO ₂ loading in the pure solution of 30% wt/wt MEA in function of time (starting absorption temperature: 303 K, gas flow: 78 Nl/h, CO ₂ concentration: 100%, solution volume: 1,00 l).....	73
Figure 5.2 Absorption rate of CO ₂ into aqueous solution of MEA, in function of temperature time (starting absorption temperature: 303 K, gas flow: 78 Nl/h, CO ₂ concentration: 100%, solution volume: 1,00 l).....	74
Figure 5.3 Absorption of CO ₂ into an aqueous solution of MEA at different temperatures. a) CO ₂ loading, b) CO ₂ uptake after 60 minutes, c) trendlines of saturation curves (absorption pressure: 1 bar, gas flow: 78 Nl/h, CO ₂ concentration: 100%, solution volume: 1,00 l).	75
Figure 5.4 The CO ₂ loading in the fresh solution of 12,5% wt/wt [Cho][Pro] in DMSO in function of time (starting absorption temperature: 303 K, gas flow: 9 Nl/h, CO ₂ concentration: 100%, solution volume: 0,50 l).....	76
Figure 5.5 Four consecutive cycle of CO ₂ absorption (absorption temperature: 30 °C, CO ₂ flow: 9 Nl/h, N ₂ flow: 18 Nl/h, solvent volume: 0,5 l, regeneration temperature: 80 °C, absorption time: 90 min, desorption time: 90 min).....	77
Figure 5.6 Regeneration efficiency related to the four absorption/desorption cycles (absorption temperature: 30 °C, CO ₂ flow: 9 Nl/h, N ₂ flow: 18 Nl/h, solvent volume: 0,5 l, regeneration temperature: 80 °C, absorption time: 90 min, desorption time: 90 min)	78
Figure 5.7 Absorption loading into 12,5% wt/wt [Cho][Pro] solution in DMSO at different temperature (gas flow: 9 Nl/h, CO ₂ concentration: 100%, solution volume: 0,50 l).....	79
Figure 5.8 Variation of CO ₂ concentration into 12,5% wt/wt [Cho][Pro] in DMSO (absorption temperature: 303 K, operating pressure: 1 bar, CO ₂ gas flow: 9 Nl/h, N ₂ gas flow: 18 Nl/h, solution volume: 0,50 l).....	80
Figure 5.9 Variation of CO ₂ concentration into 12,5% wt/wt [Cho][Pro] in DMSO. a) Starting absorption temperature: 40 °C, starting desorption temperature: 80 °C, b) Starting absorption temperature: 50 °C, starting desorption temperature: 90 °C (operating pressure: 1 bar, CO ₂ gas flow: 9 Nl/h, N ₂ gas flow: 18 Nl/h, solution volume: 0,50 l)..	81
Figure 5.10 Variation in the percentage of desorbed CO ₂ for the three desorption tests, as temperature changes	82
Figure 5.11 Absorption loading of CO ₂ into two different absorbents (absorption temperature: 303 K, operating pressure: 1 bar, CO ₂ concentration: 35%, solution volume: 0,50 l).	83

Index of Table

Table 1.1 Cumulative storage for the three scenarios of (1) stringent concentration targets, (2) less stringent concentration targets, and (3) concentration targets with the lowest penetration of renewable sources. The three types of models considered are hybrid models (synthesis of technologies and macroeconomic approaches), models focused on a macroeconomic approach and models focused on technology ⁹	8
Table 1.2 Comparison of installations with and without CO ₂ capture ¹⁵	12
Table 2.1 Chemistry of carbonate amines ²⁸	35
Table 2.2 Energy properties of alternative amines ³⁵	43
Table 4.1 Overview of the operating condition of the experimental studies	69
Table 5.1 Absorption/Desorption capacity of [Cho][Pro] solution through the four cycles	78
Table 5.2 Absorption loading expressed in terms of mol CO ₂ /mol amine and mol CO ₂ /kg absorbent of MEA and [Cho][Pro]	84

Chapter I

Introduction to Carbon Capture & Storage

1.1 Climate change and greenhouse emissions

The human influence on the climate system is evident, the atmospheric concentration of greenhouse gases (GHG), such as carbon dioxide, methane and nitrous oxide, from anthropogenic source is the largest ever. Recent climate change has caused impacts on both the human and natural systems, resulting in atmospheric and ocean's surface warming, reducing the amount of ice and rising sea levels ¹.

As shown in *Figure 1.1*, annual total CO₂ emissions have been increasing continuously since the pre-industrial era, due to economic development and population growth. By reaching unprecedented concentrations in recent decades ².

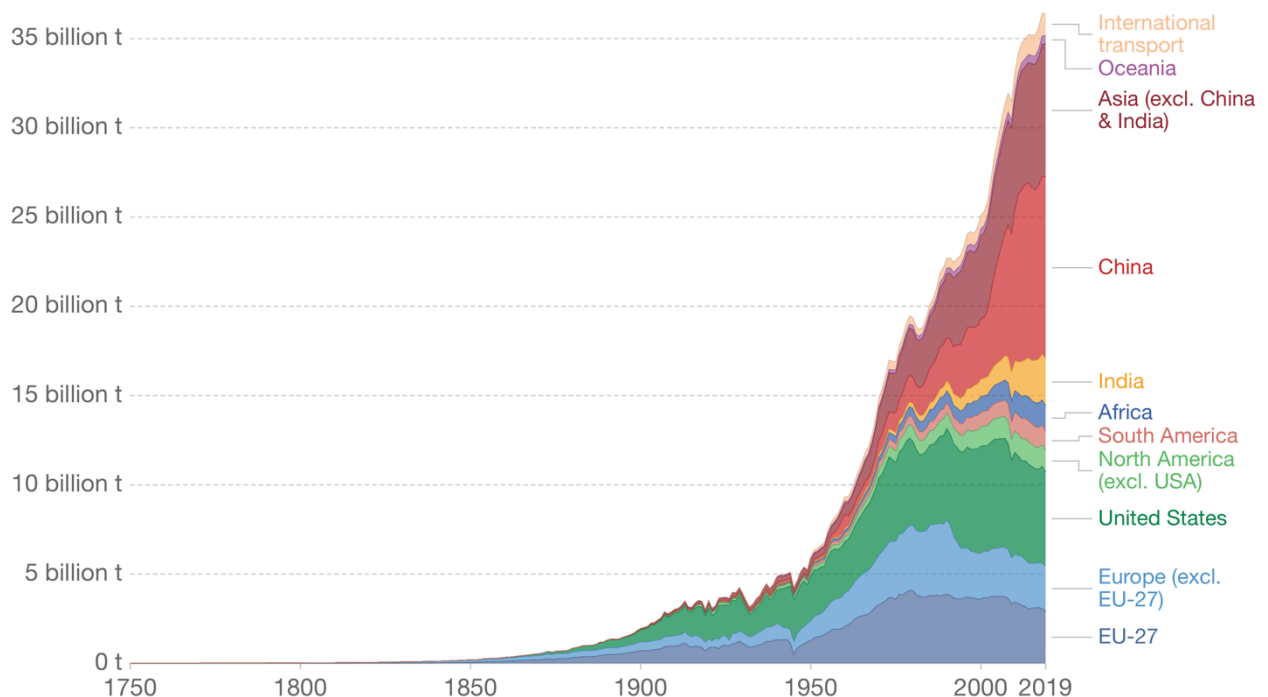


Figure 1.4 Annual total CO₂ emission (expressed in gigatonnes of CO₂ per year, Gtco₂/yr) by world region ²

To stabilize concentrations of CO₂ in the atmosphere, the world needs to reach net-zero emissions. This requires large and fast reductions in emissions ².

Moreover, the trend of anthropogenic greenhouse gas emissions shows a substantial increase since 1870, particularly in the period 2000-2020 and reaching a concentration of 49 ± 4.5 GtCO₂-equ/yr, despite the influence of policies on climate change mitigation ¹.

The main contribution to these emissions is represented by carbon dioxide, which accounted for as much as 78% of anthropogenic emissions since 1970. The overall increase in emissions can be attributed more to the use of fossil fuels in the energy sector (47%), followed by industry (30%), transport (11%) and construction (3%). The latter contribution would increase if indirect emissions were also taken into account ¹.

A continued increase in GHG emissions would cause further atmospheric warming, resulting in irreversible impacts on populations and ecosystems. Substantial reductions in anthropogenic emissions are needed to limit climate change through climate policies and socio-economic developments ¹.

1.1.1 Factors influencing CO₂ emissions

Following the *Kaya identity* ³, a mathematical structure introduced in 1995, it is possible to assess the main factors governing global CO₂ emissions:

$$CO_2 \text{ emissions} = Population \cdot \frac{GDP}{Population} \cdot \frac{Energy}{GDP} \cdot \frac{emissions}{Energy} \quad (1.1)$$

Where GDP is gross domestic production.

By considering the *Eq. (1.1)*, the global CO₂ emissions can be considered as directly linked to global population growth, per capita economic activity (GDP/P), energy intensity (E/GDP), and carbon intensity in energy consumption (emissions/E). Evaluating the population as constantly growing, and the per capita economic activity slightly decreasing in many countries, the Kaya identity reveals how, for a substantial reduction in CO₂ emissions, there is a need for strong action on energy intensity and carbon intensity ³.

For this purpose, there is a wide variety of technological options for the reduction of CO₂ emissions, and each technique is linked to the objectives to be pursued for the reduction of these emissions ⁴.

1.1.2 The Representative Concentration Pathways

Considering greenhouse gas emissions as primarily influenced by population size, economic activity, energy use, technologies and climate policy, the Representative Concentration Pathways (RCPs), presented by the *IPCC Fifth Assessment Report (AR5)* ¹ and developed using Integrated Assessment Models (IAMs), describe four different 21st-century pathways on GHG emissions and air concentrations, shown in *Figure 1.2*.

RCPs have a stringent mitigation scenario (RCP2.6), two intermediate scenarios (RCP4.5 and RCP6.0) and a scenario with very high GHG emissions (RCP8.5). The so-called *baseline scenario*, that is the scenarios that do not foresee efforts to limit emissions, lead to pathways between RCP6.0 and RCP8.5. On the contrary, RCP2.6 represents a scenario whose objective is to keep global warming below 2 °C compared to pre-industrial temperatures. RCPs are consistent with a wide range of mitigation scenarios used in WGIII, which summarise the emission scenarios published in scientific literature and defined on the basis of the estimated CO₂-equ concentration level (ppm) in 2100 ¹.

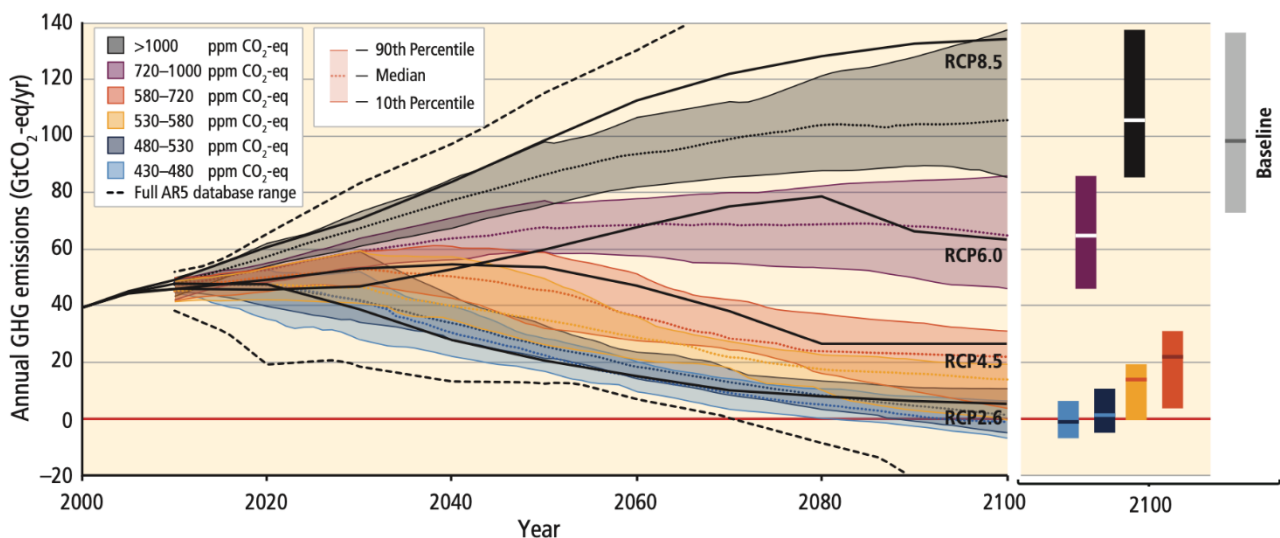


Figure 1.2 Carbon dioxide (CO₂) emissions in different RCP (lines) and the corresponding scenarios used in WGIII ¹

The analyses carried out show an almost linear relationship between the increase in CO₂ concentrations and the variation in temperatures. This relationship can be used to determine the remaining CO₂ budget that can be emitted over a given timeframe, in order to achieve a particular temperature target with a given probability. This trend is present both in the RCP and in the wider scenarios present in the literature and evaluated by the WGIII.

Mitigation scenarios for which global temperatures are likely to remain above 2 °C relative to pre-industrial levels are characterised by a concentration of approximately 450 ppm CO₂eq in 2100; and include substantial reductions in anthropogenic GHG emissions by the middle of the century, with large-scale changes in energy systems ¹.

1.1.3 ETP 2017 scenarios

According to the remain carbon budget, obtained from the IPCC projection of non-CO₂ emission to 2100, *ETP 2017* ⁵ present different pathways for the future transformation of energy sector. They differ in their level of ambition towards stated climate target but represent a significant departure from a historical business-as-usual approach. The three different scenarios identify the energy technologies and the political paths necessary to pursue the path of decarbonisation:

- *The Technological Reference Scenario (RTS)* takes into account environmental policies and commitments made by various countries. Providing a "baseline-scenario" according to which CO₂ emissions from industrial processes will be continuously growing until about 2050, with concentrations in 2060 about 16% higher than the values of 2014 and overall growth in energy demand of 50%. The global temperature is estimated to have increased by 2.7 °C for 2100, with an increasing trend in the following years ⁵.
- *The 2DS* was the main climate scenario assessed by the Energy Technology Perspectives (ETP) for many years. It reflected the commitments made during the Copenhagen agreement in 2009, consistent with a 50% probability of limiting the global average temperature increase to below 2 °C by 2100, compared to pre-industrial levels. However, it needs a substantial and ambitious change in the energy sector, with a marked reduction in the dependence of primary energy on fossil fuels, from the current share of about 80% to 35% for 2060. Achieving carbon neutrality by the end of the scenario period (2100) with an electricity production of 96% low carbon ⁵.
- *The scenario "Beyond 2 °C" (B2DS)* analyzes to what extent the development of current technologies can take us beyond the 2DS. The technological improvement of the energy sector is pushed to its maximum practicable to reach zero emissions for 2060 and negative emissions for 2100, without the need for scientific discoveries. This approach limits cumulative CO₂ emissions to below about 750 GtCO₂ by the end of the century, which is consistent with a 50% probability of keeping the increase in global temperatures below 1.75 °C, compared to pre-industrial levels. Achieving negative emissions will require the development of carbon capture technologies (CCS) in combination with bioenergy (BECCS). B2DS is part of the ambitions stated in the Paris Agreement, but does not set a specific temperature target for "well below the 2 °C" ⁵.

With the Paris Agreement for the first time, all nations come together for a common cause and make efforts to combat climate change and adapt to its effects, with greater support for developing countries; so, it tracks a new course in global climate effort. The main objective of the Paris Agreement is to strengthen the global response to the threat of climate change, maintaining an increase in global temperature well below 2 °C compared to pre-industrial levels and pursuing efforts to limit the increase in temperature to 1.5 °C ⁶.

The 2SD requires that the peak of CO₂ emissions for 2020 is reached and a subsequent reduction of a quarter for 2060. In this period, the carbon budget, that is cumulative sustainable CO₂ emissions, is 40% lower than the RTS. This cumulative reduction in emissions requires the exploitation of several technologies, the main contribution of which is made by renewables (40%) and energy efficiency (35%). A lower contribution is provided by CO₂ capture technologies CCS (14%) and nuclear (6%), as displayed in *Figure 1.2* ⁵.

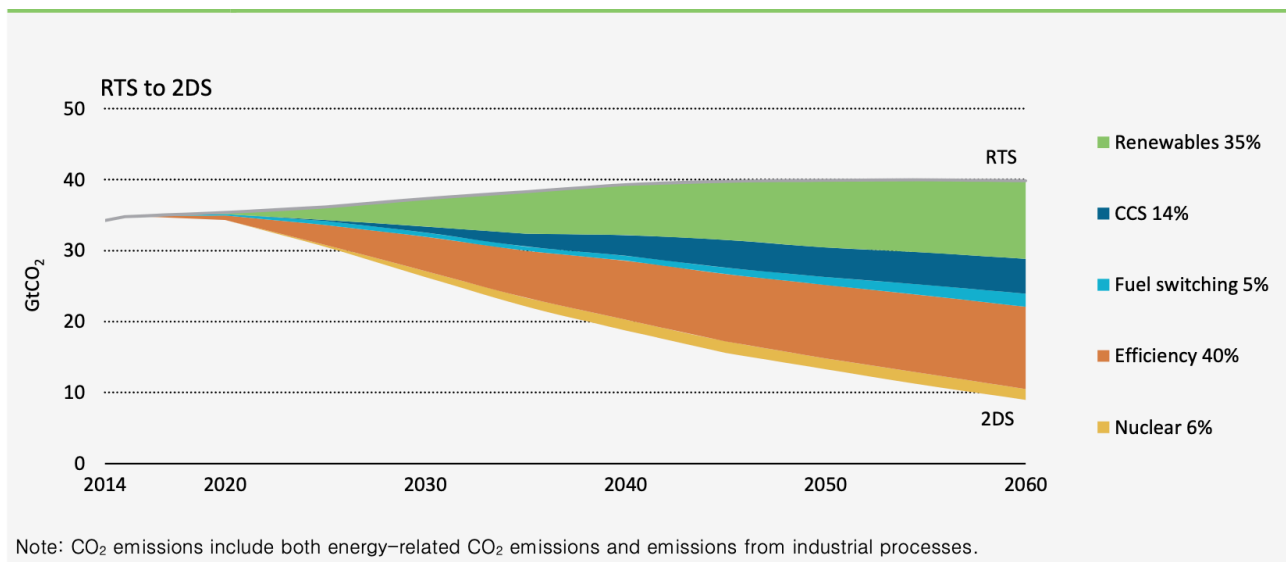


Figure 1.5 Global CO₂ emissions reductions by technology sector: from RTS to 2SD ⁵

All sectors and end-users are involved in reducing emissions: energy efficiency is targeted at the industrial, construction and transport sectors, CCS plays an important role in reducing emissions from industry and power plants, the penetration of renewables will be rapidly growing in the energy sector, due to the need for rapid decarbonisation.

If the 2SD represents a significant reduction in emissions compared to current values, going further with the B2SD is a real challenge. Concerning the 2SD, in 2060 the energy sector will already be virtually decarbonised, on the contrary, the transport and industry sectors, which will become the main sources of emissions ⁵.

The latter will be the main target of B2SD, in which the energy sector will be a source of negative emissions, necessary to balance the transport and industry sectors and to achieve total zero emissions for 2060. As highlighted in the *Figure 1.3*, in which there is a comparison of the different trends for the scenarios 2DS and B2DS.

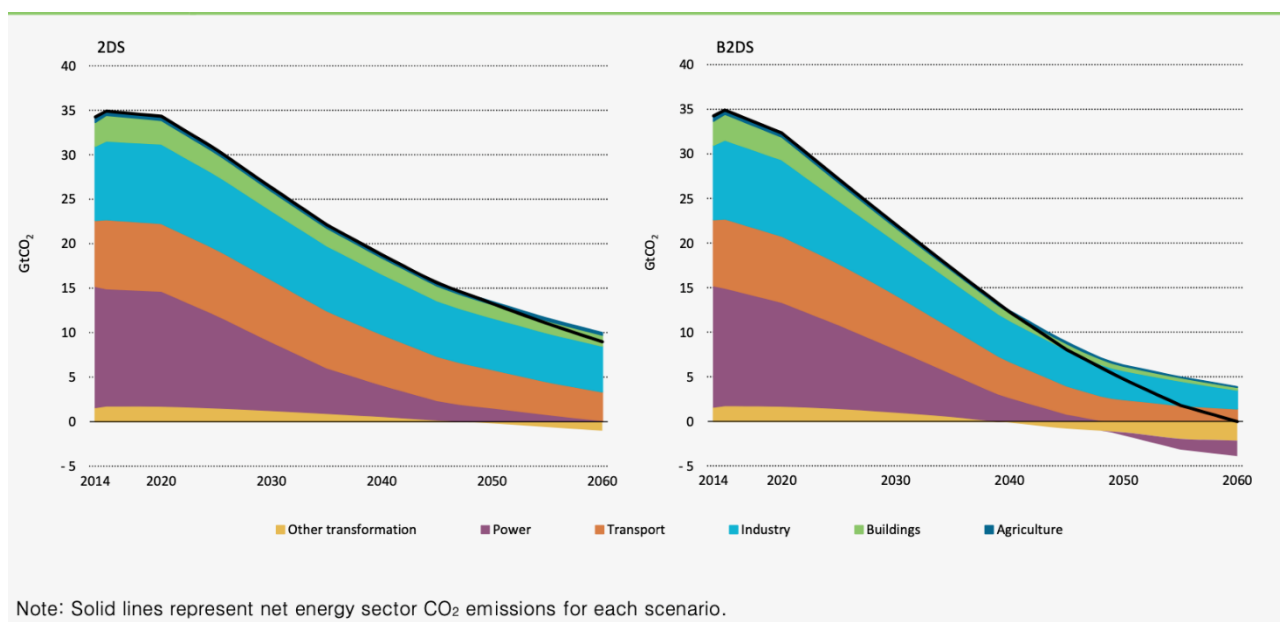


Figure 1.6 Remaining CO₂ reductions in 2SD and B2SD ⁵

In this perspective, the contribution of BECCS technologies to reducing emissions rises to 32%, becoming one of the two main contributions together with energy efficiency, which drops slightly to 34% ⁵, shown in *Figure 1.4*.

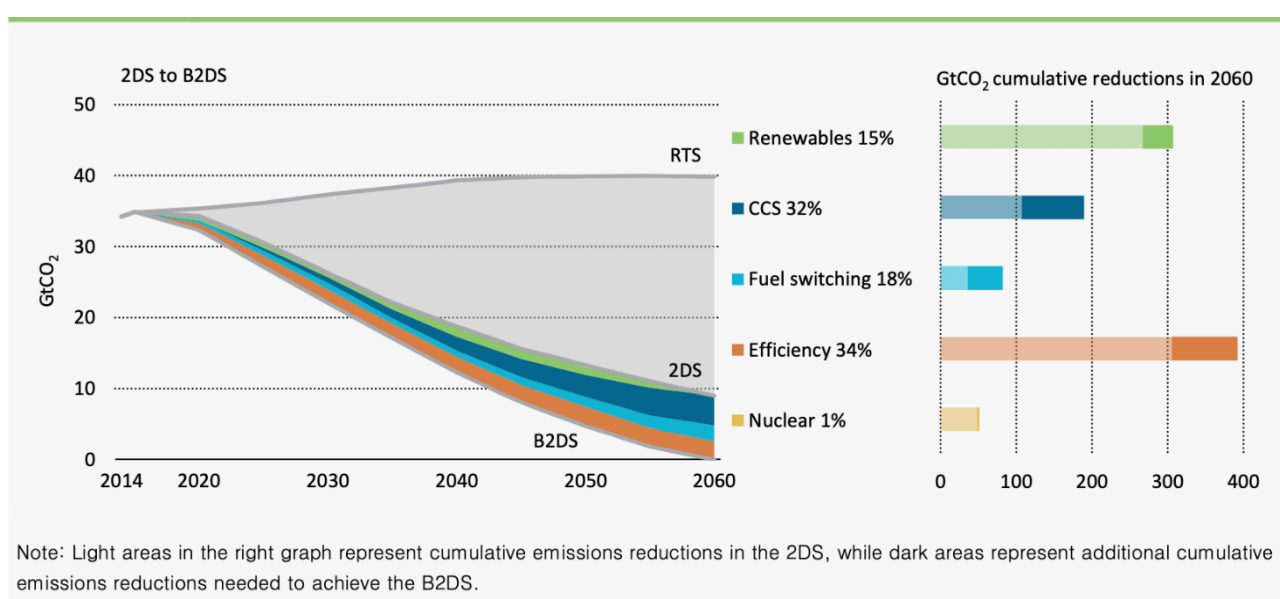


Figure 1.7 Global CO₂ emission reductions by technology and scenario ⁵

1.2 Reducing emissions by CO₂ capture and storage

CO₂ capture and storage (CCS) is a process based on the separation of CO₂ at a given stage of energy conversion or industrial processes, followed by its compression, transportation and then storage, typically in geological sites suitable for retaining it. This makes it possible to use fossil fuels with significantly reduced CO₂ emissions ⁷.

The net reduction of the concentration of CO₂ in the atmosphere also takes into account the additional CO₂ produced (*Figure 1.5*) due to the loss of efficiency of the power plant, losses due to the increased energy required for the capture, transport and storage of CO₂ ⁷.

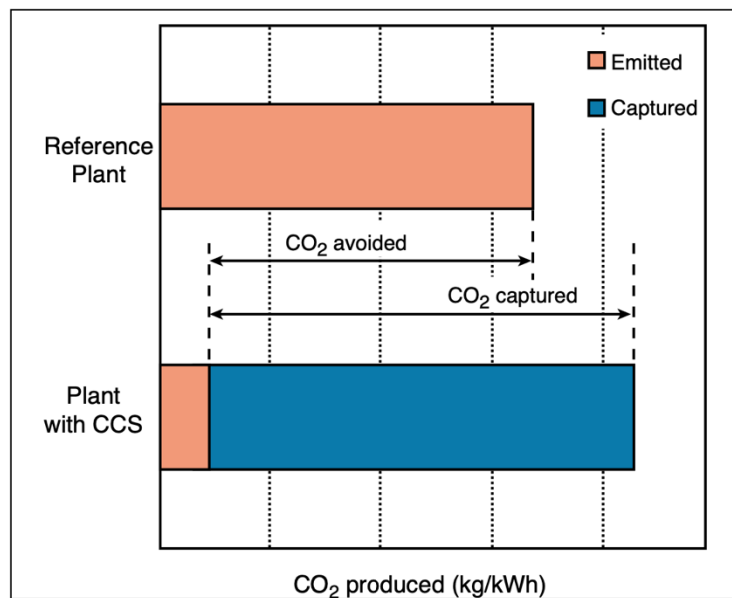


Figure 1.8 CO₂ captured and stored by a reference installation ⁷

In 2005, a special report of the IPCC WGII assessed and considered CCS as a relevant option for mitigation and attenuation of GHG concentration in the atmosphere, stating that “CO₂ capture technologies are now relatively well understood based on industrial experience in a variety of applications. Similarly, there are no major technical or knowledge barriers to the adoption of pipeline transport or the adoption of geological storage of captured CO₂”, also indicating how “CO₂ injection into deep geological formations involves many of the same technologies that have been developed in the oil and gas exploration and production industry” ⁴.

1.3 Role and value of CCS in meeting targets

CCS is often referred to as one of the key technologies for mitigating greenhouse gas emissions, the technology can be used to reduce emissions from power plants, installations for hydrogen production and industrial processes and therefore considered as a viable alternative to the use of renewable and nuclear sources ⁸.

The *Integrated Assessment Models* (IAMs), which evaluate the role of specific technologies in achieving climate objectives, consider CCS as an attractive option, also thanks to its various advantages. First of all, the CCS, in particular for the post-combustion technologies, allows the exploitation of existing energy plants, through an integration with a few adjustments to the plant itself; besides, the CCS is a viable option for the decarbonisation of industrial processes with high emissions. Finally, it is possible to combine CCS with low-carbon bioenergy (BECCS) for the generation of negative emissions: if the use of biomass allows sequestering as much CO₂ as is emitted in the production process (bioenergy or biofuel), with the addition of CCS technology, an additional capture would be achieved which would allow CO₂ to be withdrawn from the atmosphere. Thus achieving a double benefit from BECCS, both emission mitigation and energy production ⁹.

Koelbl *et al.* ⁸ studied the role of CCS in climate change mitigation scenarios. Basing this study on the results of the 27th Energy Model Forum (EMF) and with the use of 18 IAMs. In this way, he verified the important role of CCS in all mitigation models investigated, with CO₂ capture ranges that vary from model to model, but with none of them less than 600 GtCO₂-equ cumulative until 2100. *Table 1.1* shows the capture ranges of CO₂, based on different concentration targets for 2100, penetration of renewable sources and type of models used:

Table 1.1 Cumulative storage for the three scenarios of (1) stringent concentration targets, (2) less stringent concentration targets, and (3) concentration targets with the lowest penetration of renewable sources. The three types of models considered are hybrid models (synthesis of technologies and macroeconomic approaches), models focused on a macroeconomic approach and models focused on technology ⁹

	Scenario	Model type		
		Hybrid	Macro-focus	Tech-focus
1	Cumulative storage 450 ppm	730–2411 Gt _{CO₂}	—	353–1629 Gt _{CO₂}
2	Cumulative storage 550 ppm	655–2962 Gt _{CO₂}	1262 Gt _{CO₂}	846–1686 Gt _{CO₂}
3	Cumulative storage 450 ppm, limited renewables	625–2447 Gt _{CO₂}	—	1232–1366 Gt _{CO₂}

To ensure global warming of less than 2 °C compared to the pre-industrial era, cumulative emissions from 1870 must remain below about 3650 GtCO₂-equ. From this share, the remaining emissions by the end of the century are estimated to be about 800 GtCO₂-equ ¹.

From this estimation, the importance of CCS in IAMs can be assessed, which with a minimum of 600 GtCO₂-equ alone captures more than half the cumulative CO₂ required. However, it should be borne in mind that at the current emission rate it is expected to exceed the emission share of 800 GtCO₂-equ over the next 20 years ⁹.

Although CCS is often referred to as a bridging technology to more advanced renewable systems, Koelbl ⁸ verified how the role of the CCS in the IAMs does not decline in time, presenting in contrast to the largest catch ranges in the second half of the century: 5-23 GtCO₂-equ/yr in 2050 against 8-50 GtCO₂-equ/yr in 2100.

For models characterized by poor development of renewable sources, CCS technologies play an even greater role in the mitigation process, moreover, for more stringent targets the use of BECCS substantially increases for 90% of models, replacing over time the use of coal and natural gas as a primary energy source ⁹.

In the absence of CCS, the total cost of climate change mitigation would increase by 138%, while a limited availability of bioenergy would cause costs to rise by 64%. In contrast, limited availability of nuclear and renewable energy sources, such as solar and wind, would increase mitigation costs by only 7% and 6%, respectively ¹⁰. In fact, with limited availability of CCS and biomass, it would be necessary to further develop renewable energy sources, such as solar and wind, and increase the use of nuclear. The increase in mitigation costs would be due to the delay in technological development, the stabilisation of the electricity grid and the use of higher-cost technologies such as nuclear power.

Also, in the absence of CCS, there are a significant number of IAMs that find no solution to the achievement of the intended mitigation objectives. In this sense, *Riahi et al.* ¹¹ carried out a comparison of the various models in the absence of CCS, verifying an impossibility to reach the concentration of 450 ppm of CO₂ by the end of the century, in a third of the models analyzed. This ratio increases in case of further mitigation delay. So, without the use of CCS, not only do mitigation targets include higher costs to achieve, but they become unfeasible for most of the models analyzed.

1.3.1 Bioenergy with Carbon Capture and Storage (BECCS)

Negative emissions are obtained by combining CO₂ capture and sequestration technologies and the use of bioenergy (biomass and biofuels). They play a key role in a substantial reduction of greenhouse gas emissions into the atmosphere, and in maintaining the rise in temperatures below 1.75 °C compared to the pre-industrial era. There is, therefore, growing interest in bioenergy through carbon capture and storage (BECCS) ¹².

BECCS technologies developed initially to produce hydrogen, and only later, with the introduction of negative emissions associated with the production of electricity, they were combined with the use

of biomass. During the life cycle of biomass growth, there is a net transfer of atmospheric CO₂ to biomass. The CO₂ released after biomass combustion is captured and stored in a suitable geological structure. Thus, preventing the emission of CO₂ into the atmosphere, and potentially achieving a negative carbon balance. So, biomass can be considering a substituent of fossil fuels, carbon neutral. It also presents a small amount of pollutant emissions such as SO_x, NO_x, and particulates ¹².

Biomass can be used to produce renewable electricity, thermal energy, or converted to transportation fuels, such as biogas. Biogas is produced in landfills, wastewater treatment plants (WWTPs), and biogas plants by microorganisms during the degradation process of organic material. In WWTPs and biogas plants, the gas produced is generally used in energy production. Moreover, in several countries, methane rich-gas from landfills must be collected and burnt or used for energy production to prevent the methane from being released into the atmosphere. Also due to the increased interest in renewable fuels, biogas is considered a significant alternative to conventional fossil fuels, to produce electricity and heat ¹³.

Raw biogas contains about 65% CH₄, 35% CO₂, and a trace of hydrogen sulfide, water vapour, ammonia and siloxane depending on the types of raw material and digestion process. The presence of CO₂ and other pollutants reduces the economic value of biogas and limits its use. Hence, biogas needs to be pretreated to remove hydrogen sulfide, water vapour and other traces of gas. In addition to pretreatment, high-value applications such as fuel transport or biogas injection into the natural gas network require the complete removal of CO₂ for biomethane production ¹⁴, as shown in *Figure 1.6*:

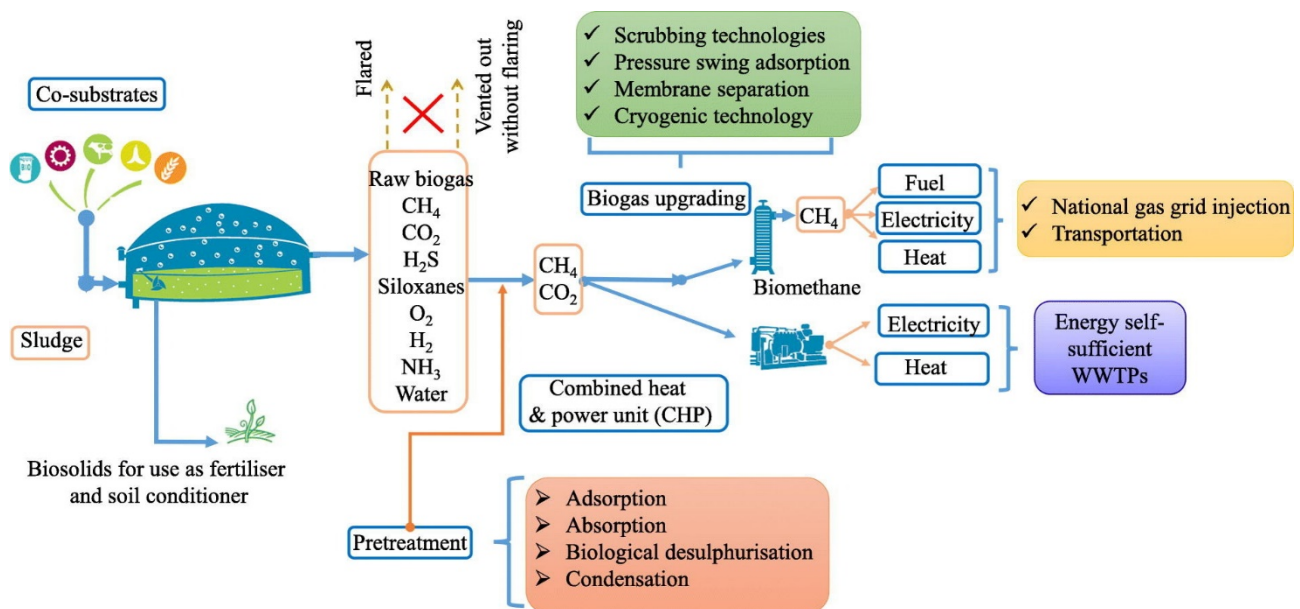


Figure 1.9 Biogas production from anaerobic co-digestion at wastewater treatment plant ¹⁴

The CO₂ removal process for the production of biomethane is called "biogas upgrading". This process can take place utilizing technologies such as physical washing of water or organic, chemical scrubbing, adsorption, pressure swing, membrane separation and cryogenic technology ¹⁴.

A further advantage of using bioenergy in combination with CCS is that it provides a reliable source of low-carbon electricity, unlike intermittent renewable energy (RES) such as wind or photovoltaic. The economic loss due to the power outage is two orders of magnitude greater than the cost of electricity. For this reason, it is necessary to combine reliable technologies with the use of renewables in the electricity system. Bio-energy with CCS is recognized as a practical and immediate approach to GHG mitigation and decarbonisation of the electrical system ¹².

1.4 CO₂ capture technologies

CO₂ is emitted mainly by the combustion of fossil fuels, both in large quantities from electricity generation plants, and in limited quantities from distributed sources, such as vehicles and heating of residential and commercial buildings. In this sense, CCS technologies are more likely to be applied to sources of large emissions, such as power plants or industrial processes.

CCS provides capture technologies necessary to collect the CO₂ produced, transport and storage in a place suitable for its conservation ⁷.

Depending on the process or application of the installation, there are three main approaches to the capture of CO₂ from fossil fuels, highlighted in *Figure 1.7*: where the operating principles of the three main CO₂ capture technologies are shown.

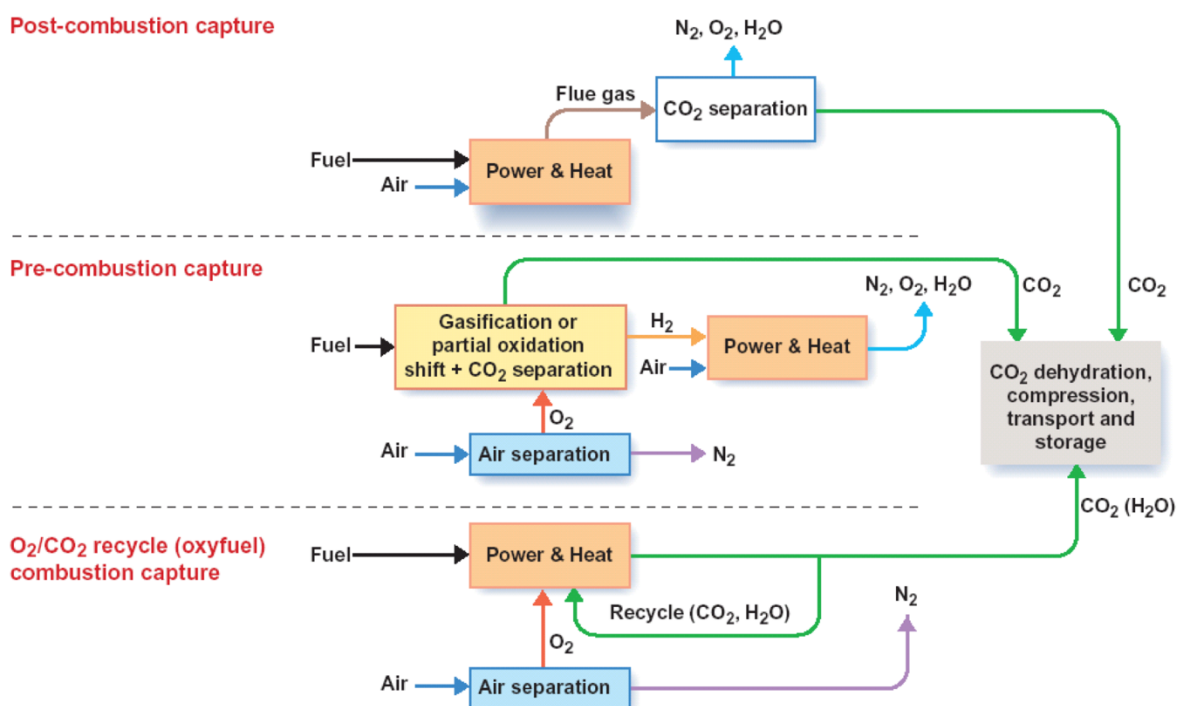


Figure 1.10 Principles of the three main CO₂ capture options ¹⁵

In *post-combustion capture*, CO₂ is removed from the flue gas before they can be expelled into the atmosphere. The most commercially used methods use a scrubbing with an aqueous amine solution. CO₂ is captured by the solvent at relatively low temperatures (40-60 °C) and then removed during the solvent regeneration process. In this process, the solvent is recovered by heating at high temperatures (100-140 °C) and then cooled to the absorption condition to be recycled for continuous use. The CO₂ removed is dried, compressed and transported to a safe geological site ¹⁵

For the *pre-combustion capture*, fossil fuel is gasified with sub-stoichiometric amounts of oxygen, and typically with steam, at high pressures (30-70 bar) to provide a mixture of synthetic gases containing predominantly CO and H₂. Further hydrogen, together with CO₂, is produced by reacting carbon monoxide with steam in an equilibrium reaction, favoured at low temperature, called *water-gas shift*:



The CO₂ produced can therefore be easily separated, releasing a gas flow rich in hydrogen H₂. This separation process typically uses a physical solvent, no heat supply is required for solvent regeneration and CO₂ can be released at about room pressure; this means that the total energy consumption of the pre-combustion capture is about half of the post-combustion capture ¹⁵.

However, such processes present an efficiency penalty due to the water-gas shift reaction. Compared to processes without capture, there is a mass loss of CO₂ that does not pass through the turbines generating power. In addition, the efficiency of a turbine burning hydrogen is lower than a conventional unit burning natural gas or synthetic gas, due to the high heat exchange coefficient of hydrogen combustion products resulting in very high temperatures, difficult to manage by the materials of the turbines. This makes it necessary to reduce the inlet temperature to the turbine causing a reduction of efficiency. Further efficiency losses should be considered in the case of gasification of liquid or solid fuels ¹⁵.

Table 1.2 Comparison of installations with and without CO₂ capture ¹⁵

Technology	Thermal efficiency (% LHV)	Capital cost (\$/kW)	Electricity cost (c/kWh)	Cost of CO ₂ avoided (\$/t CO ₂)
<i>Gas-fired plants</i>				
No capture	55.6	500	6.2	–
Post-combustion capture	47.4	870	8.0	58
Pre-combustion capture	41.5	1180	9.7	112
Oxy-combustion	44.7	1530	10.0	102
<i>Coal-fired plants</i>				
No capture	44.0	1410	5.4	–
Post-combustion capture	34.8	1980	7.5	34
Pre-combustion capture	31.5	1820	6.9	23
Oxy-combustion	35.4	2210	7.8	36

Costs for capture include CO₂ compression to 110 bar but not storage and transport costs. These are very site-specific, but indicative aquifer storage costs of \$10/t CO₂ would increase electricity costs for natural gas plants by about 0.4 c/kWh and for coal plants by about 0.8 c/kWh. LHV = lower heating value.

Consequently, post-combustion capture may be expected to have a higher thermal efficiency than pre-combustion capture, both for combined cycle gas (IGCC) and coal plants, as shown in the following *Table 1.2*.

The *Figure 1.8* shows the comparison of electricity generation costs for different technologies and the level of risk for each of the options. This shows that post-combustion capture is likely to have lower electricity costs for natural gas installations. In contrast, pre-combustion capture is expected to be slightly lower for coal plants due to high capital costs for atmospheric pressure absorbers of post-combustion technologies and the costs of replacing the degraded solvent ¹⁶.

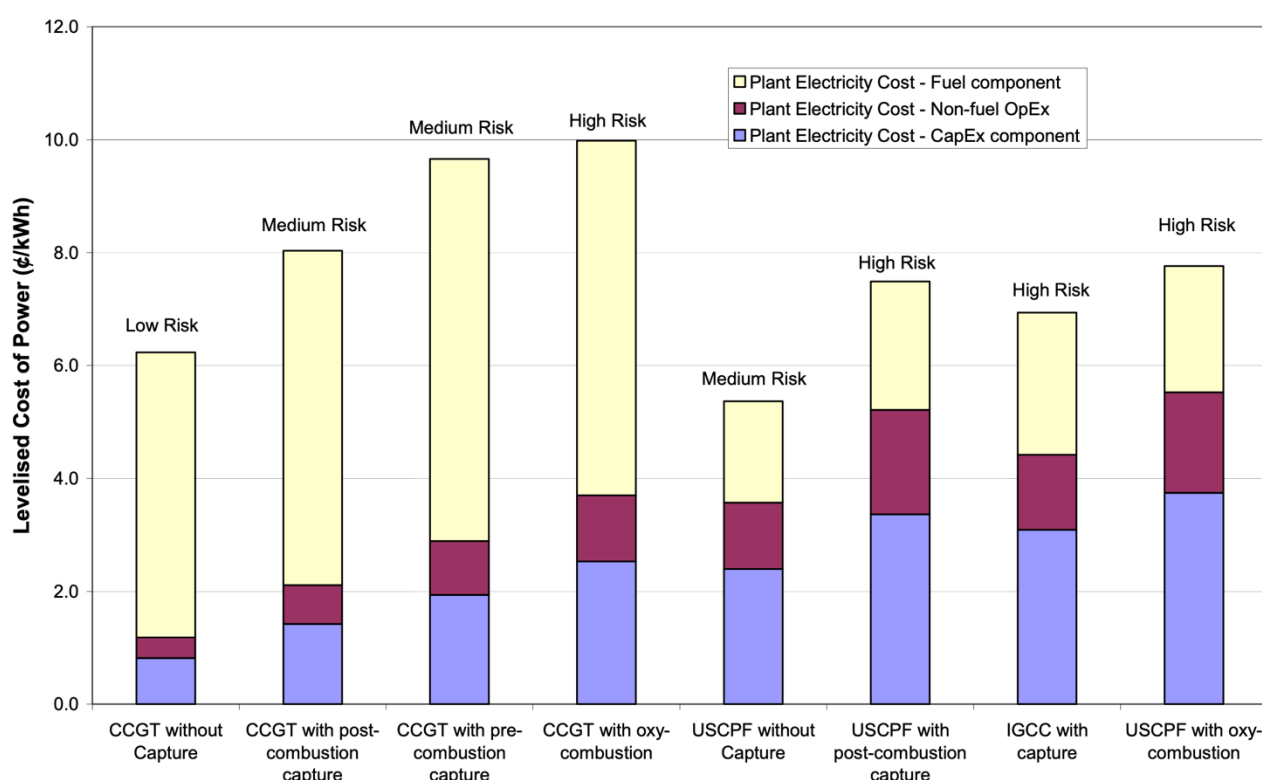


Figure 1.11 Electricity costs for gas and coal plants, with and without CO2 capture ¹⁵

Costs that, for plants equipped with capture technologies, provide the costs for the compression of CO₂ at 110 bar but not storage. It is important, however, to take into account that all costs are only estimates and that they can be expected to differ from the real costs.

The third approach to CO₂ capture is oxyfuel combustion, whose thermal efficiencies and electricity costs for gas and coal plants are shown in *Table 1.2* and *Figure 1.8*.

The concept of oxyfuel combustion was first evaluated by Abraham for increased oil recovery in the early 1980s, such a process is characterized by combustion that takes place in an environment rich in oxygen, rather than in air, with recycled combustion gas ¹⁷.

In these plants, the main separation step involves oxygen from nitrogen, the fuel is then burned in a mixture of recycled oxygen and combustible gases, providing a combustion gas mixture consisting mainly of CO₂ and condensable steam, which can be easily separated during the compression process. For coal-fired plants, removal of pollutants such as nitrogen oxides and sulphides (NO_x, SO_x) from the combustion products before or during the CO₂ compression process is required. Besides the SO_x must also be removed from recycled combustible gases, to prevent high-temperature corrosion within the boiler.

Oxyfuel combustion options for the natural gas combined cycle (IGCC) plants using cryogenic distillation technologies for O₂ oxygen production appear not to be competitive on the market (see *Table 1.2*). On the contrary, coal-fired plants appear to have competitive efficiencies and costs with amine-based post-combustion plants ¹⁵.

1.5 CO₂ conversion and utilization (CCU)

The capture of CO₂ allows not only its storage but also its use or conversion. The concept of CO₂ re-use or conversion and use (CCU) has increased significantly in recent years due to the need to mitigate climate change ⁹.

The life cycle of CCU technologies shows different CO₂ sources and possible scenarios of use:

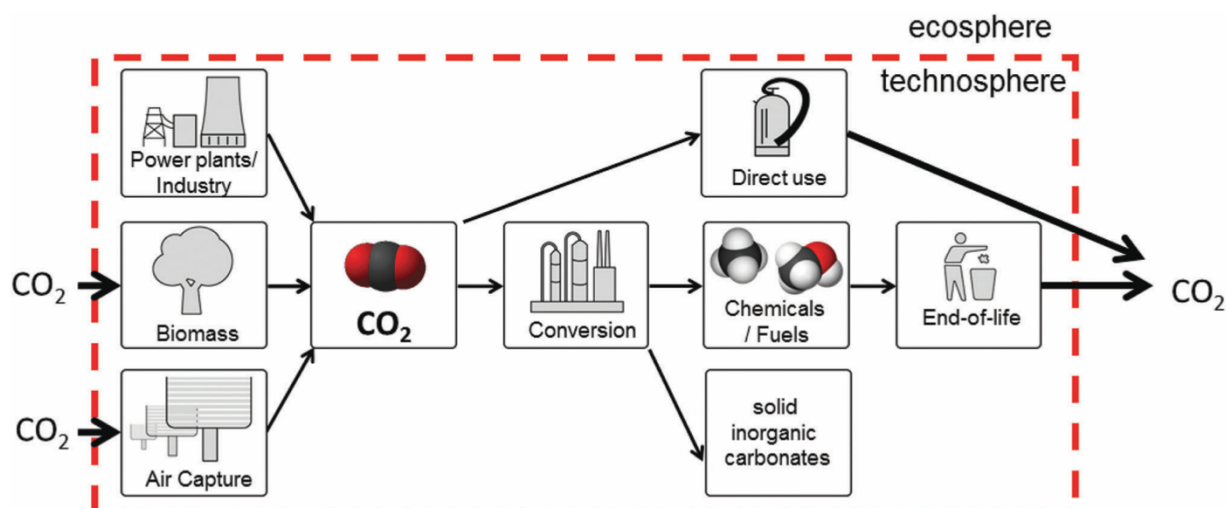


Figure 1.12 Life-cycle of carbon capture and utilization ⁹

The different roles that the CCU can play in climate change mitigation can be summarised as:

- *Carbon-negative products*: that allows storage in the form of the solid inorganic carbonate, thermodynamically more stable than CO₂, able to provide longer-term storage. However, to be considered a negative carbon product, CO₂ must be captured directly from the air or derived from the use of biomass; in the case of CO₂ capture from coal installations or industrial processes, the CCU cannot be considered as a negative carbon source over its entire life cycle.
- *Carbon-neutral products*: CCU allows a carbon-neutral scenario using atmospheric CO₂ or capturing it at the end of a life cycle of a CO₂-based product. An alternative way to obtain carbon neutral products would be the mineralisation of CO₂-based fossils.
- *Carbon-Reducing products*: in scenarios where neutral carbon products are not possible, CCU can be used to replace high-emission GHG products with alternatives to lower emissions.
- *The Temporary storage of carbon*: production of chemicals or fuels from CO₂ provides temporary storage of CO₂. In particular, compared to the fuels obtained, which provide short-term storage pending their use for energy purposes, chemicals can constitute relatively long-term storage, as in the case of polymers used for insulation in buildings.

Typically, CCU is at odds with CCS and identified as an alternative route, since both technologies involve a CO₂ capture step and have the same goal of mitigating climate change. However, the two approaches can be seen as complementary rather than conflicting. While CCS tackles the problem at the end of a process's life cycle, CCU tackles it at the beginning, focusing on raw materials and providing a sustainable carbon source. So, the two approaches can be integrated, adding a capture step at the end of the life cycle of a process, already treated by the CCU, that presents CO₂ emissions. Consequently, it is necessary to address the two approaches separately ⁹.

1.6 CO₂ transport and geological storage

Geological capture and storage provide an option to avoid CO₂ emissions into the atmosphere, capturing CO₂ from an important source (power plants or industrial processes), transporting and injecting it into a suitable rock formation ⁴.

The transport of CO₂ can take place through pipelines, ships, rail or roads. The choice of transport used is made based on of the amount of CO₂ to be transported and the distance to be travelled. Pipeline transport is the most widely used, as it is cheaper. However, for long distances (greater than 1000 km) shipping could be cheaper. As far as road transport is concerned, it is only feasible for small-scale journeys and specific applications ¹⁸.

To be transported by pipeline, CO₂ needs to be compressed to supercritical fluid conditions or the liquid state. The condition of supercritical fluid is the most efficient stage for transportation by pipelines, however, it is not possible to maintain the fluid at conditions above its critical point (31.1 °C and 74 bar) for all situations. Therefore, management of pressure drops is necessary in order to maintain the conditions above the vapour-liquid equilibrium and ensure a flow of CO₂ mono-phase. In this sense, the operating pressures of the pipelines are in the range of 85-210 bar¹⁸, so that CO₂ is in the liquid state for a wide range of temperatures.

For the management of pressure drops over long distances, pumping stations are distributed at regular intervals. For short distances, such stations can be avoided by increasing pressure at the pipeline inlet, while increasing energy expenditure for compression¹⁸.

As far as ship transport is concerned, it is more efficient to transport CO₂ as a cryogenic liquid, at 6.5 bar and -51.2 °C. Such transport provides greater flexibility compared to pipelines, being able to transport CO₂ in much smaller volumes than the project ones, thus being able to collect CO₂ from more than one production site, and ensuring greater adaptation to fluctuations in production rates¹⁸.

While the capture of CO₂ is the phase of the CCS process characterized by higher expenses, both in economic and energy terms, the phase of storage of CO₂ is the phase of great uncertainty. This uncertainty is linked to the quantification of storage potential and verification of the traceability and monitoring of injected CO₂, as well as the presence of several engineering challenges to ensure that CO₂ remains underground for hundreds or thousands of years¹⁸.

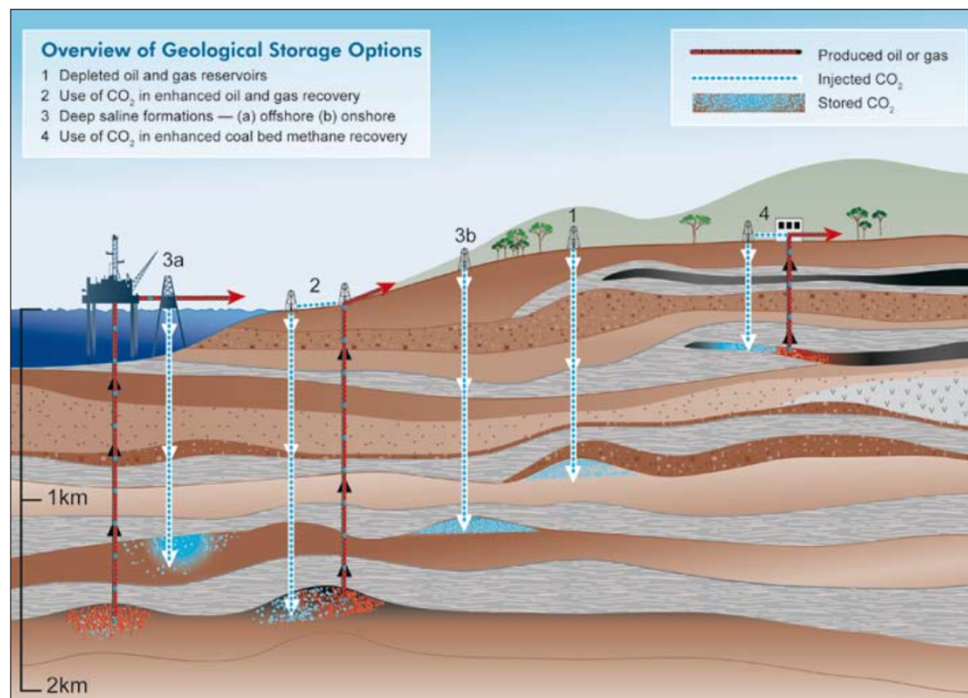


Figure 1.13 Methods for storage of CO₂ in underground geological formations⁴

CO₂ is injected at high pressures deep underground, and the main storage sites are salt aquifers, depleted oil and gas fields, and deep coal deposits. Most assessments of storage capacity identify salt aquifers as the site with the greatest storage potential, while oil and gas fields offer the economic incentive for additional hydrocarbon recovery by injection of CO₂.

The injection of CO₂ can be considered as an already well-developed technology for the oil industry, where it is exploited to improve the recovery of hydrocarbons, with many projects around the world. The most publicized example is in Sleipner, a Norwegian offshore site in the North Sea, where since 1996, to avoid the payment of the carbon tax, is injected about one Mt per year of CO₂ separated from the condensed hydrocarbon produced ¹⁸.

The storage of CO₂ in deep saline formations typically takes place at depths greater than 800 m, where the pressures and temperatures exerted lead to a liquid or the supercritical state of CO₂. Under such conditions, the CO₂ density will vary between 50 and 80% of the water density, with a consequent upward movement of the CO₂. Once injected, the retained CO₂ fraction will depend on a combination of physical and geochemical capture mechanisms. The physical entrapment avoids the release of CO₂ towards the surface, and the need for the presence of a well-sealed cover rock, called *caprock*. A further physical entrapment is given by the capillary forces that hold the CO₂ inside the porous spaces of the rocks ⁴.

However, in many cases, one or more sides of the rock formation allow the release of CO₂ laterally, below cap rock. In such cases, additional catch mechanisms are necessary to ensure long-term storage. Geochemical capture mechanisms occur as a result of a reaction between the injected CO₂ and the fluids already present within the rock formation, the so-called *in situ fluids*. Once injected, the CO₂ dissolves in the water in situ, in a time scale of hundreds of years, thus obtaining water charged with CO₂ that increases its density and sinks the fluid downwards. Subsequently, from the reactions between the dissolved CO₂ and the minerals of rock, they come to create ionic species such to convert a fraction of the injected CO₂ in minerals of solid carbon, in a process of the arc of millions of years. Finally, there is a further method of entrapment that occurs following the adsorption of CO₂ on coal or shale of organic substances in place of other gases, such as methane. In these cases, the CO₂ will remain trapped until the pressure and temperature conditions remain unperturbed ⁴.

Critical factors in geological storage are related to the identification of injection potential, the monitoring of injected CO₂ and possible losses. The quickest loss situations, including the most likely to occur in case of malfunctioning of wells, present obvious injection problems, and can therefore be identified and resolved relatively quickly. While, in case of lower infiltration, for example through unforeseen permeable faults, they can cause local damage in the terrestrial or marine environment. Even for low loss rates (in the order of 0.1% of the annual storage volume) such infiltrations can lead to increases in atmospheric CO₂ concentration ¹⁵.

1.7 Current status of CCS development

As can be seen from the previous paragraphs, the CCS will play an important role in meeting the objectives set by the IPCC and COP 21. Linked to the various stages of capture, transport and storage, there are several developing technologies. Typically, such technological development follows a series of steps of scale-up: (i) bench or laboratory scale, (ii) pilot-scale, (iii) demonstration scale, and finally (iv) commercial-scale ⁹.

Figure 1.11 summarises the current state of development of the different CCS technologies, based on a *Technology Readiness Level* (TRL) scale. The TRL traces, in fact, the state of the different technologies and their progress in the different stages of research and development (R&D). Based on this scale, there is a grouping of the different technologies between the development phases TRL 3, TRL 6 and TR 7. In particular, the progression of technology beyond TR 3 requires additional funds for research, while in order to overcome TRL 6 and TRL 7, substantial investment and/or commercial interests are required ⁹.

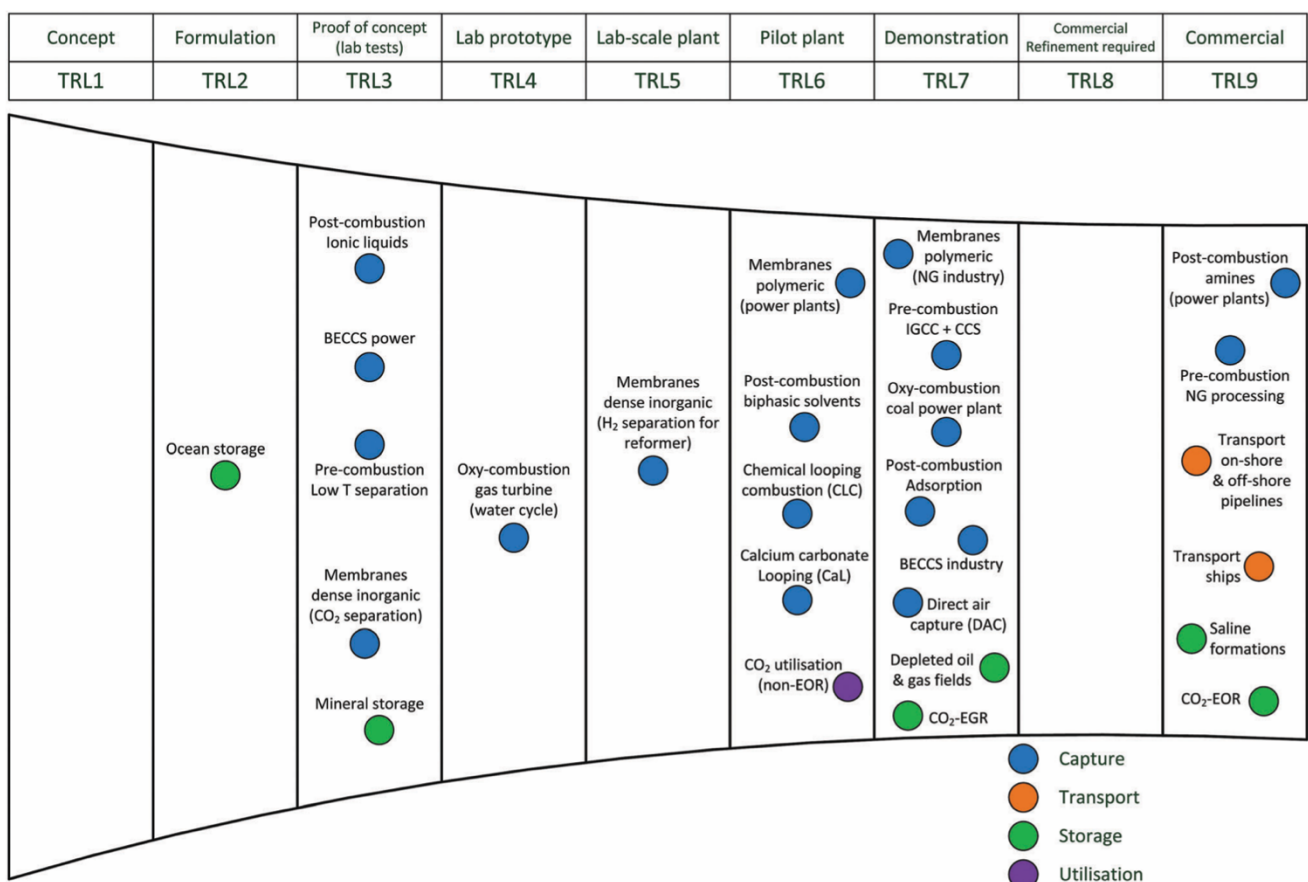


Figure 1.14 Current progress of Carbon Capture, Storage and Utilization, in terms of TRL. BECCS: bioenergy con CCS; IGCC: integrated gasification combined cycle; EGR: enhanced gas recovery; EOR: enhanced oil recovery; NG: natural gas ⁹

- **CO₂ capture**

The post-combustion capture of CO₂ by chemical absorption is considered a mature technology, exploited on a commercial scale structure, such as the coal-fired power plants Boundary Dam and Petra Nova ¹⁹, and therefore considered on a development phase TRL 9.

Recent developments in polymer membrane studies have allowed this technology to reach the demonstration-scale TRL 7, which also includes oxyfuel combustion, a technology that could reach the commercial-scale soon. In contrast, the CCS applied to combined-cycle plants presented some difficulties in development, leading also to the suspension of projects initiated, such as the IGCCS of Kemper Country ²⁰.

- **CO₂ transport**

CO₂ transport technologies are well established, with more than 6500 km of CO₂ pipelines worldwide (both on-shore and off-shore), the majority of which are linked to the recovery of hydrocarbons (EOR) operations in the United States. Ship transport is also relatively mature, and as these technologies are currently used in commercial applications, they all have a TRL of 9 ⁹.

- **CO₂ storage**

Many commercial-scale CCS projects already use EOR technology to improve oil recovery by injection of CO₂. There is, therefore, a solid base of experience and knowledge on the subject, which led the CO₂-EOR technology to a TRL of 9. Similarly, the storage of CO₂ in salt formations has reached the commercial scale, including sites such as Sleipner CO₂ Storage, Snøhvit CO₂ Storage and Quest (on-shore and off-shore). In contrast, the storage of CO₂ from EGR (enhanced gas recovery) and storage in exhausted oil and gas fields, both remain at a demonstrative scale (TRL 7). Ocean storage and geochemical storage are in the early stages of development ⁹.

- **CO₂ utilization**

Several structures use CO₂ for various applications. Such processes present a TRL of 9 being mature and commercially available technologies. Most of them in the food industry and some in chemical production. In Saga City, Japan, CO₂ captured from the incineration of solid waste is used for growing crops and algae. The necessary CO₂ is obtained mainly from industrial processes, and only in some cases from CO₂ capture processes from the combustion gases of the plants ⁹.

- **Commercial-scale CCS projects**

The implementation of large-scale projects has been slow; there are currently 51 large-scale CCS plants globally, of which 19 are in operation, four under construction and 28 at various development stages with an estimated combined capture capacity of 96 million tonnes of CO₂ per year ²¹.

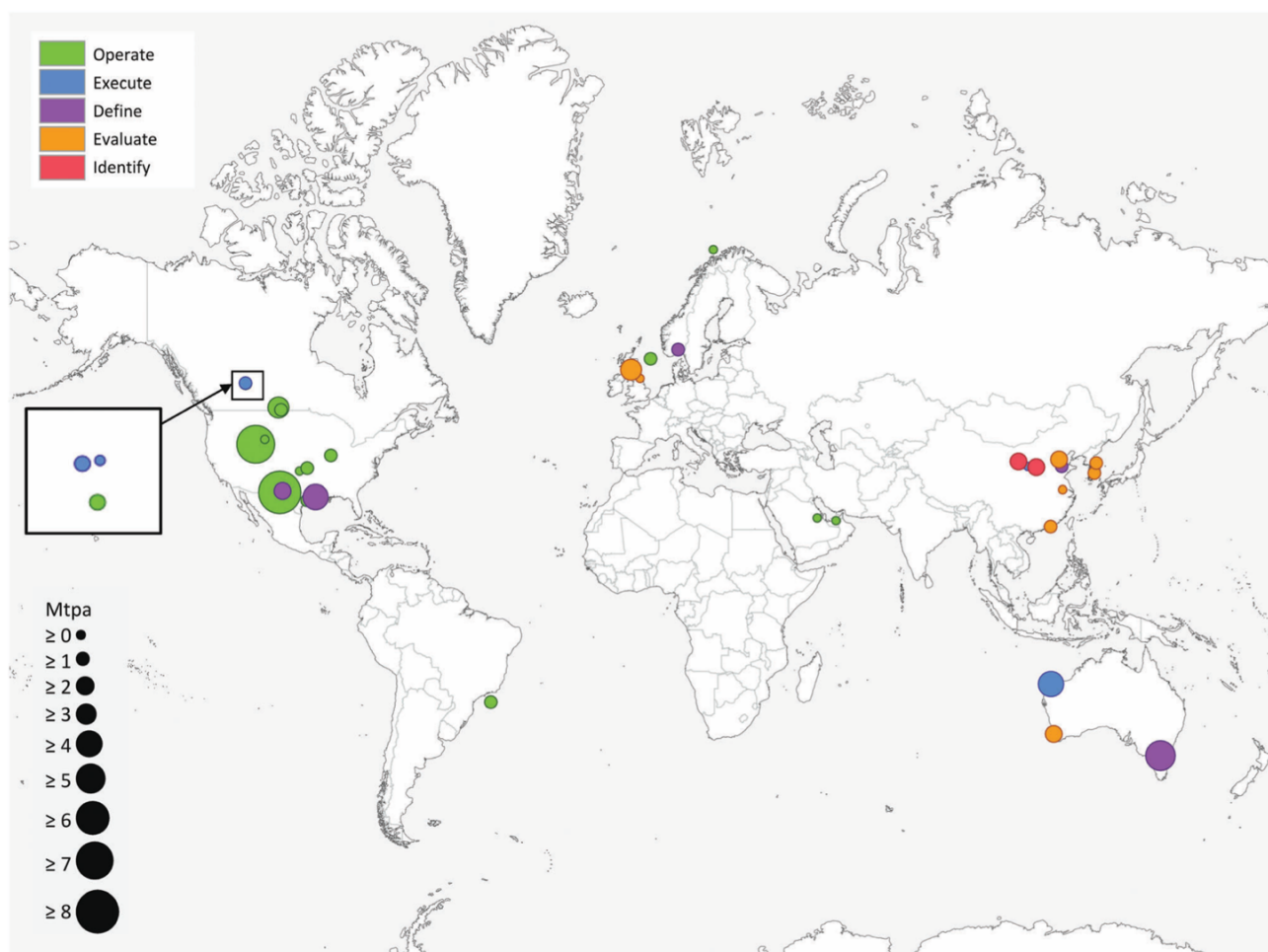


Figure 1.15 Large-scale CCS projects for the world. The size of the circles is proportional to the CO₂ capture capacity of the project to the colour indicates the life-cycle of the project⁹

As shown in *Figure 1.12*, most commercial-scale CCS projects are located in the United States. In terms of "lifecycle" of the project (identify, evaluate, define, execute and operate), the US also present the majority of projects in operation. In addition, projects in the US have the largest CO₂ capture capacity compared to projects in the rest of the world: Century Plant captures 8.4 Mtco₂ per year, while Shute Creek Gas Processing Facility captures 7 Mtco₂ per year. Although China has the second-largest number of projects, only one of them is in the implementation phase (Yanchang Integrated CCS Demonstration), and most are still in the early stages of development. The CO₂ capture capacity of projects in China varies between 0.4-2 Mtco₂ per year. Europe follows with the third-largest number of projects on a commercial scale, with two operational projects in Norway: the Sleipner CO₂ Storage project captures 1 Mtco₂ per year and the Snøhvit CO₂ Storage Project 0.7 Mtco₂ per year. Of the five projects in Canada, three are operational: Great Plains Synfuel Plant and Weyburn-Midale Project (3 Mtco₂ per year), Boundary Dam CCS Project (1 Mtco₂ per year) and Quest (about 1 Mtco₂ per year). There are also CCS projects operating in Brazil, Saudi Arabia and the United Arab Emirates, with a CO₂ capture capacity ranging from 0.8-1 Mtco₂ per year⁹.

1.8 The case for post-combustion

Due to population growth and economic development, energy needs in recent years have been growing steadily, particularly in countries such as China, South Africa and Brazil, where there is an abundance of fossil fuels that allow the production of large-scale energy at low cost. This means more investment in conventional power plants, which have a lifetime of decades and will have a significant impact on future CO₂ emissions ²².

In fact, in conventional power plants, fossil fuel is burned with an excess of air resulting in the emission of flue gas, rich in CO₂ and various pollutants into the atmosphere. Emission reductions in such installations can be achieved by post-combustion CO₂ capture (PCC). PCC has the advantage of not requiring major technical changes to existing plants, but simple additions and interfaces to specific areas, in particular:

- Integration with flue gas path
- Supply of electricity to pumps and fans
- Interfacing with the central control system
- Integration with the power plant's steam cycle to provide the heat needed for the capture process, if not available separately.

The required modifications to the plant can be achieved with standard engineering techniques, but in some cases, there may be physical limitations to the implementation. Therefore, the integration of PCC systems is not possible in every power plant. In addition to technical and economic limitations, access to a potential CO₂ storage site could also limit the use of such systems ²².

1.9 Amine-based processes for post-combustion CO₂ capture

The conventional post-combustion separation process is based on the use of an aqueous solution of monoethanolamine (MEA) as an absorptive species. In this process, the combustible gases come into contact with the absorbing liquid inside an absorption column, where the CO₂ is absorbed by reacting with the solvent. The CO₂ is then released by heating the rich solvent. The capture process is selective, as only acidic gases react ²².

Research activities initially focused on the study of the uptake process of reactive amines, and in recent decades the range of amines has been expanded to compounds such as piperazine, amino-methyl propanol, amino-ethyl-amino-ethanol, aminomethyl-propane-diol, diethyl-amino-ethanol and

various mixtures. Besides, interest has been renewed for absorbents based on carbon and ammonia solutions, as viable alternatives to amines, which are generally subject to degradation. Alternative separation methods based on solid adsorbents, membranes and cryogenics are also subject to active research. However, although they may offer advantages in terms of energy efficiency and cost, they have yet to be demonstrated on a pilot scale and therefore cannot be considered a viable alternative to liquid solvents ²².

Historically, amine-based liquid absorption processes have been widely applied in acid gas (CO₂, H₂S) treatments of natural gas and with industrial gas flows. This provided the technical and scientific basis for extending this operation to the treatment of flue gas. However, there are several significant differences in the conditions for treating acidic gases in PCC processes, leading some challenges to overcome:

- Large volumetric flow rates of flue gas require larger equipment and consequently higher investment costs.
- The low partial pressure of CO₂ in combustion gases will result in higher energy expenditure for separation.
- The constant presence of oxygen in the supply gas will result in increased oxidative degradation by organic capture species such as amines ²².

1.10 Objective of my thesis

In the following chapter, the role of the CCS in achieving the stringent objectives of COP 21 on energy transition was analysed. The main carbon capture technologies have been presented, describing the key principles. In addition, a look at the different methods of transport and storage of CO₂ captured, in the different geological sites used. Finally, the current state of the various CO₂ capture and sequestration technologies was discussed, differentiating between those already on the market and those in the developing state.

Chapter 2 will address the issue of post-combustion capture by liquid solvents. Analyzing, in particular, the mechanisms of physical and chemical absorption, and the description of the capture and desorption process. Advanced technologies will also be illustrated, to improve absorption and regeneration performance, and reduce energy consumption. The conventional solvents will be analyzed, describing the properties that influence their energy performance, focusing on the problems of managing these solvents.

In the next chapter, liquid ions will be treated as possible substitute solvents for carbon capture. The properties and advantages of conventional liquid solvents will be described. The reaction mechanisms for which CO₂ capture is possible at competitive levels for trade in these substances will be explained. Focusing in particular on ILs of organic origin, characterized by a high biodegradability and low or zero toxicity.

Chapters 4 and 5 present the experimental methods and results of my work. In particular, in chapter 4 there is a description of the bench used to carry out CO₂ capture tests by two different solvents: a 30% wt/wt aqueous solution of MEA, and an IL of organic nature based on choline. In addition, the operating conditions of the different tests are reported.

The thesis aims to evaluate the reliability of the bench by comparing the results of the absorption tests by the aqueous solution of MEA, with the literature. In addition, the absorption performance of the IL will be evaluated, verifying that the experimental results reach the theoretical load capacity levels of this solvent. In addition, we want to verify for which conditions it is possible to obtain a complete regeneration of the material. Finally, I want to compare the performance of the two solvents highlighting the advantages of using IL.

Chapter II

The Post-Combustion Capture by liquid solvents

2.1 Introduction to PCC

CCS technologies consist of the capture, compression, transport, and storage of CO₂. There is a further path in which the CO₂ produced is used (CCU), and therefore not stored but exploited to produce chemical species or fuels usable later for a useful effect. In the case of post-combustion capture, CO₂ is separated from the flue gas, consisting mainly of N₂, H₂O, O₂ and minor constituents, such as NO_x and SO_x, before they are expelled into the atmosphere. As described in the previous chapter, there are alternative approaches to CO₂ capture (pre-combustion capture and oxyfuel combustion), but post-combustion capture is the most mature and already widely available technology on the market ²³.

For removal of CO₂ from combustion fumes, physical separation based on a diffusion process or difference of boiling points may be applied, however, such processes are typically slow. The conventional process of PCC, based on an aqueous solution of amine, exploits a selective chemical absorption that affects only acidic gases, thus exploiting the different nature of CO₂ from the remaining gases present in the mixture. CO₂ can react with water to form carbonic acid, H₂CO₃, and that acid reacts further with the bases in proton exchange reactions to produce non-volatile bicarbonate, HCO₃⁻, and potentially carbonate ions, CO₃²⁻. In this way, the bicarbonate is trapped in the basic aqueous solution, while the remaining gases of the mixture do not give rise to any reaction. Although SO_x may be present within the combustible gas mixture, acidic gases that may react with water, only CO₂ can react with the amines in solution, which gives to the aqueous amines a CO₂ absorption capacity ²³.

However, the production of the chemical species necessary for absorption leads to higher CO₂ production than can be captured and requires significant energy expenditure; therefore, this process must be reversible, being able to exploit in this way the absorbing species in a continuous cycle of absorption and desorption. This cyclic process is based on a temperature variation: CO₂ is absorbed into an aqueous amine solution at a relatively low temperature, so it has a high affinity with CO₂. The rich solution is then brought to high temperatures to shift the chemical equilibrium and reduce affinity with CO₂, thus allowing the regeneration of the absorbing species and the separation of the previously captured CO₂ ²³.

A schematic representation of a PCC installation is given in *Figure 2.1*:

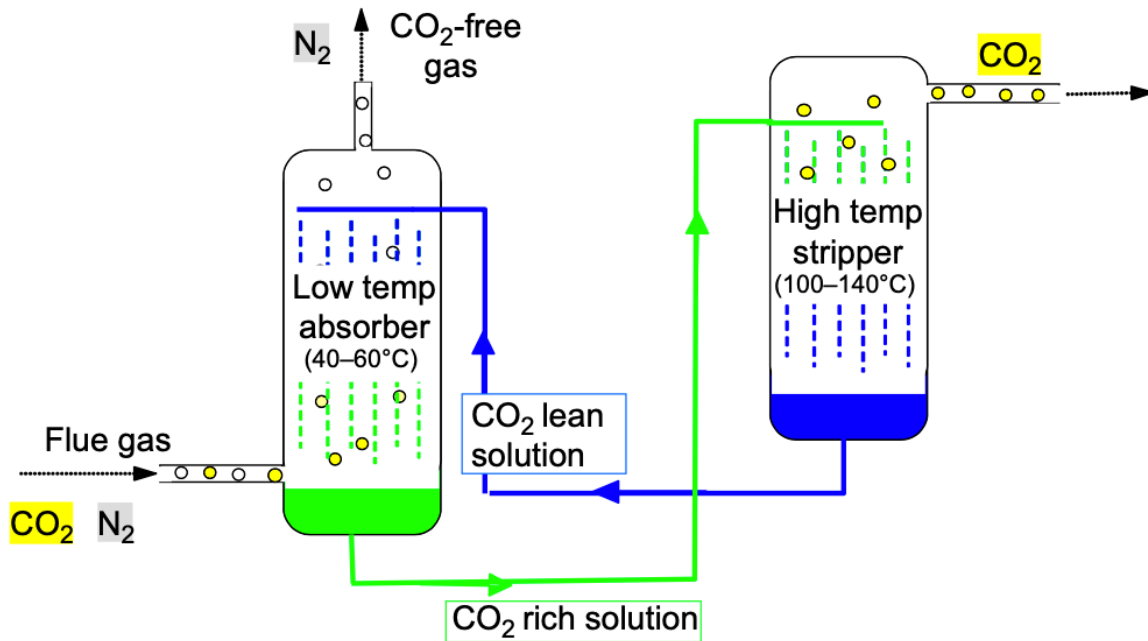


Figure 2.3 Schematic diagram of the amine-based PCC plant ²³

The mixture of CO₂-containing gas and the absorbent comes into contact within a packed column, that is, a column filled with grossly porous packaging material. The fresh absorbent is inserted into the upper part of the column and flows downwards by gravity along the solid surface of the packaging material. The flue gasses are introduced from the bottom of the column and pumped upwards. This is a typical counter-current process that generates a large contact surface between the gases and the liquid. As the absorber moves along the column it absorbs increasing amounts of CO₂, until it reaches saturation. Once the absorbent reaches the base of the column, it is collected, pumped into the stripping column, and heated. The stripping column is quite similar to the absorption column, and again, the CO₂-rich absorbent is introduced from the top. For conventional processes, steam is produced at the base of the stripping column, used both to transport heat along the column and to dilute the CO₂ released. The absorbent flowing downwards releases CO₂, which flows upwards along with the steam produced at the bottom of the column. Steam dilutes CO₂ and releases heat by condensation. Therefore, this process allows obtaining free combustion gases of CO₂ at the exit of the absorber, and the production of almost pure CO₂ at the exit of the stripping column ²³.

The separation of CO₂ from a gas mixture, using reactive chemical absorption, is based on a combination of physical and chemical processes. These processes occur as a result of the direct counter between the liquid and gaseous phases and are favoured by providing or removing heat.

At the interface between the liquid and the gaseous phase, there is a continuous migration of molecules between one phase and another: the gaseous molecules dissolve in the liquid, and the liquid evaporates in the gaseous phase. *Figure 2.2* shows the absorption of CO₂ gas by a liquid:

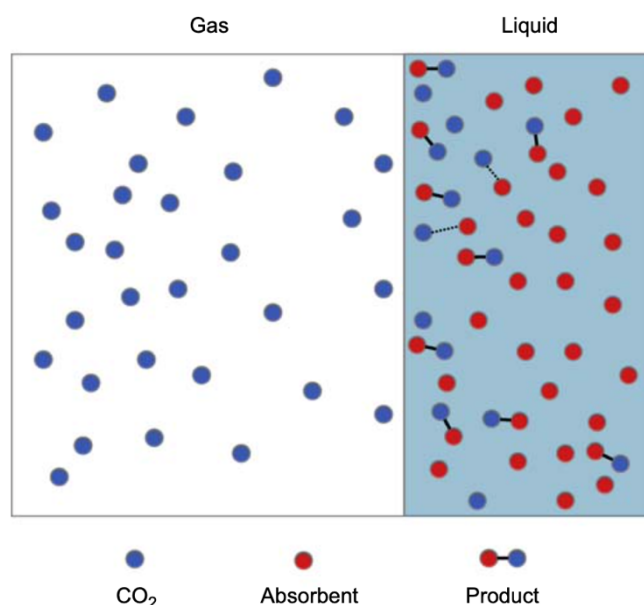


Figure 2.4 Graphical representation of gaseous CO₂ passing through the gas-liquid interface and undergoing chemical reactions with the absorbent ²³

The gaseous CO₂ at the interface dissolves within the liquid phase, in this way, coming into contact with a molecule of the absorbing species, reacts chemically to give rise to a distinct chemical product. This reduces the concentration of dissolved CO₂ in the liquid phase and encourages more migration of gaseous CO₂ to the gas-liquid interface. The product of the reactions is then free to migrate into the liquid phase. From this point of view, the only difference between CO₂ absorption and desorption is the direction of migration from one phase to another. This migration is driven by the diffusion process, that is, a spontaneous movement of molecules from a region with a higher concentration to one with a lower concentration. This diffusive transport is influenced by the properties of the liquid (temperature, viscosity, and flow rate) and the speed and magnitude of the chemical reaction that occurs. The properties of the liquid influence the diffusion coefficient while the chemical reactions modify the concentrations of the species and consequently the concentration gradient ²³.

2.2 The physics of absorption

With the physics of absorption, we refer to the transport of matter that takes place between the different phases, and the properties that govern this movement ²³.

2.2.1 Solubility, driving force, and diffusion

Solubility defines the amount of matter that can be dissolved within another before saturation. It is important to note that, when a material dissolves, mainly does not undergo any chemical change, what changes is the environment that surrounds it. As already pointed out, the diffusion process is activated by the presence of a concentration gradient of the gas between the gaseous and liquid phases, this process continues until an equilibrium is reached between the two phases, where the liquid is saturated under gas conditions. The same concept applies to CO_{2(g)} and absorbent: when CO_{2(g)} comes into contact with the absorbent species, within the liquid phase, there is already a concentration gradient that drives the CO_{2(g)} diffusion process within the absorbent species until saturation is reached. The concentration gradient is called the *driving force* (DF), and can be quantified as follows:

$$DF = P_{CO_2} - P_{CO_2}^* \quad (2.1)$$

Where P_{CO_2} is the concentration of CO_{2(g)} defined as partial pressure (kPa) and $P_{CO_2}^*$ is the concentration of dissolved CO₂ defined as partial equilibrium pressure (kPa), or the resulting partial pressure for a certain concentration at the equilibrium of CO₂, $[CO_2]^*$ (mol/m³). the relationship between $P_{CO_2}^*$ and $[CO_2]^*$ is constant at a given temperature, and is referred to as *Henry constant*, expressed by the following equation ²⁴:

$$H_{CO_2,L} = \frac{P_{CO_2}^*}{[CO_2]^*} \quad (2.2)$$

In which $H_{CO_2,L}$ is the Henry constant for the solubility of CO₂ in liquid L.

The speed with which molecules move between the gaseous and liquid phase defines the time taken by the system to reach equilibrium. This speed is proportional to the driving force DF and the diffusion coefficient $D_{A,L}$ of the species A in the liquid L. This coefficient can be quantified by the *Wilke-Chang correlation* ²⁵, and is a function of the molecular volume of diffuse molecules and the viscosity of the liquid:

$$D_{A,L} = 7,4 \cdot \frac{(10^{-8} \cdot (\phi_L M_L))^{\frac{1}{2}} T}{\mu_L V_A^{0,6}} \quad (2.3)$$

In which ϕ_L is the binding factor of the absorber; M_L is the molecular weight of the absorber L (g/mol); T is the temperature (K); μ_L the viscosity of the absorbing liquid (mPa s); V_A the molecular volume of the species A (m³/mol).

2.2.2 Mass transfer across the gas-liquid interface

Mass transfer occurs when a gaseous phase A component passes through a gas-liquid interface, characterized by two regions of stagnant film of thickness d_G (m) and d_L (m), until it reaches the bulk of the liquid phase ²⁶, as shown the *Figure 2.3*.

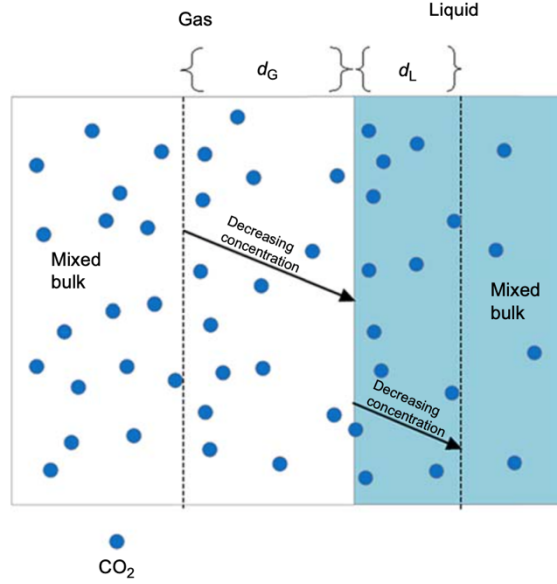


Figure 2.5 Mass transfer across the stagnant film regions of thickness d_G and d_L at the gas-liquid interface ²³

The mass transfer rate is influenced by the concentration gradient of the gaseous species (i.e., CO₂) between the two stagnant films. The mass flow of component A, N_{CO_2} (mol/m²/s), may be expressed in terms of the total mass transfer coefficient K_G (mol/m²/s/KPa) and driving force ²⁶:

$$N_{CO_2} = K_G(P_{CO_2} - P_{CO_2}^*) \quad (2.4)$$

To assess the overall mass transfer coefficient K_G , the resistance-in-series model can be used. By relating the mass transfer coefficient of the gaseous phase, k_G , and liquid phase, k_L^* ²⁷:

$$\frac{1}{K_G} = \frac{1}{k_L^*} + \frac{1}{k_G} \quad (2.5)$$

Excluding the chemical reaction occurring in the liquid phase, the two mass transfer coefficients are expressed as a function of the Henry coefficient and the diffusion coefficient ²³:

$$k_L^* = \frac{D_{CO_2,L}}{d_L H_{CO_2,L}} \quad (2.6)$$

$$k_G = \frac{D_{CO_2,G}}{d_G RT} \quad (2.7)$$

Assuming that the resistance to mass transfer in the gaseous phase is negligible (i.e., $k_G \gg k_L^*$), the total mass transfer coefficient can be assumed as $K_G \approx k_L^*$ ²⁷.

2.3 The chemistry of absorption

The overall reactions occurring during a cyclic PCC process are set out below, of which essentially instantaneous reactions, characterised by protonation balances, can be distinguished, and those occurring over a measurable period, which include reactions between CO₂ and water, hydroxide and amines ²³:



The use of the two arrows \rightleftharpoons indicates a relatively slow and observable reaction, while the double arrow \leftrightarrow indicates an instantaneous protonation equilibrium reaction; the reaction enthalpy is indicated with ΔH_i .

The complete set of reactions is shown graphically in *Figure 2.4*:

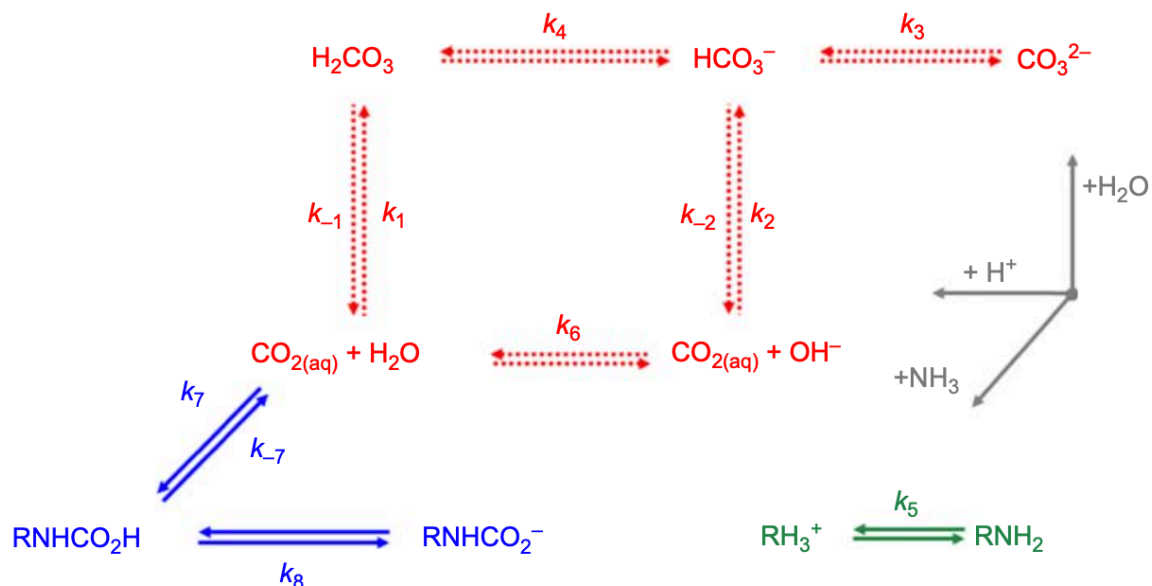


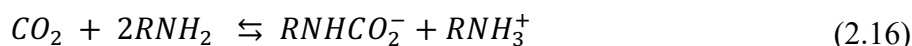
*Figure 2.6 Set of reactions*²³

All reactions between CO₂ and water/hydroxide are independent of amines. The secondary and sterically hindered amines do not form carbamate, and so their only contribution to the overall reaction is the protonation balance, K_5 . Primary and some secondary amines react directly with CO₂ to form carbamide acid, *Eq. (2.14)* which, under typical PCC operating conditions, deprotonates to carbamate, *Eq. (2.15)*. There is an additional direct reaction between bicarbonate and amines to form carbamate, but it has been omitted as a slow reaction and does not significantly contribute to the uptake kinetics, nor does it influence equilibrium positions²³.

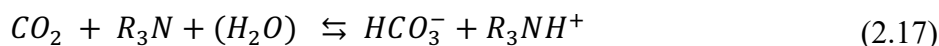
2.3.1 The kinetics of the reaction of CO₂ in aqueous amine solutions

Amines are bases, and therefore the pH of an amine solution will be basic. The K_5 protonation constant of the amines covers a wide range of values: from 8,2 per methyl diethanolamine (MDEA) to 9,04 per monoethanolamine (MEA) (all values reported at 40 °C); amines with a higher protonation constant will produce a higher pH which corresponds to a higher concentration of hydroxide. Being the rate constant for the reaction of CO₂ with hydroxide, k_2 , is much faster than the rate constant of the reaction with water, k_1 , a higher concentration of hydroxide OH⁻ will lead to a significant acceleration of absorption²³.

Reactive amines, those for which carbamate is formed, provide an additional pathway for the absorption of dissolved CO₂, the *Eq. (2.14)*. For high reactive amine concentrations (~0.5-5 mol/L or higher) this reaction dominates the others, with a rate constant that also varies over a wide range of values: from $1,29 \cdot 10^{-3}$ L/mol/s for 2-amino-2-methyl-propanol (AMP), through $8,34 \cdot 10^{-3}$ L/mol/s for MEA, to $24,3 \cdot 10^{-3}$ L/mol/s for piperazine (PZ) (AMP and MEA at 40 °C, PZ at 25 °C)²³. Reactive amines with a high protonation constant have an advantage. However, the way in which amines react with CO₂ is of greater importance. For primary amines, the overall reaction that occurs is as follows:



In which two amine molecules are needed for each absorbed CO₂ molecule: the carbamide acid initially formed deprotonates for high pH values, and the proton released is then captured by the second amine. Tertiary amines and sterically hindered amines do not present such disadvantage:



The overall reaction involves the use of a single molecule of amine per molecule of CO₂. Allowing, theoretically, to absorb twice as much CO₂ as reactive amines. However, tertiary amines and sterically hindered amines lose the rapid reaction k_7 , for this reason, all practical processes based on the use of tertiary amines include a certain amount of promoter, a rapid reactive amine added at lower concentrations²³.

A further interesting absorber is potassium carbonate, K₂CO₃, which is not amine-based and uses carbonate ion to deprotonate carbonic acid. These absorbers are very cheap and have high stability, making them particularly attractive as reagents. By analogy with tertiary amines, however, they have the disadvantage of not involving rapid reaction k_7 , and therefore need the addition of a rapid reaction amine²³.

2.3.2 Chemical kinetics and enhanced mass transfer

According to the *Eqs. (2.4) - (2.7)*, the mass transfer can be defined in terms of mass transfer coefficients and a concentration differential, expressed as driving force. In particular, the liquid-side mass transfer coefficient k_L^* was defined as a function of the diffusion coefficient of CO₂, $D_{CO_2,L}$, and the solubility or Henry coefficient, $H_{CO_2,L}$. In the presence of a chemical reaction, the mass transfer coefficient on the liquid side increases. This increase is caused by the maintenance of the driving force, due to the rapid transformation of CO₂ into reaction products. This effect is quantified by the enhanced mass transfer, k_L , function of liquid-side mass transfer, k_L^* , and enhancement factor, E ²³.

As expressed by the Eq. (2.18):

$$k_L = E \cdot k_L^* \quad (2.18)$$

When a primary or secondary amine that react rapidly with CO₂ to form carbamate via k_7 , Eq. (2.14), is present at large concentration, this dominates the reaction rate and reaction with water and hydroxide can be neglected. In this situation, it's possible to consider the reaction between amine and CO₂ as pseudo first order²³.

Based on *Penetration Theory*, when both mass transfer and chemical reaction phenomena occur, the Hatta number is used to correlate the mass transfer rate and the reaction rate²⁷:

$$Ha^2 = \frac{\delta^2/D_{CO_2}}{1/k_L} = \frac{\tau_{diffusion}}{\tau_{reaction}} \quad (2.19)$$

The physical meaning of the Hatta number can be expressed as the ratio of diffusion time to chemical reaction. A high value of Ha implies that the diffusion time is much greater than the reaction time and therefore the reaction takes place in the liquid film. Assuming that reaction between amine and CO₂ is a pseudo first order the Hatta number can be given by Eq. (2.20)²⁷:

$$Ha = \frac{\sqrt{k_7 C_L D_{CO_2,L}}}{k_L} \quad (2.20)$$

where k_7 is reaction rate constant, $D_{CO_2,L}$ is diffusivity of CO₂ in liquid, C_L is liquid concentration and k_L is liquid enhanced mass transfer coefficient.

The enhancement factor, E , in the case of pseudo first order reaction is defined by expression:

$$E = \sqrt{1 + Ha^2} \quad (2.21)$$

The enhancement factor, E , is a measure of the absorption rate within the liquid phase. It is the ratio of mass flow in the presence of a chemical reaction to mass flow in the presence of a single physical absorption. When the reaction is slow compared to the diffusion process, E is close to unity, indicating how absorption is controlled by the physical mechanism. When the chemical reaction is faster, E is greater than the unit and the mass transfer is enriched with the chemical reaction²⁷.

As far as desorption is concerned, the reverse reaction for CO₂ stripping is very fast for primary, secondary, and tertiary amine. In fact, they can be considered instantaneous. The desorption rate is limited only by diffusion, hence by time in which the CO₂ is transferred from the liquid phase to the gas phase. For the stripper, the packing is used to maximize the surface area for the CO₂ release ²³.

2.4 The cyclic capacity

Considering the absorption column, to ensure that the concentration of CO₂ in the combustible gases at the outlet of the absorber is minimal, the height of the column must be sufficiently high, and the flow of absorbent and gases must be sufficiently slow. In this way, the CO₂ concentration at the bottom of the absorption column will be maximum, since the partial pressure of CO₂ reaches the highest value ²³.

The CO₂-rich solution is then pumped into the upper part of the stripper, where it is brought to high temperatures to allow the solvent to regenerate and separate CO₂. As temperatures rise, chemical balances shift accordingly, reducing the partial pressure of CO₂ and bringing the CO₂ load to much lower levels.

The difference between the maximum loading of CO₂ at the bottom of the absorption column and the minimum at the bottom of the stripping column is called cyclic capacity: the higher the value, the greater the amount of CO₂ captured by a certain amount of absorbent ²³.

The heating of the CO₂-rich absorbent inside the stripper requires a large amount of energy, which is an important part of the operating expenses of the PCC system, so its reduction is of the utmost importance. This energy expenditure is due to three main components ²³:

- *Reaction enthalpy*: shifting the chemical equilibrium to release CO₂ at higher temperatures requires energy since these reactions are necessarily endothermic.
- *The thermal capacity of the absorbent*: the solvent must be heated to be regenerated. The smaller the amount of solvent, the lower the contribution to energy expenditure, defined by cyclical capacity.
- *Dilution vapour requirement*: throughout the stripping column, the CO₂ released must be diluted to keep its partial pressure below the partial pressure of equilibrium CO₂, thus maintaining a driving force for desorption. The higher the partial equilibrium pressure of the CO₂, the lower the demand for dilution vapour. This is regulated by the fact that the affinity of CO₂ absorption decreases with increasing temperature, which in turn is regulated by the shift in chemical equilibrium.

Of crucial importance for cyclical capacity is the overall stoichiometry of the reactions between amine and CO₂; tertiary amines are attractive from the point of view of cyclical capacity, but the slow absorption of CO₂ is too high a price to pay ²³.

A relevant factor, influenced in turn by the choice of amine, is the reaction enthalpy for amine protonation, ΔH_5 . A high value of ΔH_5 leads to lower CO₂ absorption values at high temperatures, reducing the basicity of the amine. With reference to Eq. (5) this is described by van't Hoff's equation:

$$\frac{d \ln K_5}{dT} = \frac{\Delta H_5}{RT^2} \quad (2.22)$$

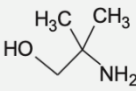
That is, the amines lose basicity as the temperature increases. The basicity of the amine determines the absorption of CO₂ in the solvent by deprotonation of the initially formed carbamic acid (or carbonic acid) to produce the carbamate ion (or bicarbonate ion). A lower basic amine at higher temperatures will absorb less.

Although this seems counter-intuitive (an increase in enthalpy reaction ΔH_5 will result in increased energy demand to shift chemical equilibrium), this additional expenditure is fully balanced by the effect of the shift in equilibrium, which has a positive effect on cyclical capacity and consequently on the decrease in dilution vapour demand ²³.

2.5 Conventional aqueous ammine and carbonate

The four classes of amine-based liquid absorbers most commonly used for CO₂ absorption/stripping are shown in *Table 2.1*:

Table 2.1 Chemistry of carbonate amines ²⁸

Class	Typical reaction	$-\Delta H_{\text{abs}}$ (kJ/mol)	Kinetics
Carbonate	$\text{CO}_3^{2-} + \text{CO}_2 + \text{H}_2\text{O} \leftrightarrow 2\text{HCO}_3^-$	40	Very slow
Tertiary amine	$\text{R}_3\text{N} + \text{CO}_2 \leftrightarrow \text{R}_3\text{NH}^+ + \text{HCO}_3^-$	60	Slow
Hindered amine	 $\text{AMP} + \text{CO}_2 \leftrightarrow \text{AMPH}^+ + \text{HCO}_3^-$	60–70	Moderate
Secondary or primary amines	$2\text{R}_2\text{NH} + \text{CO}_2 \leftrightarrow \text{R}_2\text{NHCOO}^- + \text{R}_2\text{NH}_2^+$	70–80	Fast

They differ in heat of absorption, CO₂ absorption kinetics and inherent stoichiometry. Potassium carbonate, K₂CO₃, operates isothermally at 100 °C per pressure change, as its low absorption heat does not promote regeneration by temperature variation. Tertiary amines such as methyl diethanolamine (MDEA) are used in mixtures with velocity promoters such as piperazine (PZ). Hindered amines such as aminomethyl propanol (AMP) can be used alone or in combination with speed enhancers. Primary or secondary amines, such as MEA and PZ, may be used individually or as velocity promoters for tertiary amines, hindered amines or potassium carbonate ²⁸.

Water is a key component of these amine solutions; its concentration is optimized to balance the viscosity and intrinsic capacity of CO₂. Lower viscosity increases heat exchange and mass transfer performance.

Water also provides stripping steam for solvent regeneration, allowing working at higher pressures. However, in simple stripper configurations, water reduces energy performance; disadvantage that is eliminated with the use of advanced regeneration systems such as flash stripper ²⁸.

2.6 Equivalent work

The scrubbing of amines is based on temperature variation to promote solvent regeneration. This process is optimized by working the absorber at low temperatures and the stripper at high temperatures. Typically the flue gas and the poor solvent are cooled up to 30-40 °C with cooling water or ambient air; while the high temperatures of the stripper are limited by the thermal degradation of the solvent or by the temperature that can be reached with condensation vapour or other heat sources ²⁸. The energy consumption of the adsorption/desorption process is currently considered to be still too high. In particular, the energy demand for solvent regeneration, for a basic pilot plant and considering the use of an aqueous solution at the 0,3 g/g MEA (the solvent conventionally used), is estimated at 3.6-3.8 GJ/tCO₂, for which a thermal efficiency loss is estimated at 11-15%. Approximately 70-80% of total energy demand, including the CO₂ compression stage, is considered to be due to solvent regeneration alone; for this reason, research only focused on the reduction of such energy consumption ²⁹.

The energy required for regeneration is considered an indicator of process performance but is not sufficient to classify the various capture processes. For this reason, the *equivalent work* is used in the literature to compare the total energy consumption (thermal and electrical) of the different capture processes ³⁰.

*Rochelle et al.*³¹ defined the equivalent specific work as the sum of the electrical power consumed in the processes (energy required to compress CO₂ up to 100-150 bar, and for the transport of flue and liquid gases) and the energy supplied by the condensation of steam in the reboiler Q (reboiler duty):

$$W_{eq} = 0,75 \cdot Q_{reb} \left(1 - \frac{313}{T_{reb} + 10} \right) + W_{comp} + W_{pump} \quad (2.23)$$

The effect of the reboiler's energy expenditure is then expressed as the amount of work that could reasonably be extracted from steam if it were expanded into a turbine, as a function of temperature (T_{reb}), assuming a Carnot efficiency of 75% a heat sinks at 313 K and by including a ΔT at the reboiler of 5-10 K.

2.7 CO₂ loading

The CO₂ load is a measure of the CO₂ concentration in the solution. It is defined as the ratio of CO₂ molecules to alkalinity groups. For example, MEA has one alkalinity group per molecule while piperazine has two, hence, for an MEA, PZ or MEA / PZ system, the definition of CO₂ load is expressed mathematically by equation³²:

$$CO_2 Loading = \frac{n_{CO_2}}{n_{MEA} + 2n_{PZ}} \quad (2.24)$$

In particular, rich loading can be defined as the molar ratio between CO₂ and absorbing species in the solvent flow at the outlet of the absorber, and lean loading as the molar ratio between CO₂ and absorbing species in the solvent flow at the inlet of the absorption column.

A low lean loading means a high solvent capacity to absorb CO₂, but also a lower partial pressure of CO₂ at the bottom of the stripper which involves a higher energy demand to desorbs CO₂³⁰.

Figure 2.5 shows how the chosen of lean loading can be used to minimize the equivalent work, depending on the configuration of the stripper used:

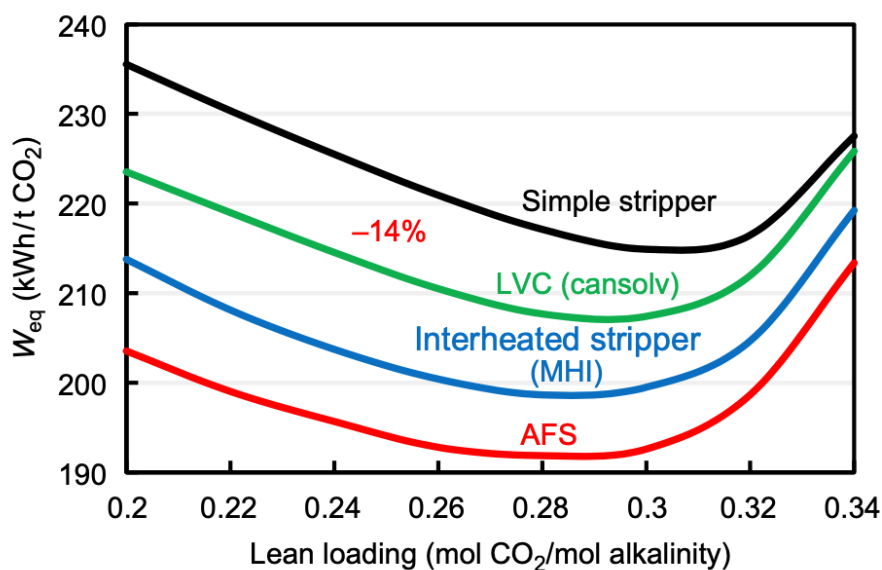


Figure 2.7 Power consumption with different stripper configurations. AFS, advanced flash stripper; LVC, lean vapour compression; MHI, Mitsubishi Heavy Industries ³⁰

Although several studies account for lean loading greater than 0,3 (mol CO₂/mol alkalinity), lower loading levels are preferred in the market to reduce the capital cost of the absorption column ³⁰.

2.8 Advanced absorption

The reactions accompanying the absorption of CO₂ by liquid solvents are exothermic and this results in a heat release that generates a temperature peak within the absorption column. High solvent temperatures limit the cyclic capacity of the solvent and reduce the driving force within the absorption column, with a consequent deterioration of the energetic performances to the stripper and greater demand of packaging area for the absorber that involves greater costs of capital. To ensure dissipation of the heat generated by CO₂ absorption, an intercooler is typically used to mitigate limitations on absorption capacity and driving force ³³.

Figure 2.7 shows the design of an in-and-out intercooling, in which the solvent is extracted from the absorption column and cooled to 40 °C in a single point. The overall temperature profile, as well as the peak point within the column, is affected by operating parameters such as the CO₂ concentration in the flue gas, the CO₂ loading and the liquid rate (gas-liquid ratio L/G), so the beneficial contribution offered by intercooling will depend on the operating parameters of the absorption column ³³.

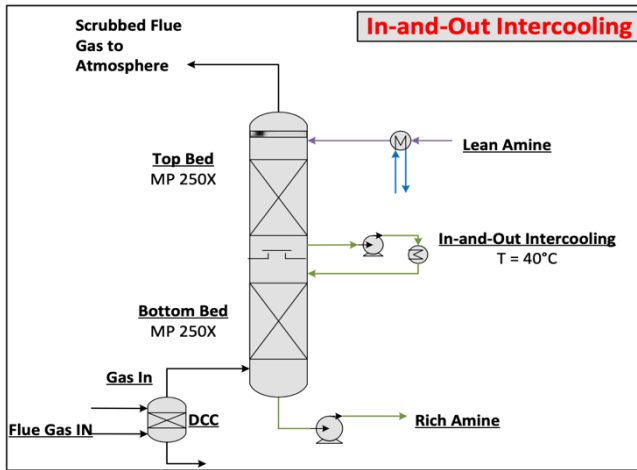


Figure 2.9 Design of an in-and-out intercooling³³

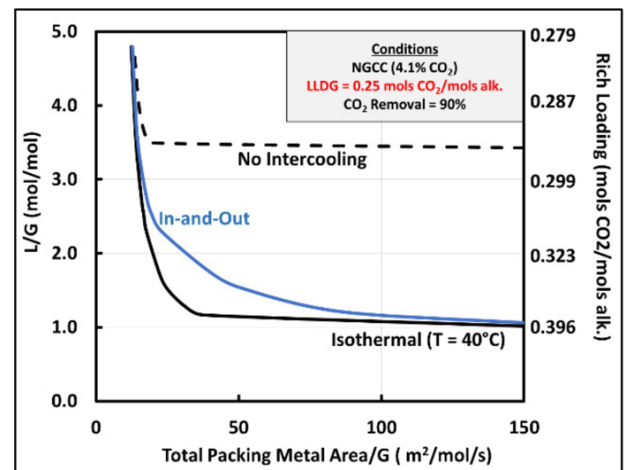


Figure 2.8 Design curves for an adiabatic absorption column (dashed curve), in-and-out intercooling (blue curve), and isothermal (black curve)³³

Each curve in Figure 2.6 represents the packing area required to reach 90% CO₂ removed for a given liquid-gas ratio (L/G). Moving between a vertical asymptotic limit, for which there are an infinite solvent rate and a minimum packaging area, and a horizontal asymptotic limit, which corresponds to an infinite packaging area and minimum solvent rate. Where the minimum liquid L_{MIN} rate is defined as the solvent rate required to achieve a specific gas composition at the inlet or outlet of the column, for a given solvent composition at the inlet (rich loading) with an infinite mass transfer surface³³.

Low L_{MIN} values result in a high cyclical solvent capacity and thus in the better overall energy performance of the process. The ratio of the minimum solvent rate L_{MIN} of the adiabatic and isothermal process provides an estimate of the potential benefit of using intercooling: a high report indicates a potentially significant improvement in the performance of the process, on the contrary, a close-to-unit report indicates a non-significant contribution.

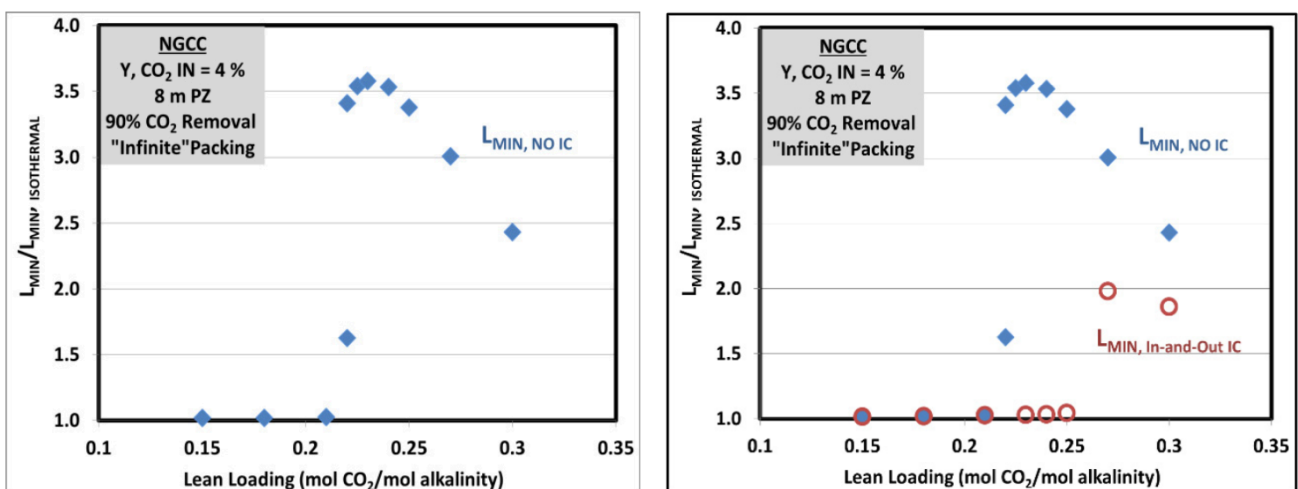


Figure 2.10 Ratio of minimum solvent rate to an adiabatic absorber (no intercooling) and an intercooler absorber³³

For intermediate values of lean loading, there are higher deviations of performance compared to ideal isothermal absorbers, so the use of an intercooler would lead to significant improvements. At extreme loading values (both lower and higher values) the ratio is approximated to the unit ³³.

Figure 2.8 shows the potential effect of intercooling on a liquid flow with 8 m PZ at 4% CO₂ input. For a critical lean loading of 0,21 (mol CO₂/equiv PZ) the minimum liquid rate of the adiabatic absorber is more than 3,5 times that of the isothermal absorber. A single intercooling stage near the center of the column reduces this effect to a factor of 2 for lean loading greater than 0.26 ²⁸.

2.9 Advanced regeneration systems

The basic configuration of the PCC post-combustion capture process is shown in Figure 2.9. The low-temperature rich solvent at the outlet from the absorber is heated by the pure solvent inside a heat exchanger and then sent to the top of the stripper. The reboiler covers the demand for sensitive heat, CO₂ desorption heat and latent vaporization heat within the stripping column. The pure solvent at high temperature at the outlet from the stripping column is sent to the heat exchanger and then further cooled to be able to return inside the absorber at a temperature of around 40 °C.

CO₂ separated from the solvent and diluted with the vapour produced escapes from the upper part of the stripper and is cooled inside a condenser, where the latent heat of the excess vapour leaving with the CO₂ is lost ³⁴.

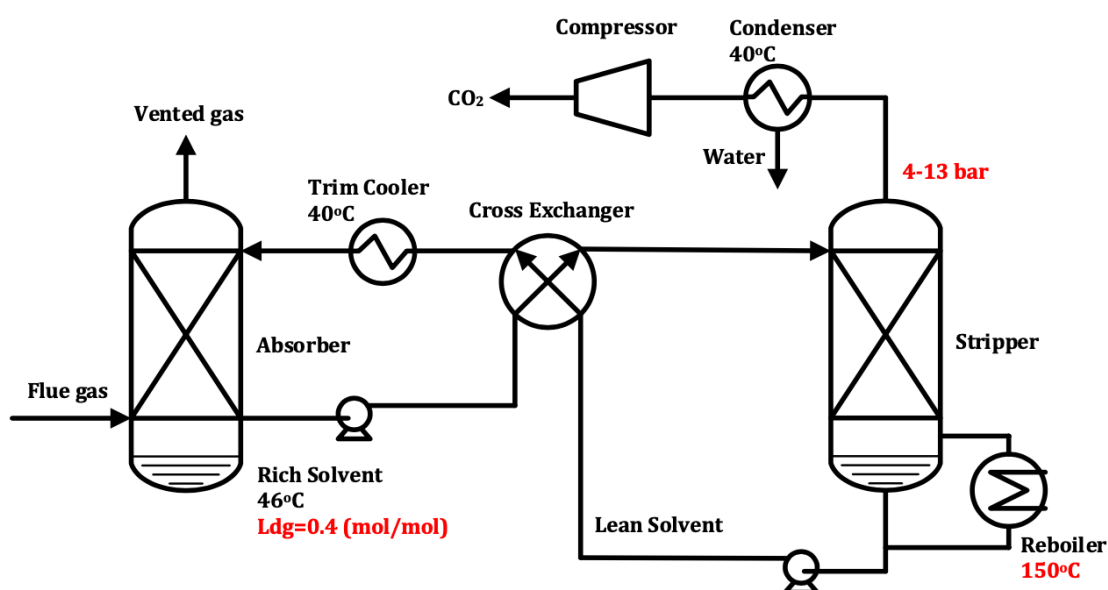


Figure 2.11 Scrubbing di ammine con simple stripper ³³

One of the reasons why the simple configuration of the stripper is inefficient is the heat loss generated by the condensation of the superheated steam that is not in any way recovered. *Figure 2.4* compares the energy performance of the three main configurations that are used to maximize heat recovery, comparing them to the simple stripper ²⁸.

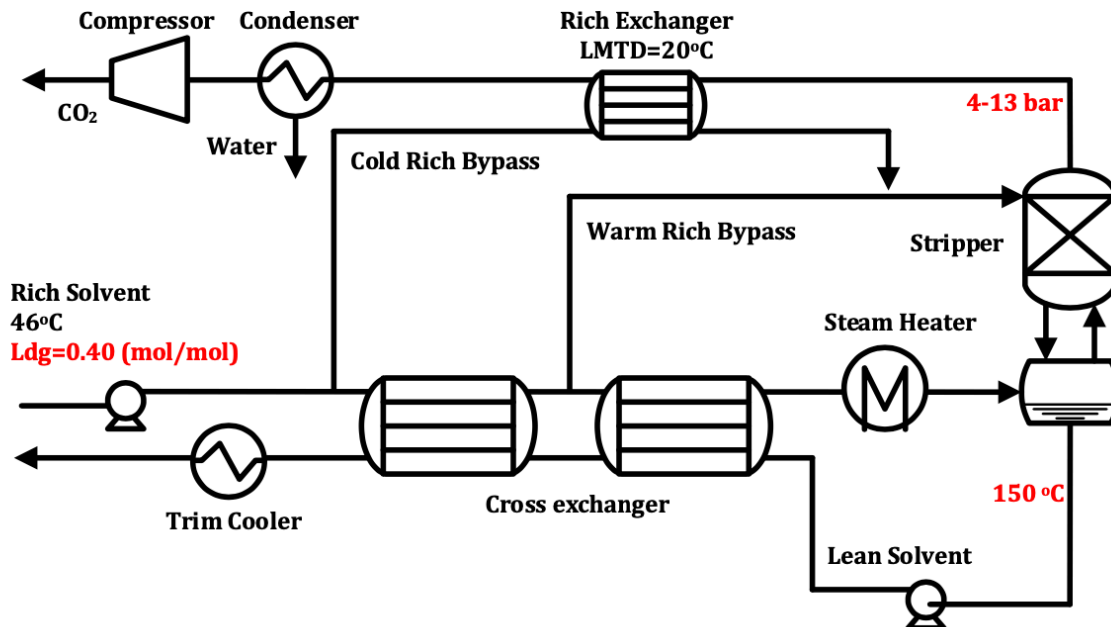


Figure 2.12 Advanced Flash Stripper AFS ²⁸

Figure 2.10 shows an *advanced flash stripper* (AFS). In this configuration, the rich solvent at the outlet from the absorption column feeds two heat exchangers in series with a convective Steam Heater connected to the bottom of the stripper. A portion of the rich solvent is preheated employing the CO₂ at high temperature at the exit from the stripping column, inside a Rich Exchanger. In this way, the latent heat of excess steam is not lost but exploited to preheat a portion of the rich solvent. The heated rich solvent is extracted between the two heat exchangers, close to its boiling point and stripper pressure, to be mixed with the preheated rich solvent and subsequently sent to the top of the stripper. The remaining rich solvent is heated by the "Steam Heater" and feeds the lower part of the stripping column. In this configuration, the reboiler is replaced by the Steam heater and a flash vessel ³⁴.

The AFS is designed to optimize the rate of cold and hot solvent to bypass the heat exchangers, so it can recover virtually the entire latent heat of the superheated steam ²⁸.

Figure 2.11 shows the configuration of the *interheated stripper*:

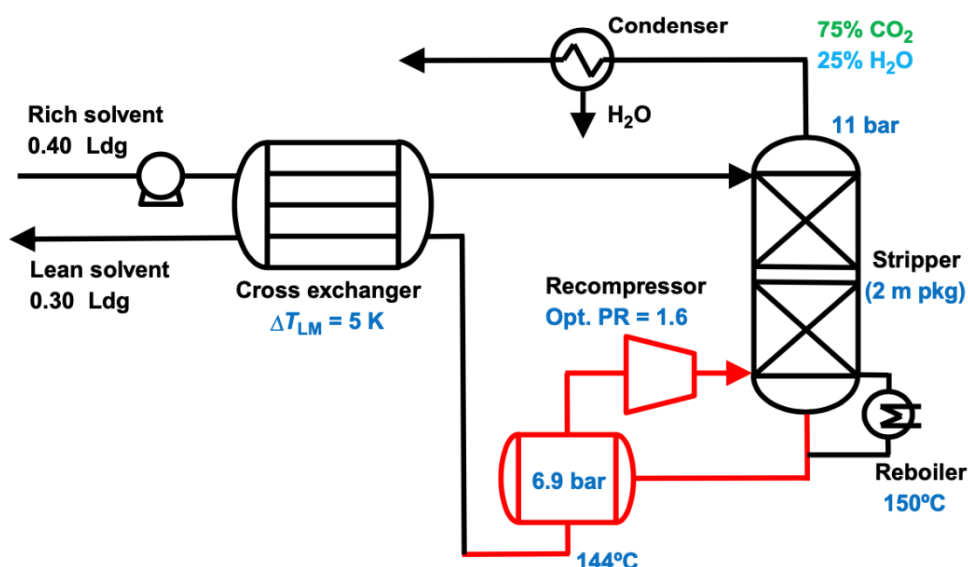


Figure 2.13 Interheated stripper, 8 m PZ²⁸

The absorbing liquid is extracted from the center of the stripper and pumped through an additional heat exchanger, where it exchanges heat with the pure high-temperature solvent at the exit from the bottom of the stripper, in series with the main heat exchanger. As with the AFS, this system recovers much of the latent heat generated within the stripper. This project has no optimized variables, so it is typically less efficient than the AFS²⁸.

Lean vapour compression (LVC) is shown in Figure 2.12:

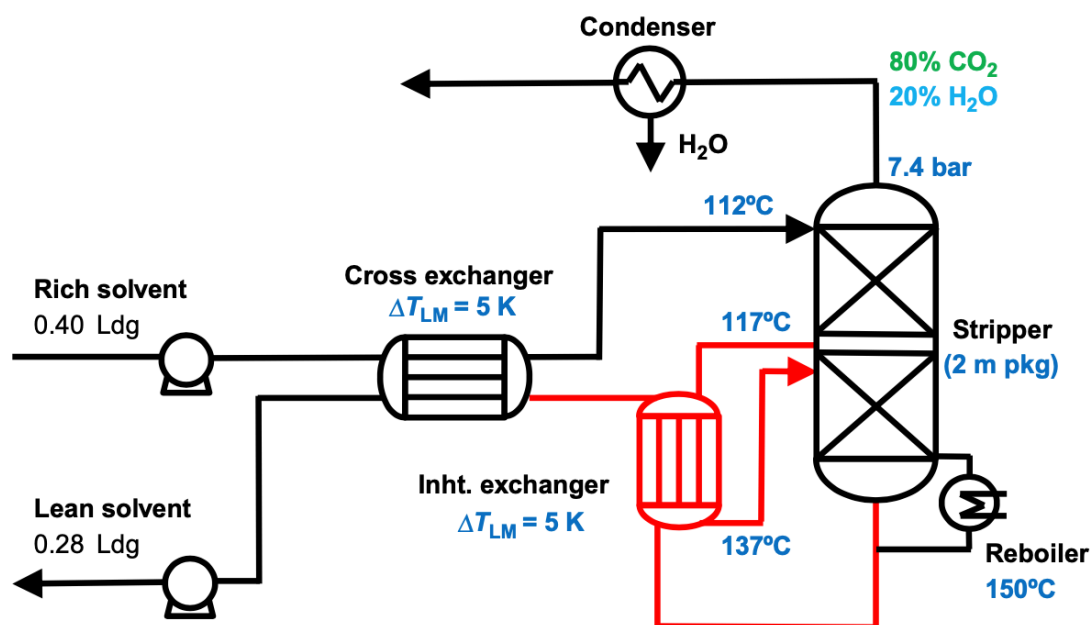


Figure 2.14 Lean vapour compression LVC²⁸

The LVC has been tested in several pilot plants, it flashes the pure solution to the outlet of the column and compresses the resulting steam and then repacks it on the bottom of the stripper. As a result of the flash, the temperature of the pure solvent is reduced, resulting in a decrease in the temperature of the rich solvent at the entrance of the stripper. This allows you to recover much of the latent heat released by steam condensation at the top of the stripper. Although this configuration involves a further compression stage, the overall effect leads to a decrease in equivalent work ²⁸.

2.10 Solvent selection for energy performance

The energy performance of a given solvent is influenced by four properties: *absorption capacity*, *absorption rate*, *absorption heat* and *thermal degradation*. Each of which is linked to a compromise between the cost of capital and the use of energy.

The CO₂ absorption capacity determines the capital cost and energy losses of the heat exchanger. The absorption rate determines the packing area demand of the absorber and the loss of work as a driving force. Heat absorption and maximum operating temperature determine the cost of capital and loss of work of compressor, reboiler and stripper ²⁸.

These properties are summarised in *Table 2.2* for several potential solvents ³⁵:

Table 2.2 Energy properties of alternative amines ³⁵

Amine	m	$k'_{g \text{ avg}} \times 10^7$	Capacity mol kg ⁻¹	$-H_{\text{abs}}$ kJ mol ⁻¹	T_{max} °C	P_{max} bar	$P_{\text{H}_2\text{O}}/P_{\text{CO}_2}$
Piperazine (PZ)	8	8.5	0.79	64	163	14.3	0.33
PZ/bis-aminoethylether	6/2	7.3	0.67	69	162	16.3	0.28
2-Methyl PZ/PZ	4/4	7.1	0.84	70	155	10.3	0.41
2-Methyl PZ	8	5.9	0.93	72	151	9.9	0.37
2-Amino-2-methyl propanol (AMP)	5	2.4	0.96	73	140	6.1	0.49
PZ/aminoethyl PZ	5/2	8.1	0.67	71	138	5.0	0.55
PZ/AMP	5/2.3	7.5	0.7	71	134	4.5	0.54
Diglycolamine (registered trademark)	10	3.6	0.38	81	132	9.1	0.25
Hydroxyethyl PZ	8	5.3	0.68	69	130	2.3	0.98
PZ/AMP	2/4	8.6	0.78	72	128	3.4	0.63
2-Piperidine ethanol	8	3.5	1.23	73	127	3.3	0.61
Monoethanolamine (MEA)	11	3.6	0.66	70	125	2.7	0.67
MEA	7	4.3	0.47	70	121	2.2	0.81
Methyldiethanolamine (MDEA)/PZ	5/5	8.3	0.99	70	120	1.8	0.92
MDEA/PZ	7/2	6.9	0.8	68	120	1.4	1.15
Kglycinate	6	3.2	0.35	69	120	1.08	1.46
Ksarconinate	6	5	0.35	54	120	0.73	2.17
MEA/PZ	7/2	7.2	0.62	80	104	0.7	1.38

2.10.1 Normalised capacity

The working capacity of the solvent influences the capital cost and the energy consumption of the heat exchanger; there is always an economic compromise between the size of the exchanger and the pinch point. For an infinitely large heat exchange surface, the effect of absorption capacity would be negligible but would involve prohibitive economic costs ²⁸.

The capacity of a solvent is reflected in the stripper's sensitive heat demand, given by *Eq. (2.25)* ¹⁸:

$$Q_{sensible} \left(\frac{kJ}{mol CO_2} \right) = \frac{C_p \Delta T}{C} \quad (2.25)$$

Where C_p is the specific heat of the solvent (kJ/kg (H₂O+amine) K), ΔT is the hot side approach temperature of the heat exchanger, and C is the solvent capacity (mol CO₂/ kg (H₂O+amine)).

A quantitative measure of the intrinsic capacity of the solvent can be obtained by assessing the difference between the equilibrium concentration of CO₂ at 40 °C and 5 kPa and the equilibrium concentration of CO₂ at 40 °C and 0,5 kPa. Values for which a sufficient driving force is obtained to provide absorption of 90% CO₂ from the flue gas ¹⁸.

However, it is necessary to weigh the intrinsic capacity for the viscosity of the solvent, as high viscosity values will reduce the heat exchange coefficient of the heat exchanger. This is reflected in the normalised capacity, $capacity/(\mu/10)^{0,25}$.

As shown in *Table 2.2*, several amine systems provide a normalized capacity greater than 7 m MEA. Hindered and tertiary amines provide a higher normalized capacity due to their intrinsic stoichiometry requiring only one mole of amine per mole of CO₂ absorbed, compared to two moles for MEA systems. Methyldiethanolamine (a tertiary amine) with piperazine and aminomethylpiperazine (an inhibited amine) with piperazine are quite competitive. Besides, increased capacity is also provided by diamines such as piperazine PZ since more amine equivalents can be loaded into the solvent before the viscosity is too high ¹⁸.

2.10.2 Rate of CO₂ absorption

Solvents with a high absorption rate require less packing area with equal CO₂ consumption, which results in lower capital costs for the process. Moreover, a high absorption rate reduces the driving force for mass transfer in the absorber and the overall irreversibility of the process ³⁵.

CO₂ is usually absorbed by a liquid solvent in a mass transfer mechanism with a fast reaction in the boundary layer of the liquid. The standard CO₂ absorption rate (k'_g , mol/m²Pa) may be expressed in terms of the driving force of the partial CO₂ pressure ³², and depends intrinsically on the properties of the solvent and the hydrodynamic gas-liquid contact:

$$k'_g = \frac{Flux}{P_{CO_2} - P_{CO_2}^*} \approx \frac{\sqrt{k_{am}[amina]D_{CO_2}}}{H_{CO_2,L}} \quad (2.26)$$

Assuming that the concentration of the amines at the boundary layer of the liquid is the same present in the bulk of the liquid phase, k'_g is approximated according to the diffusivity of CO₂ in the liquid (D_{CO_2}), the reaction rate of CO₂ with the amine (k_{am}), the concentration of the amine in the bulk of the liquid phase and the Henry constant of the solubility of CO₂ in the liquid L ($H_{CO_2,L}$) ³⁵.

Piperazine or piperazine derivatives provide the highest values of k'_g . In contrast, tertiary amines and hindered amines are generally too slow to be used individually and require velocity promoters, such as secondary or primary amines, useful to provide an acceptable CO₂ uptake rate ¹⁸.

The optimal concentration for most solvents involves a compromise between an undesirably high viscosity for a higher amine concentration and low kinetics with a lower amine.

Figure 2.13 shows this optimization for PZ:

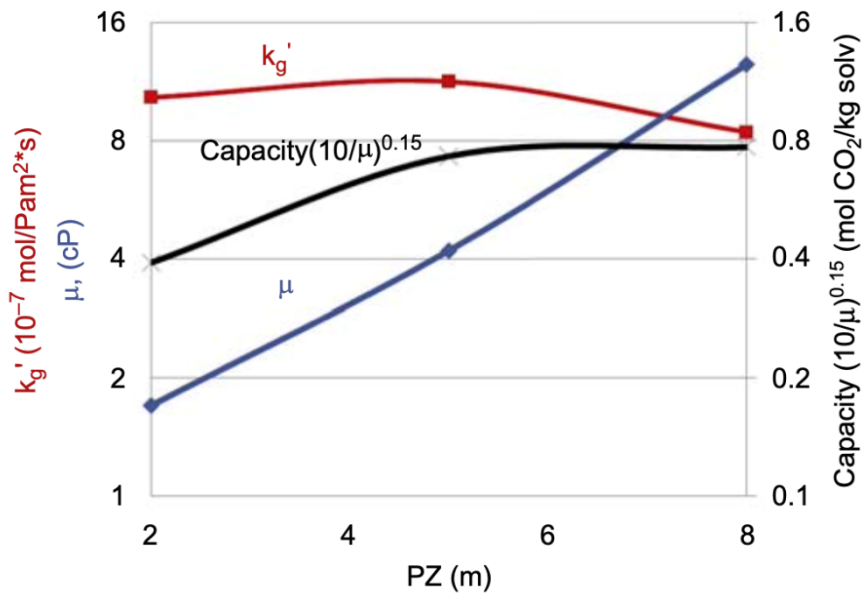


Figure 2.15 Optimal concentration of PZ to maximize energy properties at 40° C ²⁸

The normalized capacity reaches the maximum value between 5 and 8 m PZ; the absorption rate has a peak for 5 m PZ because high viscosity values also hinder the diffusion coefficient.

Therefore, it can be assumed that 5 m PZ is an optimal concentration. In the case of PZ the low concentration of amine may also help to minimize problems of solids solubility ²⁸.

2.10.3 Thermal degradation

The thermal degradation of amines to 100-150 °C limits maximum T temperatures and operating P pressures, and consequently negatively impacts the energy performance of solvent regeneration. Thermal degradation also leads to the formation of products with greater volatility than their amine counterparts, so excessive degradation must be avoided to minimise the economic loss and environmental impact of degradation products ³⁶.

Although thermal degradation is easily managed by reducing the operating temperature at the bottom of the stripper, high temperatures, for conventional processes based on amine, favour the reduction of the overall energy demand for regeneration. Moreover, high pressures minimize the size, and cost of capital, stripper and compressor. Therefore, the stripper is expected to be optimized in such a way as to operate under conditions where energy performance is maximized, limiting economic loss and secondary environmental impact ³⁶.

Davis et al. ³⁷ estimated that the optimum temperature for 7 m MEA should be around 132 °C with an operating pressure of 3 bar. However, most MEA-based processes have been designed to operate at a maximum temperature of 120 °C.

2.10.4 Heat of absorption

The scrubbing of amines is a process that is based on the regeneration of the solvent by temperature variation, so a greater heat absorption allows to maximize the heat exchange by reducing energy consumption. However, the regeneration process depends on the temperature of the desorption column, which is limited by the thermal degradation of the solvent.

A quantitative measure of the effect of absorption heat and T_{max} is the reboiler pressure estimate for a representative pure solvent, assuming that it is saturated at 40 °C and 0,5 kPa CO₂, expressed as ¹⁸:

$$P_{max} = P_{H_2O} + P_{CO_2} \quad (2.27)$$

Where P_{H_2O} is the water vapour pressure at T_{max} and P_{CO₂} is given by Eq. (2.28):

$$P_{CO_2} = 0,5 \text{ kPa} \cdot \exp\left(\frac{\Delta H_{abs}}{R}\right)\left(\frac{1}{T_{max}} - \frac{1}{313}\right) \quad (2.28)$$

As revised by *Rochelle et al.*³⁶, piperazine or its derivatives have been identified as solvents with the maximum value of T_{max} , resulting in higher values of P_{max} . Solvents with low absorption heat (<60 kJ mol⁻¹) will not be competitive. These include systems based on sodium or potassium carbonate.

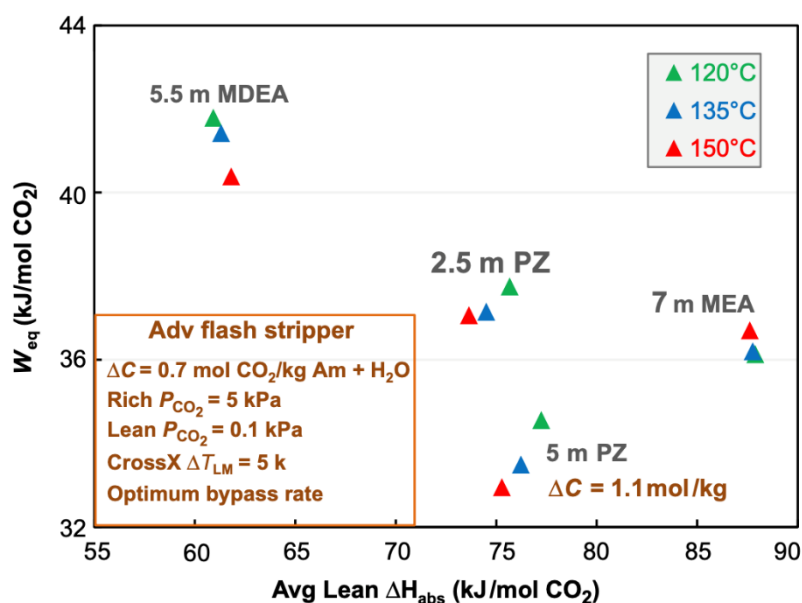


Figure 2.16 A large absorption heat reduce the equivalent work. MDEA, methyl diethanolamine; MEA, monoethanolamine; PZ, piperazine²⁸

Figure 2.14 shows the effect of absorption heat on the equivalent work in the AFS modelled by *Lin e Rochelle*³⁴, demonstrating how a greater heat of absorption allows reducing the total energy consumption²⁸:

2.11 Solvent management

Additional solvent properties may result in the loss of active components and consequent secondary environmental impact. Oxidative degradation is a problem that concerns only the treatment of fumes. The formation and decomposition of nitrosamine are linked to reactions occurring in the presence of impurities in the flue gas. The volatility of the amine and its loss as aerosols represent the most significant secondary environmental impact²⁸.

2.11.1 Oxidative degradation

Oxidative degradation of the amine is a common problem of scrubbing processes in capturing CO₂ from oxygen-containing flue gas. Although many studies have been carried out on this subject in recent decades, the mechanism by which this oxidation occurs is not yet clear²⁸.

The sensitivity of MEA, and other amines, to oxidation, has been under study since 1950. The oxidation rate is a function of temperature, CO₂ loading and oxygen concentration, MEA and dissolved metals. Many of the experiments carried out simulated the oxidative degradation conditions within the absorption column, where the flue gasses containing excess oxygen are in continuous contact with the amine. The most studied amine was MEA, being subject to rapid oxidation at low absorber temperatures. The presence of dissolved metals, such as iron and magnese, significantly increases the oxidation rate, acting as powerful catalysts. In addition to MEA, other primary and secondary amines have a certain sensitivity to oxidation at low temperatures, while amines such as piperazine PZ, tertiary amines and hindered amines have been identified as resistant to absorber conditions and can be used as oxidation inhibitors ¹⁸.

The second route of oxidation, in CO₂ capture processes, is through the reaction with the oxygen transported (including dissolved oxygen, oxidized metal ions, peroxides and nitrites) in the heat exchanger, stripper and reboiler, where high operating temperatures are present. Under these conditions, even amines with certain stability at low absorber temperatures will be subject to oxidative degradation ³⁸. Therefore, since the oxidation rate is linked to the solubility of oxygen in the solvent, it is possible to minimise it by removing dissolved oxygen in the rich solution, either by nitrogen or by means of a low-temperature flash of CO₂/H₂O ¹⁸.

Moreover, *Voice et al.* ³⁸ showed how the choice of amine can significantly influence the oxidation rate:

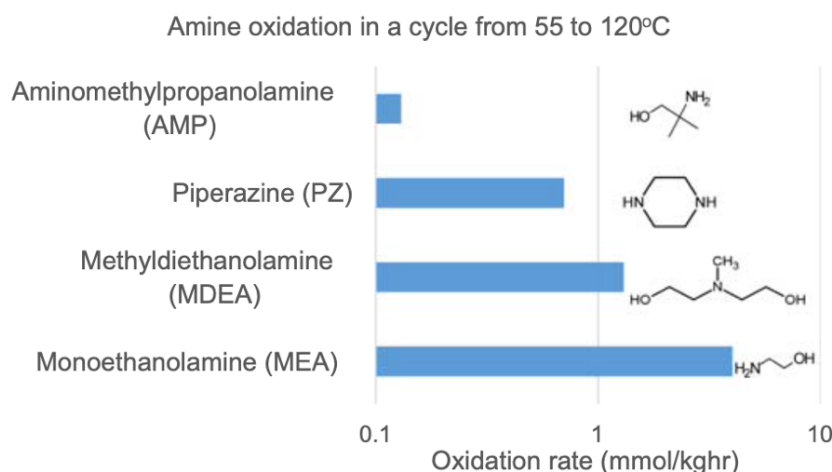


Figure 2.17 Oxidation rates of common amines with cycles from 55 to 120 °C ³⁸

Tertiary amines, such as methyl diethanolamine (MDEA), which are not subject to oxidation at low absorber temperatures, undergo oxidative degradation to the stripper due to reactions with dissolved oxygen at high temperatures. Aminomethyl propanol (AMP) shows the highest oxidation resistance, followed by PZ which shows significant resistance when compared to MEA. Although the PZ, in comparison with the MEA, is undergoing a net increase in the oxidation rate at high stripper temperatures compared to the low absorber temperatures.

2.11.2 Flue gas impurities

Flue gas from coal-fired power plants contains several impurities which affect the post-combustion capture processes. Typically these plants have processes of gas pretreatment, such as to remove most impurities such as SO₂, HCl and grosser ash, which, however, are generally not able to capture the remaining impurities such as NO_x, Hg, and submicron H₂SO₄ aerosol ¹⁸.

2.11.3 Nitrosamine

Secondary amines react with nitrites under stripping conditions to produce carcinogenic nitrosamines which can create significant secondary environmental impacts. *Fine* ³⁹ proposed a sequence of processes that determines the accumulation of nitrosamines in the processes of scrubbing amines.

The figure shows its nitrosamine cycle model:

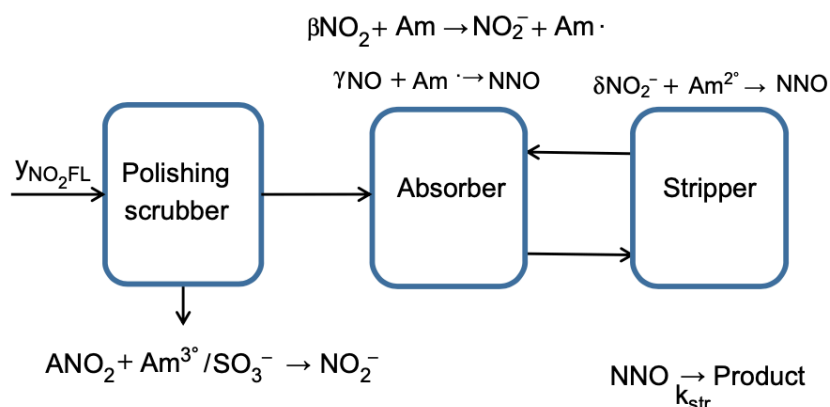


Figure 2.18 The nitrosamine cycle ³⁹

Combustion fumes containing NO_x enter a typical Polishing scrubber, where a part of NO₂ can be removed by reaction with sulphites or tertiary amines. The remaining NO₂ will be mostly absorbed in the inlet of the absorption column by reaction with secondary or tertiary amines, forming nitrites. At high stripper temperatures, nitrites react with secondary amines to produce nitrosamine. Once formed, the nitrosamine will thermally decompose inside the stripper, until it reaches a stationary concentration, such that the decomposition rate will be equal to the rate at which the NO₂ enter inside the absorption column ¹⁸.

The thermal decomposition is catalyzed by high pH values, therefore by performing a solvent regeneration at 150 ° C and with the addition of NaOH, there are suitable conditions for the decomposition of nitrosamine. Therefore, the concentration of nitrosamine can be controlled by amine selection, high-temperature stripping, removal of NO₂ at the scrubber and upstream NO_x controls. Limited accumulations of nitrosamine can be managed by means of water washes, with

minimal risks of emissions. In worst case degradation products consist of volatile secondary amines, otherwise, the most significant risk is losses of liquid substances containing nitrosamines ²⁸.

2.11.4 Amine volatility

Moderate levels of amine volatility (10-100 ppm) can be managed by treating the exit gases from the absorber with water washes, higher volatility levels will require more expensive washing systems. Although the use of highly volatile amines may reduce emissions of amine aerosols, volatility above 100 ppm should be avoided under the operating conditions of the absorption column. At the same time, amines with low volatility make recovery by evaporation difficult but are effective in avoiding emissions into aerosols.

Considering the different effects, the best compromise is represented by a solution of the amine with moderate or low volatility, characterized by the presence of at least two hydrophilic groups (N, O, OH, etc.), amines with three hydrophilic groups are considered essentially non-volatile ^{18,28}.

The effect of the CO₂ load on the volatility of the amines varies depending on the type of amine. In methyl diethanolamine (MDEA) or aminomethyl propanol (AMP) the volatility of the amine increases slightly with the CO₂ load because the bicarbonate makes the amine quite hydrophobic. For PZ, the CO₂ load significantly reduces the volatility of the amine by producing carbamate or protonated amine ^{18,28}.

2.11.5 Amine aerosol emissions

The amine vapour may condense on particulates inside the absorption column, generating small drops of aerosol difficult to remove even with washing processes with water. The resulting aerosol can, however, be removed effectively using fibre filters or using a low or zero volatility amino acid or amine ¹⁸.

Chapter III

Ionic Liquids for Post-combustion CO₂ Capture

3.1 Ionic liquids properties

Ionic liquids are more commonly defined as materials consisting of cations and anions that melt at a temperature of 100 °C or less. This temperature has no chemical or physical significance but has persisted over the years ⁴⁰.

In the last decade, ionic liquids (IL) have emerged as a promising alternative to *conventional amines* due to their remarkable properties, such as negligible volatility, high chemical/thermal stability and tunability. The latter is considered to be the most important property of ionic liquids, as it allows the design of activity-specific ionic liquids (TSIL) ⁴¹.

The number of possible ILs is very high. Some examples of commonly used IL cations and anions are shown in *Figure 3.1*:

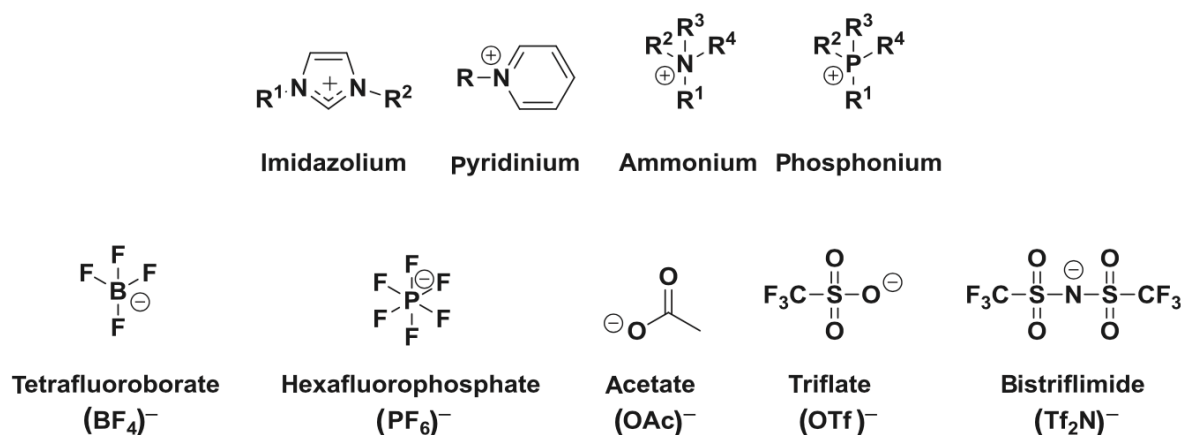


Figure 3.2 Examples of the most common cations (above) and anions (below) used for ILs ⁴²

where the "R" groups are often alkyl groups. Among these IL, the imidazolium class is the most widely studied and reported in the literature. ILs can be synthesized by different mechanisms from countless materials and with a great possibility of structural variations provided by the selection of "R" groups.

ILs are also referred to as *designers*, as their physical, chemical, and biological properties are influenced by the choice of cations, anions, and functional groups selected during synthesizing reactions. Being composed of cations and anions, the ILs are subject to strong intermolecular Colombian forces, therefore they are characterized by intrinsically very low vapour pressures and high vaporization enthalpies. This property is considered to be advantageous in absorption-based processes, as steam losses will be essentially zero for the aqueous solutions ⁴².

The non-volatility of ILs allows separation of CO₂ from the rich solvent more facilitated, with a reduced energy consumption compared to CO₂ capture methods, more commonly used, based on the scrubbing of amines. Moreover, the use of ILs, compared to conventional volatile solvents, allows avoiding the loss of solvent by preventing air pollution caused by organic substances. Therefore, ILs can be considered as an advantageous option for CO₂ capture, with reduced energy consumption and costs ⁴³.

In addition to CO₂ absorption performance, IL viscosity is also a key property. In general, the viscosities of functionalized ILs are relatively high and increase further as a result of CO₂ absorption due to chemical reactions. As previously analysed, high viscosity values will reduce the heat transfer coefficient as well as hinder the CO₂ diffusion process. Therefore, the reduction of the viscosity of the IL through structural variations is at the center of significant and continuous research efforts ⁴².

The main advantage of the use of ILs as absorbing species in PCC processes is, in addition to the use of molecular species with minimal or negligible volatility, the non-use (or in limited quantities for aqueous IL solutions) of water. This allows to reduce the overall energy requirement of the process, due to a reduction in the demand for sensitive heat and latent heat during the phase of solvent regeneration. The sensitive heat decreases as the specific heat of IL-based solvents is lower than the conventional solution at 30% MEA, which is greatly influenced by the high specific heat of the water. Moreover, the contribution of latent heat to energy expenditure for ILs is significantly reduced, if not nil, as no steam production is required for CO₂ dilution in such processes, thus allowing the use of significantly lower operating temperatures ⁴⁴.

3.2 CO₂ Solubility in ionic liquids

Thanks to tuning, ILs possess unique properties compared to other organic solvents. Millions of possible combinations of different cations, anions and functional groups, provide the IL with specific physicochemical properties and influence their CO₂ capture performance ⁴³.

Most ILs absorb CO₂ through a physical mechanism, through the physical interaction between cations, anions and CO₂. For this reason, the solubility of CO₂ is determined by the type of cations and anions constituting the IL. Anions are considered to play a more important role in CO₂ absorption than cations. *Anthony et al.*⁴⁵ studied the effect of different cations (such as imidazolium, ammonium, pyrrolidinium and phosphonium) and anions (Tf₂n, PF₆ and BF₄) on the solubility of CO₂, discovering that with the same anion, the choice of the cation slightly affects the solubility. On the contrary, the anion effect is more relevant.

However, although the contribution of cations to CO₂ solubility is less than that of anions, the cationic effects are not negligible. Considering IL with the same anion, the presence of long alkyl chains and the fluorination of cations marginally favour the solubility of CO₂. This is because these effects increase the free volume necessary for the capture of CO₂ in the gaseous phase and in stronger interactions between CO₂ and fluorinated alkyl chains, effects which favour the physical dilution of CO₂ in the IL⁴³.

Although ILs represent a different option for CO₂ capture, the physical mechanism of absorption of ILs cannot yet compete with the solvents currently on the market, due to the lower CO₂ absorption capacity found for post-combustion capture, interacting with flue gas at atmospheric pressure and low CO₂ concentration⁴³.

In fact, although the molar fraction of CO₂ dissolved within the IL, at a given temperature T and pressure P, seems to be higher than that observed for common organic solvents, such perception of "high" solubility is affected by the large molecular weights of ILs compared to the molecule of CO₂. Considering the solubility in terms of moles per volume of IL, or moles per mass of IL, then the amount of CO₂ dissolved physically is quite similar to that observed for ordinary liquid organic solvents and polymeric materials. From this point of view, the physical absorption of CO₂ by ILs could be competitive for PCC technologies if IL were used inside membranes rather than as absorbent. Physical absorption cannot be considered as a viable option for capturing low-pressure CO₂ from combustion fumes. Therefore, to be considered as competitive absorbers for PCC applications, ILs need to incorporate some form of chemical reactivity⁴².

3.3 Task-specific ionic liquids

Many of the most commonly used ILs in the literature (*Figure 3.1*) have only physical absorption mechanisms of CO₂. ILs that do not have reactive functional groups (such as an *amine*) are not considered to be competitive absorbers for PCC processes.

Indeed, the aqueous solutions of MEA, while presenting problems associated with degradation, corrosion and volatility, are characterized by high CO₂ capture capacity. As a result, ILs need to incorporate reactive sites in their structures, to increase the CO₂ absorption capacity at the low pressures found in PCC processes, thus constituting a viable alternative to conventional solvents. The first task-specific IL was designed by Davis⁴⁶, bonding a *primary amine group covalently* to an imidazolium cation, with the primary objective of increasing the CO₂ absorption capacity. When exposed to CO₂, this amine-functionalized TSIL reacts by a 2:1 mechanism, through the formation of an ammonium carbamate salt, as shown in Figure 3.2⁴².

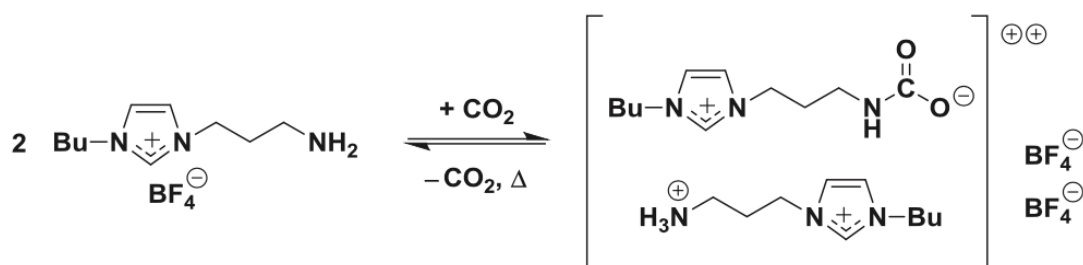


Figure 3.3 TSIL Davis structure and reaction mechanism for CO₂ absorption⁴²

The addition of an *amine group* to an imidazolium cation is a relatively simple approach with which to greatly improve the absorption of low-pressure CO₂. However, functionalization often leads to greater intermolecular interactions, resulting in increased viscosity as a result of CO₂ absorption. To solve this problem, ILs are used in solution with liquids at high boiling point, to counterbalance the high viscosity of ILs. Moreover, these blends have the advantage of reducing the costs associated with the use of ILs, which are typically very high⁴⁷.

3.4 Amine-CO₂ chemical interaction

Generally, the groups of amines connected to the cations or anions of the ILs, react with the CO₂ by means of different mechanisms. For cation-functionalized IL containing amine groups, such as single amine-based IL [Nh2p-bim] [BF₄] and dual amine-based IL DAIL, they are expected to react with CO₂ through a carbamate-forming mechanism, completely similar to that already presented for aqueous amines. Resulting in a 1:2 stoichiometric ratio between the reacted CO₂ moles and the amine moles used, as shown in Figure 3.3⁴³.

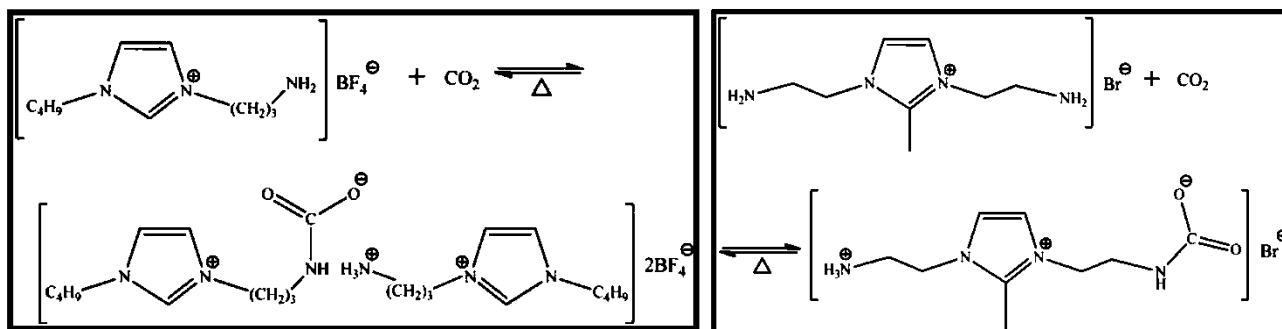


Figure 3.4 Reaction mechanism between CO₂ and [Nh2p-bim] [BF₄] and DIAL, respectively⁴³

However, studies on CO₂ absorption by 2-dimethyl-(3- aminoethyl) imidazolium-based ILs including [aEMMIM] [F], [aEMMIM][Cl], [aEMMIM][Br], and [aEMMIM][I] showed that this four amine-functionalized ILs can absorb CO₂ through a 1:1 mechanism of reaction, by forming carbamic acid⁴³.

The introduction of an NH₂ group to the imidazolium ring effectively increases the CO₂ absorption capacity, but this is not the case for all cations with NH₂ groups. Zhang *et al*⁴⁸. studied the absorption performances of 1,1,3,3-tetramethylguanidinium lactate ([TMG][L]) with NH₂ groups connected to the cation. [TMG][L] showed very low physical solubility values and a molar absorption ratio between CO₂ and NH₂ far from the 1:2 value shown by [Nh2p-bim] [BF₄].

Tethering an amino group to the anion of the IL, the formation of carbamide acid is encouraged, which is reflected in an almost equimolar ratio, following the 1:1 stoichiometric reaction mechanism, as shown in Figure 3.4. Moreover, dual functionalized ILs, in which both cation and anion are functionalized with amine groups, the CO₂ absorption capacity is further increased, approaching 1,00 mol CO₂/mol IL⁴³.

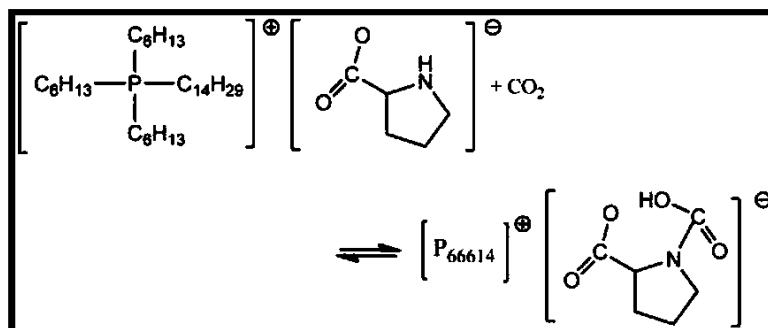


Figure 3.5 Proposed reaction mechanism of CO₂ with [P66614]- [Pro]⁴³

3.5 Ionic liquids degradation

Although ILs have often been referred to as "green solvents", some of them may cause inhibition in plant and animal growth. In addition, some ILs structures may be persistent pollutants in the atmosphere due to their resistance to abiotic and biotic degradation processes.

It is, therefore, necessary to understand and determine the hazard associated with the presence of ILs in the environment ⁴³.

3.5.1 Degradation in presence of the microorganism

The tenth principle of Green Chemistry proposed by Anastas and Warner in 1998, indicates how a chemical compound, at the end of its use, should be able to degrade in the environment in harmless and persistent ways. Biodegradability criteria for chemical compounds are defined by the Organization for Economic Cooperation and Development (OECD) ⁴³.

The biodegradation of 37 on imidazolium, pyridinium, pyrrolidinium, ammonium, and phosphonium based ILs, in the presence of the *Sphingomonas paucimobilis* bacterium, was analysed by measuring carbon dioxide produced using an indirect impedance technique. With a biodegradation rate greater than 60%, after an incubation period of 28 days in the presence of the bacterium at 45 C, for 54% of the samples analyzed. These samples should be considered as readily biodegradable compounds. Consequently, the choice of an effective micro-organism is crucial for the assessment of ILs biodegradability. In addition, the rate of biodegradation is strongly influenced by the choice of the IL constituent anion, as well as by the different alkyl chains and IL cation head groups ⁴³.

Liwarska-Bizukojc et al. ⁴⁹ investigated the biodegradation of seven imidazolium ILs, such as 1-ethyl-3-methylimidazolium bromide ([Emim][Br]), 1-hexyl-3-methylimidazolium bromide ([Hmim][Br]), and 1-decyl-3-methylimidazolium bromide ([Dmim][Br]), by activated sludge microorganisms. It was found that longer alkyl side chains are more susceptible to oxidation of the terminal carbon atom. IL, having a decyl side chain, is the easiest biotransformed of the ILs studied. Nevertheless, no products of cleavage of the imidazolium ring were observed. The increase in the number of substituents of the imidazolium ring does not favour biodegradation of ionic liquids. The completely substituted ionic liquids were less susceptible to biodegradation than the ionic liquids with a lower number of alkyl side chains. Ionic liquids, which are completely substituted by short alkyl chains (up to two carbon atoms), are the most difficult to be decomposed microbiologically.

Deng *et al.*⁵⁰ focused on antimicrobial activities and biodegradation kinetics of ten pyridinium, pyrrolidinium, and ammonium-based ILs incubated with either a pure strain of *Rhodococcus rhodochrous* ATCC 29672 or an activated sludge. Nine ILs showed a more than 75% biodegradability percentage in the first 28 days, except for [Hmpy][Tf2n]. The kinetic study showed that the rate of decomposition varies from IL to IL, with a slower degradation for pyridinium ILs. The ammonium-based ILs, if there is no complete substitution with long alkyl chains, are characterized by a fast degradation, especially in the presence of the anion acetate. As far as pyrrolidinium-based ILs as concerned, the rate of degradation, in the presence of pure strain bacteria, does not seem to be significantly affected by the length of the alkyl chain, in a range of C1 to C4 carbon atoms.

Studies on the biodegradability of ILs have mainly focused on the aerobic side. However, the anaerobic biodegradation of many compounds plays an important role in the environment. Neumann *et al.*⁵¹ studied the biodegradability of imidazolium, pyridinium and dimethylaminopyridinium-based ILs, such as [Emim][Cl], [Omim][Cl], 1-(8-hydroxyoctyl)-3-methylimidazolium bromide ([OOHmim][Br]), 1-ethylpyridinium chloride ([EPy][Cl]), 1-octylpyridinium chloride ([OPy][Cl]), over 11 months. Many of the ILs analysed, except for [OOHmim][Br], showed non-biodegradability, highlighting worse degradation than aerobic condition.

3.5.2 Thermal degradation

The thermal stability of an IL is an important factor that limits the maximum operating temperature and consequently also the performance of the system. In particular, amine-functionalized ILs are widely used for CO₂ capture processes. Capture and desorption processes that subject ILs to relatively high temperatures for a long time; therefore, studying the thermal stability of ILs, and their decomposition temperatures, is of paramount importance⁴³.

3.6 Ionic liquids from renewable biomaterials

As highlighted by the above studies, the most common cations (such as imidazolium and pyridinium) and anions (often fluorine) are produced from non-renewable material, showing weak biocompatibility and biodegradability, and high toxicity. For this reason, in recent years studies have focused on the synthesis of IL from renewable materials and low toxicity.

Amino acids are one of the most abundant biomaterials in nature and are recognized as non-toxic, biodegradable and biocompatible. As a result, they can be considered as an excellent raw material for the synthesis of ILs, also thanks to their moderate costs⁵².

In 2005, the group of *Fukumoto*⁵³ synthesized for the first time liquid ions based on amino acids (AAILs), and since then many of the anions used for the production of IL have a natural origin. Also, recently IL-based choline, an essential micronutrient of natural origin, have been synthesized and characterized, showing a high biodegradability and low toxicity. Less attention, however, has been paid to Choline-based AAILs, which show promising physicochemical and thermal properties.

*Tao et al.*⁴⁷ synthesized a series of choline-based AAILs, featuring physicochemical properties such as viscosity, density and conductivity, over a wide temperature range.

As for viscosity, one of the most important factors influencing the performance of processes associated with the use of ILs, the values are in the range of 121-5600 mPa·s at 25 °C, with a dependence on the size of the anionic structure. An increase in the complexity of the structure results in higher viscosity, probably due to greater internal interactions (van der Waals forces or hydrogen bond interactions). In particular, the [Cho][Gly] has the lower viscosity value (above 121 mPa·s), while the [Cho][Ser] shows the highest viscosity, due to the introduction of a hydroxyl group in the anionic structure accompanied by hydrogen bond interactions. The viscosity, as well as the density, of [Cho][AA], decreases linearly as temperature increases, in contrast to conductivity, which increases exponentially, as shown in *Figure 3.3*.

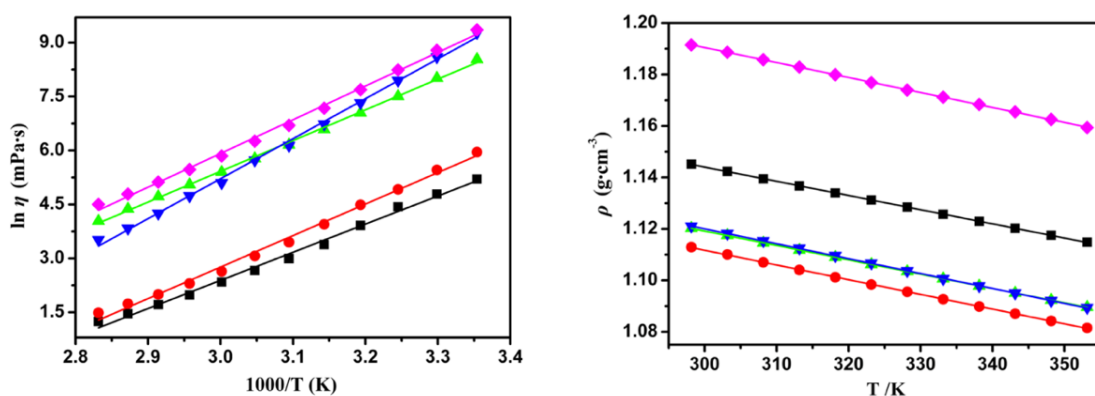


Figure 3.6 Viscosities η and Densities ρ as a function of temperature: ■, [Ch][Gly]; red ●, [Ch][L-Ala]; green ▲, [Ch][β-Ala]; blue ▼, [Ch][Pro]; pink ◆, [Ch][Ser]⁴⁷

All [Cho][AA] are liquid at room temperature, with a glass transition temperature range T_g running from -74 to -10 °C. T_g varies according to the structure of the anions, usually, an increase in the number of carbon atoms on the side of the amino acid chain results in a higher glass transition temperature.

As *Figure 3.4* shows, the decomposition temperature T_d for the [Cho][AA] analyzed is in the range of 150-200 °C, showing also, in this case a dependence on the anionic structure.

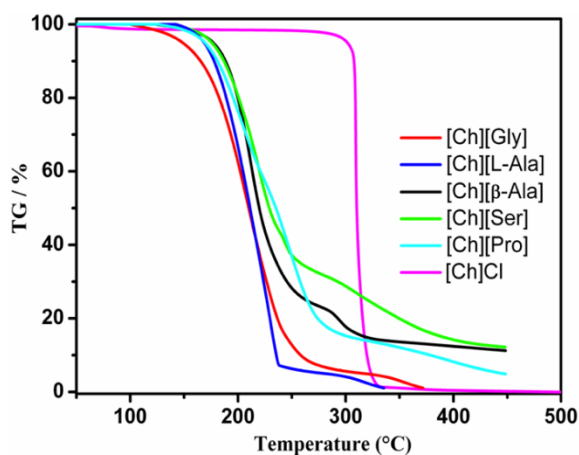


Figure 3.7 Decomposition temperature for several [Cho][AA] ⁴⁷

In particular, the [Cho][Gly] presents a T_d around 150 °C presenting the simplest anionic structure. In contrast, structures with a hydroxyl group and a pyrrolidine ring, such as [Cho][Ser] and [Cho][Pro], show a higher decomposition temperature. Demonstrating how the thermal stability of [Cho][AA] is mainly related to the anionic structure, a larger anion size involves thermal decomposition of [Cho][AA] at higher temperatures ^{47,52}.

3.7 CO₂ absorption in Choline-based AAILs

Each AA contains functionalized amines, so IL based on AA (AAILs) can be considered as task-specific anions optimal for the synthesis of IL in CO₂ capture processes ⁵⁴.

Davarpanah *et al.* ⁵⁵ have studied the CO₂ absorption performance for four different biological-based TSILs in industrial fume treatment processes. The choline-based amino acids [Cho][AA] examined are shown in the figure:

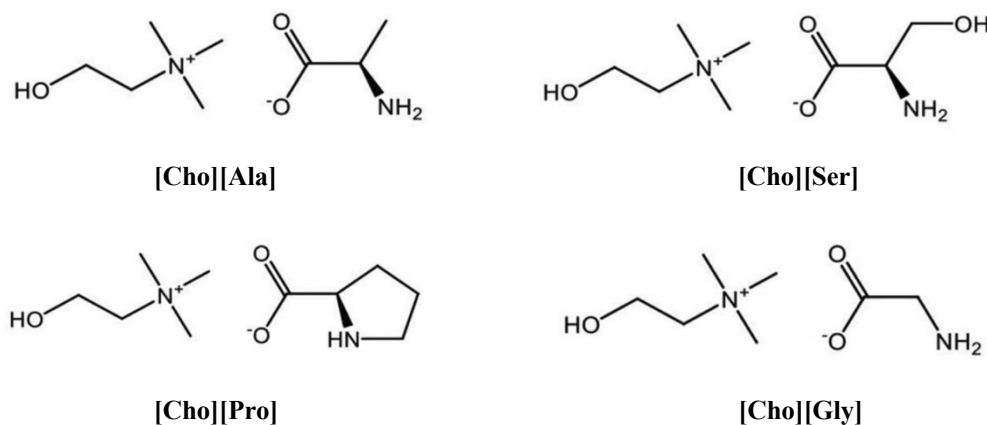


Figure 3.8 Chemical structure of the four [Cho][AA] IL ⁵⁵

For the four ILs, CO₂ is absorbed and fixed by the formation of two different species, carbamate and carbamide acid; in fact, two different reactions can occur:

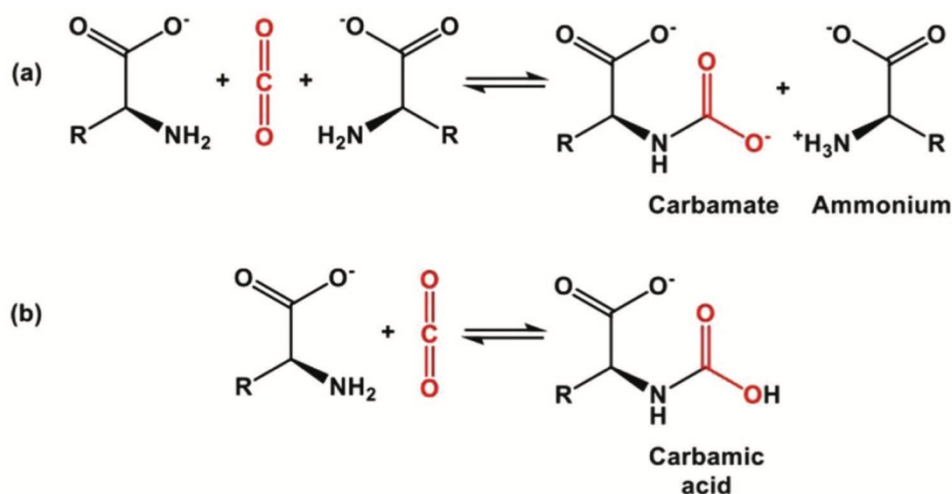


Figure 3.9 Possible scenarios of reaction between CO₂ and amines. **a)** Formation of ammonium carbamate by a 2:1 reaction mechanism; **b)** formation of carbamide acid by a 1:1 reaction mechanism ⁵⁵

Carbamate along with ammonium is formed by the reaction of two amine molecules and one CO₂ molecule (2:1 mechanism), while carbamide is produced by a 1:1 stoichiometric reaction mechanism. During the CO₂ absorption process, some amino acids change in composition due to the formation of a white precipitate. This is particularly true for [Cho][Ala] and [Cho][Gly], and the reason for this formation is obtained by analyzing the 2:1 mechanism of stoichiometric reaction ⁵⁵.

From the studies carried out by *Latini et al.* ⁵⁴, the following path of reactions between [Cho][Gly] and CO₂ can be assumed:

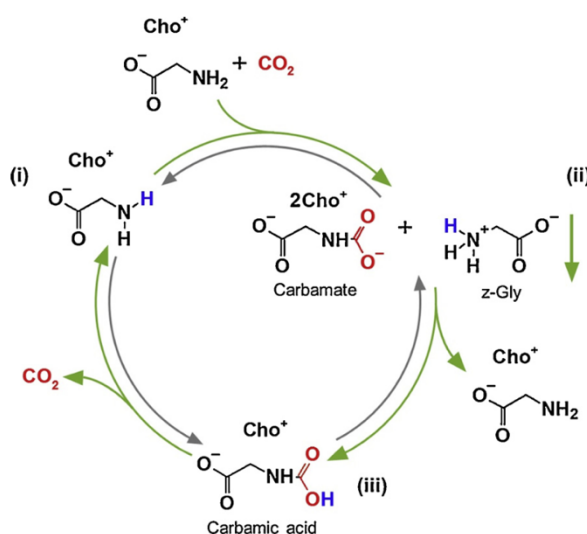


Figure 3.10 Path of reactions between [Cho][Gly] and CO₂. Observed reactions indicated in green; possible unobserved reactions indicated in grey ⁵⁴

In which two amino groups of glycinate anions react with CO₂ in a 2:1 mechanism. In the process (i) to (ii), the first amine reacts with CO₂ producing a carbamate species, while the proton moves towards the second amine forming ammonium counter ion. In particular, the second amine, extracting a proton from the first, gives rise to a fraction NH₃⁺, which produces z-glycine. Subsequently, ammonium carbamate is converted to carbamic acid by means of a proton transfer process (ii) to (iii). During the desorption process, direct conversion of carbamide acid to the starting IL occurs, through a simple release of CO₂, process (iii) to (i). However, since the first reaction process, the [Cho][Gly] loses its purity due to the formation of the white precipitate, which turns out to be solid glycine. The low solubility of z-glycine in the DMSO is probably the cause of the precipitation of the solid. This irreversible behaviour results in a loss of CO₂ absorption capacity, resulting in a reduction in the efficiency of solvent regeneration ⁵⁴.

Conversely, the formation of the white precipitate is not observed for the [Cho][Pro], for which two different CO₂ absorption mechanisms occur simultaneously: a 2:1 reaction mechanism, like [Cho][Gly], in which two amino groups of anions proline react with CO₂, and a 1:1 reaction mechanism. In contrast to [Cho][Gly], carbamide is not produced by proton transfer from ammonium carbamate, but the two species develop independently. This could be due to the presence of the heterocyclic ring of proline, which would favour a 1:1 mechanism, in which carbamide acid is produced through a direct reaction between a single molecule of [Cho][Pro] and CO₂, process (i) a (iii) in *Figure 3.8*. During the desorption phase, CO₂ is released from carbamide acid, through a direct reaction that regenerates the starting IL, process (iii) to (i) ⁵⁴.

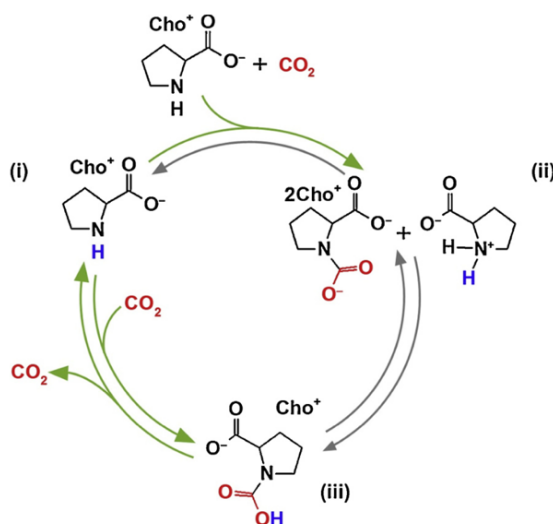
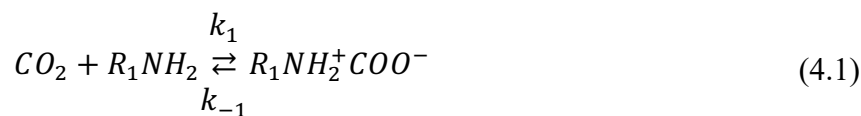


Figure 3.11 Path of reactions between [Cho][Pro] and CO₂. Observed reactions indicated in green; possible unobserved reactions indicated in grey ⁵⁴

Thus, for [Cho][Pro], the absorption of CO₂ occurs via the formation of two different species (carbamate and carbamic acid) related to two different reaction mechanism. A carbamate moiety is

formed together with an ammonium counter-ion, by a reaction of two amine with one CO₂ molecule, Eq. (4.1), whereas carbamic acid is formed by a 1:1 reactions stoichiometry, Eq (4.2) ⁵⁵.



Where R_1NH_2 represents $H_2N - CHR' - COO^-$. Although proline, unlike serine, is a secondary amine, the [Cho][Pro] solution react with CO₂ in a similar way to [Cho][Ser] and therefore the reaction between the secondary amine R_1R_2NH and CO₂ is not indicated ⁵⁶.

As concerning the [Cho][Pro], during the entire absorption and desorption process, unlike [Cho][Gly], the solution remains pure and no white precipitate formations are observed, probably due to the increased solubility of z-proline in the DMSO, formed in the process (ii) ⁵⁴.

Therefore, the choice of AA significantly affects the absorption performance of the resulting IL. Overall, TSIL solutions from renewable biomaterials provide several benefits such as low costs, low environmental impacts, low viscosity values, low energy consumption and high regeneration capacity. These features make the solutions based on [Cho][AA] optimal absorbent and competitive for post-combustion CO₂ capture processes ⁵⁵.

3.8 [Cho][AA]s-based solutions

The relative high cost and large viscosity of ILs means that pure [Cho][AA]s cannot be used directly in CO₂ capture processes. In particular, the high viscosity value, which increases further as a result of absorption, leads to an extremely low mass transfer rate between the gaseous and liquid phases. Causing a slowing of the absorption process. In order to address this obstacle to the commercial use of ILs, [Cho][AA]s are mixed with compatible fluids, such as PEG200 and H₂O ⁵⁶.

Li et al. ⁵⁷ investigated the process of CO₂ absorption/desorption in [Cho][Pro]/PEG200 mixtures and observed that the addition of PEG200 can significantly accelerate the process of CO₂ absorption and desorption. *Feng et al.* ⁵⁸ studied the CO₂ absorption in four AAILs including [N1111][Gly], [N1111][Lys], [N2222][Gly], and [N2222][Lys] mixed with H₂O or MDEA/H₂O mixture. Showing an increased absorption capacity and absorption rate of AAIL in mixtures with MDEA.

McDonald *et al.*⁵⁹ studied the effect of water on CO₂ absorption in aqueous solutions of AAILs ([N1111] [Gly] and [N2222] [Pro]). They found that the select amino acid-derivated ionic liquids may show a molar CO₂ absorption ratio of 1:1 in dry conditions. However, they concluded that high viscosity values discouraged their direct use, regardless their high absorption capacity values.

In my thesis, the performance of conventional aqueous solutions of amine is compared with a Choline-based AAIL. [Cho][Pro] was selected for the study of the process of CO₂ absorption/desorption by ILs. To overcome the issues deriving from their extremely high viscosity, [Cho][Pro] was diluted in dimethyl sulfoxide (DMSO, supplied by Merck, purity $\geq 99\%$).

DMSO is an aprotic solvent but exhibits properties like water, and it is completely miscible with the ILs utilized. It is non-toxic, and it has a high boiling point. The DMSO allows performing a process of absorption/desorption of CO₂ by a simple change of pressure or temperature, without the need to produce steam inside the desorption column. This allows reducing the energy required for CO₂ desorption in comparison with aqueous amines systems⁵⁴.

3.9 Synthesis of [Cho][Pro]

The synthesis of [Cho][AA] ILs usually relies on the water solution of choline hydroxide, [Cho][OH]. [Cho][OH] solution is a convenient starting reagent for AAILs synthesis via acid-base titration. Such a synthesis method leads to the production of ILs with very high purity without any byproduct. However, the [Cho][OH] solution is corrosive, reactive, and expensive⁵⁵.

To overcome drawbacks related to the corrosivity and cost of choline hydroxide, the two different choline based AAILs (exploiting proline and serine as anions) were synthesized following the innovative method reported for the first time by *Latini et al.*⁵⁴. This method makes use of choline chloride as a choline cation source, being cheap and easy to handle salts.

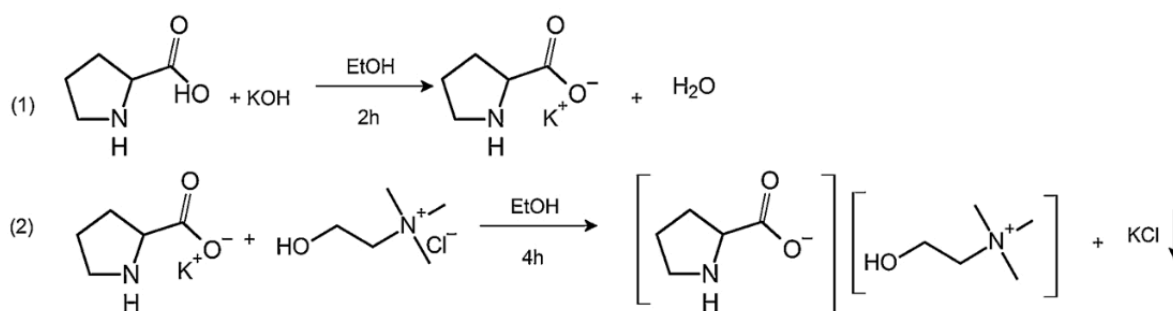


Figure 3.12 Synthesis pathways of [Cho][Pro]⁵⁴

In a 250 ml flask, proline (45 g, supplied by Merck, purity $\geq 99\%$) and an excess of potassium hydroxide (30.9g, Carlo Erba, purity $\geq 85\%$) are mixed at RT in ethanol (200 ml, supplied by Merck, purity $\geq 99.8\%$) under stirring. The potassium salt of the proline is formed, the suspension turned white while the excess of the potassium salt of the proline precipitates. Once the potassium hydroxide pellets dissolved completely (c.ca 2h), the proline chloride (69.8g, supplied by Alfa Aesar, purity $\geq 98\%$) was added. The mixture was left under stirring for 4h. The potassium salt of proline dissolves and potassium chloride precipitated as white powder leaving choline glycinate in solution upon the exchange of K^+ by choline cations. The potassium chloride crystals were separated by centrifugation, and then ethanol and water produced during the reaction were removed using a rotary evaporator. The so obtained IL was preliminary checked by means of ATR-IR spectroscopy and then, outgassed under dynamic vacuum at 30 °C overnight to remove the possible residual ethanol and water, before the experiments. The reaction describing the whole process is summarized in *Figure 3.12*⁵⁴.

Chapter IV

Experimental Section and Methods

4.1 Plant description

As shown in *Figure 4.1*, the bench consists of two stainless steel packed columns used to investigate the CO₂ absorption and stripping process. The first column ($V = 2$ l, $p < 25$ bar, $T < 65$ °C) act as an absorption section where CO₂ is removed from the simulated flue gas stream by a solvent, and the second one ($V = 4$ l, $p < 4.5$ bar; $T < 125$ °C) is a regeneration section where the absorption capability of the rich solvent is restored. The feed gas mixture was prepared by mixing pure gas with a typical composition of the post-combustion process.

The bench can work in the "continuous" configuration or the "batch" configuration. In continuous, it has a poor solvent recirculation from the stripper to the absorber. In the batch cycle, the first column carries out at first the absorption (at low temperature and high pressures), and at a second moment, raising the temperature and/or varying the pressure, acts as a desorption column regenerating the solvent, reaching temperatures up to 125 °C.

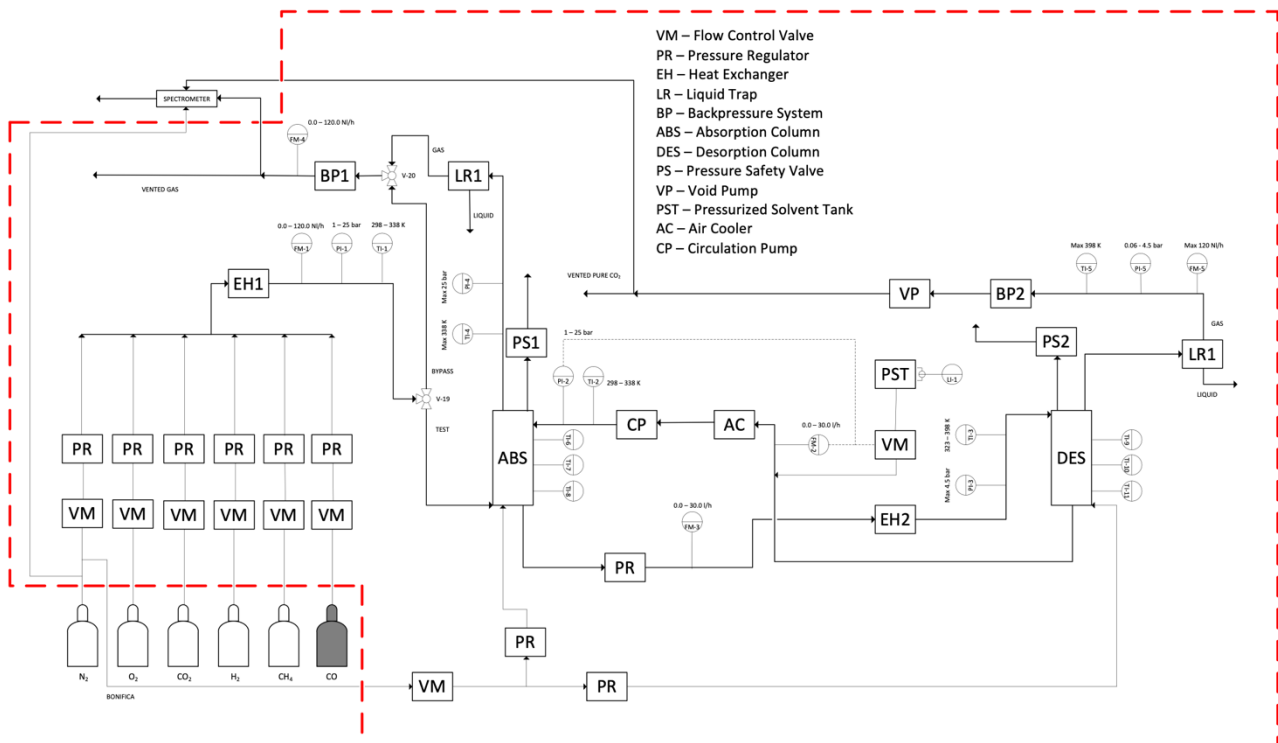


Figure 4.2 Schematic diagram of the experimental setup

The bench will be used primarily for absorption tests with an aqueous monoethanolamine solution (MEA, 30% by weight) used as a benchmark. The alternative of chemical absorption with ionic fluids based on choline and amino acids will be investigated. The bench has been designed based on information in the literature to verify the CO₂ removal efficiency by liquid solvents in operating conditions similar to those in real life and a plant with the scheme replicable on an industrial scale.

4.1.1 Experimental set-up

The potential for post-combustion CO₂ capture by two different solvent, aqueous monoethanolamine, MEA, and a choline-based amino acid IL, [Cho][Pro], is to be verified through chemical/physical absorption and desorption cycles under different operating conditions. Gaseous mixtures containing carbon dioxide simulate different processes of production and use of energy and materials. The bench has three operating conditions:

- **Preparation for the test.**

The individual gas flows (conditions: ambient temperature and pressure reduction from 25 bar up to the test run pressure) necessary to simulate the mixture of interest shall be introduced. Pressure regulators (PR) shall be capable of modulating the gas pressure between a value close to the maximum operating and storage value (25 bar) and a minimum of 1 bar, controlled by a pressure gauge with a transmitter placed downstream of mixing.

The resulting mixture is heated by an electric heater to the inlet temperature in the absorber for the test. A three-way valve system bypasses the absorption reactor: part of the mixture is analysed by the mass spectrometer. The flow rates of the individual gases in the mixture are varied until the desired composition is reached. In the meantime, the intended solvent flow rate for the correct conduct of the test is circulated in the closed circuit between the two reactors, thanks to the pump (CP). Then reach the operating temperature of the reactors, thanks to the activation of the electric heater (EH2) in the inlet to the stripper and the air cooler (AC) in the inlet to the absorber.

The electric heater (EH1) that conditions the gaseous mixture has a heating cable that brings the absorber to the operating temperature foreseen for the test (controlled by the indicator with transmitter TI7). The electric solvent heater performs the same operation on the stripper (controlled by the indicator with transmitter TI10). The vacuum pump ensures a possible depression of the stripper.

- **Test**

At the end of the previous step, the operating conditions are reached which are then maintained during the entire test (flow rate, temperature, pressure, and composition of the gaseous mixture; flow rate,

pressure, and temperature of the solvent; constant pressure and temperature in reactors). The bypass valve is closed, and the mixture is directed to the absorbing reactor.

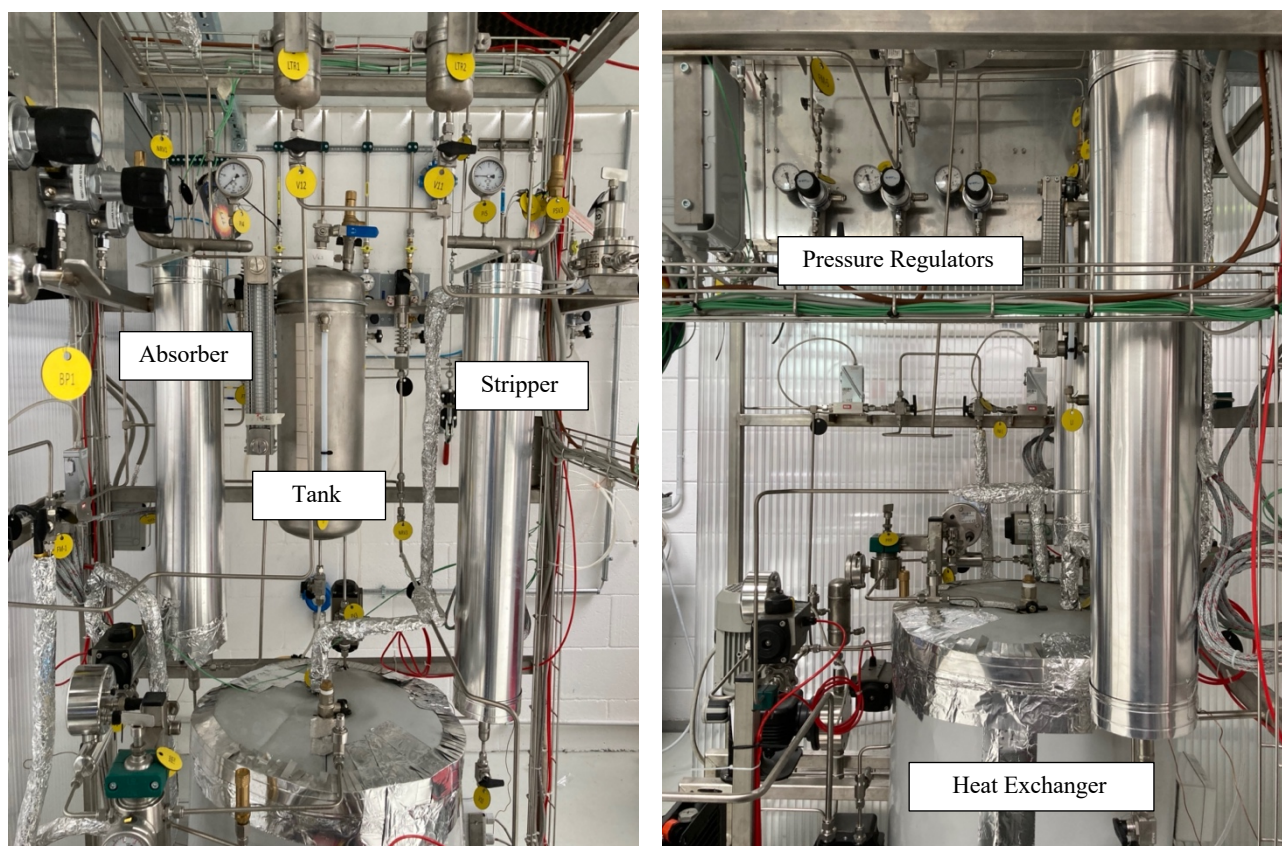


Figure 4.3 Photos of CO₂ capture bench in the lab A1 of Environment Park, science, and technology park in Turin

For the continuous configuration, the mixture fed into the base of the reactor meets the counter-current solvent flow rate: the regenerated absorbent is introduced from the top of the absorber column meanwhile the gas mixture is continuously introduced from the bottom. By means of the counter-flow almost all the carbon dioxide is chemical absorbed.

The residual gaseous mixture leaves the absorption reactor; before the derivation to the mass spectrometer through a capillary, traces of liquid solvent are separated. The rich solvent, on the other hand, is heated and reduced in pressure before entering the desorption reactor, where a large part of the previously captured CO₂ is released. Traces of liquid solvent shall be retained from the released gas before analysis in the spectrometer. The solvent, on the other hand, is recirculated and brought to the uptake operating conditions to start a new capture cycle, with a possible refill to ensure a constant flow rate.

For batch configuration, the absorption and desorption process are performed by means of a single column, varying the operating conditions of temperature and pressure. For this configuration, there is no counter-flow between solvent and gas mixture. In fact, the solvent is introduced inside the

absorption column, forming a flat surface of heat exchange between the gaseous and liquid phase. The gas mixture is continuously introduced from the bottom of the column, coming directly into contact with the liquid solvent.

The temperature of the reactors during the test varies due to the thermochemical reaction and is kept constant by regulating the current in the electrical windings around the walls. Backpressure systems (BP) ensure constant pressure operation of reactors. Safety valves are required with a calibration certificate with pressure values of 25 bar and 4.5 bar for absorber and stripper, respectively. The vent of these valves is sucked from the hood.

○ **Clean-up**

At the end of the test (gas and solvent inlet valves closed, electric heaters and pump/e/s turned off), any residual gases present in the pipes and reactors shall be removed by pure nitrogen cleaning. A dedicated line of nitrogen is also provided for the cleaning of mass spectrometer lines.

4.2 CO₂ Absorption and Desorption measurements tests

The absorption experiments were designed to assess the loading capacity of CO₂ by an aqueous solution of MEA, and the liquid ion [Cho][Pro] in DMSO, for different conditions of temperature and partial pressure of CO₂. The tests were performed in batch configuration, thus using a single column to perform the absorption and desorption of CO₂.

A mixture of two different gas compositions, pure CO₂, and a mixture of 35% CO₂ and 65% CH₄ (simulating the composition of biogas) was used for the two liquid solutions: 30% by weight of MEA in aqueous solution and 12.5% by weight of [Cho][Pro] in DMSO. The amount of solution used varies between 500 and 1000 ml, always maintaining a wide safety range from the threshold value (equal to 70% of the volume of the absorption column). The gas flow rate used has been varied based on the volume of solvent used and by the moles of amine present in solution. As a comparison parameter between the different tests, the same ratio was maintained between the NI/h of CO₂ sent during an entire absorption test, and the moles of amine present in solution (i.e., 15 NI/h CO₂/mol amine in solution).

Each complete process consisted of three consecutive absorption, desorption, and cooling operations at initial conditions (ambient temperature and pressure). The molar fraction of the output CO₂ was analysed using an analytical method. Each test has been carried out for 90 minutes, the absorption

process, under specific conditions of temperature and partial pressure of CO₂, was considered to be terminated with a CO₂ flow at the output equal to the CO₂ flow at the inlet.

The operating conditions of the different tests are shown in *Table 4.1*.

In addition, the desorption process was investigated for the solution of IL-DMSO, at the end of the different absorption tests. The regeneration of IL was evaluated by heating the solution to different temperature conditions (70, 80, and 90° C) and with a constant flow of pure N₂ (18 NI/h). The system has been brought to a temperature and maintained to the operating conditions by means of the electrical heaters present around the column and at the inlet of the gas mixture. Finally, the regeneration efficiency of the IL-DMSO solution, which plays a key role in practical applications, was evaluated by means of three repeated cycles of absorption and desorption.

Table 4.1 Overview of the operating condition of the experimental studies

Experiment	Solvent	Process	T	P	Solvent Volume	Flow Composition	Total flowrate	CO ₂ Concentration
			[°C]	[bara]	[mL]		[NI/h]	[vol%]
A1	30% MEA	Absorption	30	1	1000	CO ₂	78	100
			40	1	850	CO ₂	66,4	100
			50	1	500	CO ₂	39	100
A2	12,5% IL	Absorption	30	1	500	CO ₂	9	100
			40	1	500	CO ₂	9	100
			50	1	500	CO ₂	9	100
B1	30% MEA	Absorption	30	1	550	CO ₂ +CH ₄	123,5	35
B2	12,5% IL	Absorption	30	1	550	CO ₂ +CH ₄	25,7	35
C1	12,5% IL	Absorption	30	1	500	CO ₂	9	100
		Desorption	80	1	500	N ₂	18	0
D1	12,5% IL	Desorption	70	1	500	N ₂	18	0
			80	1	500	N ₂	18	0
			90	1	500	N ₂	18	0

4.2.1 Absorption loading

During the test, all relevant process parameters, such as temperature, pressure, inlet and outlet gas flow rate and molar fraction of CO₂, shall be accessible to the time plot. In addition, all bench data is stored every second.

This allows to obtain important derived quantities such as the amount of CO₂ absorbed, the removal rate, and the loading of CO₂. These parameters are calculated using the following equations:

$$\dot{m}_{CO_2}^{abs} = \dot{m}_{CO_2}^{FG,in} - \dot{m}_{CO_2}^{FG,out} \quad (4.1)$$

$$\psi = \dot{m}_{CO_2}^{abs} / \dot{m}_{CO_2}^{FG,in} \quad (4.2)$$

$$m^{IL} = \frac{n_{CO_2}}{m_{IL} + m_{DMSO}} \quad (4.3)$$

$$m^{MEA} = \frac{n_{CO_2}}{m_{MEA} + m_{H_2O}} \quad (4.4)$$

$$\alpha^{IL} = \frac{n_{CO_2}}{n_{IL}} \quad (4.5)$$

$$\alpha^{MEA} = \frac{n_{CO_2}}{n_{MEA}} \quad (4.6)$$

where $\dot{m}_{CO_2}^{abs}$ is the absorbed CO₂ flow rate, $\dot{m}_{CO_2}^{FG,in}$ e $\dot{m}_{CO_2}^{FG,out}$ are the CO₂ flow rate at the inlet and outlet of the absorption column respectively. ψ is the CO₂ removal rate, expressed as a percentage. n_{CO_2} is the amount of mol of CO₂ absorbed by the liquid solvent, m and α are the absorption loading in units of *mol CO₂/kg absorbent* and *mol CO₂/mol MEA ÷ IL*.

4.2.2 Regeneration efficiency

The regeneration efficiency can be expressed as following:

$$\eta = m_n / m_1 \quad (4.7)$$

where η is the regeneration efficiency (%). m is the CO₂ absorption loading ($\text{mol CO}_2/\text{mol IL}$), 1 represent the first cycle, n represent the nth cycle.

4.2.3 Saturation of the solution

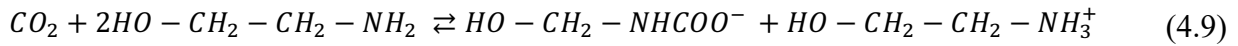
The degree of saturation of the solution during the absorption test is calculated as follows:

$$\Delta CO_2 = \frac{\dot{m}_{CO_2}^{FG,in} - \dot{m}_{CO_2}^{abs}}{\dot{m}_{CO_2}^{in}} \quad (4.8)$$

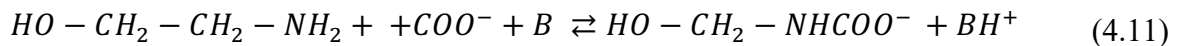
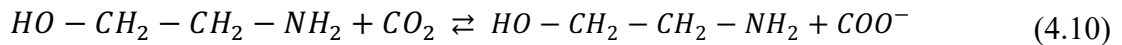
where $\dot{m}_{CO_2}^{abs}$ is the absorbed CO₂ flow rate and $\dot{m}_{CO_2}^{FG,in}$ is the CO₂ flow rate at the inlet of the absorption column.

4.3 CO₂ Absorption and Desorption mechanisms

In aqueous solution of MEA, the CO₂ absorption is described by the zwitterion mechanism proposed by Danckwert⁶⁰:



According to the zwitterion mechanism, this reaction involved two steps. Firstly, the zwitterion is obtained through the reaction between CO₂ with MEA. Then, the zwitterion is deprotonated by a base in the solution:

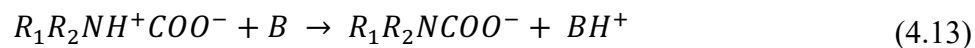


where B is a base existing in the solution, including MEA or H₂O⁶¹.

Similar to the reaction mechanism between CO₂ and aqueous amine, the zwitterion theory is also used to describe the reaction mechanism between CO₂ and [Cho][Pro]⁶². First, the zwitterion (i.e., $R_1R_2NH^+COO^-$) was generated between CO₂ and [Cho][Pro]:

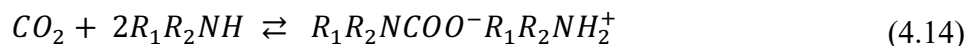


The, the deprotonation of the zwitterion in [Cho][Pro]-DMSO by a base (B) is illustrated:



where B in [Cho][Pro]-DMSO solution is largely R_1R_2NH , the other few bases involved are neglected ⁵⁶.

In addition, as illustrated in the previous chapter, there is a second independent and parallel reaction involving CO₂ and [Cho][Pro], characterized by a 1:2 reaction mechanism. This reaction is considered faster and requires two moles of [Cho][Pro] ⁵⁶, as illustrated by Eq. (4.13):



Chapter V

Results and Discussion

5.1 Absorption of CO₂ with an aqueous solution of MEA

The bench was used originally for absorption tests with an aqueous monoethanolamine solution (MEA, 30% by weight) to compare the results with the literature and ensure the reliability of experimental results.

To measure the experimental loading capacity of the MEA, pure CO₂ was flowed through 1,00 dm³, until no more CO₂ was absorbed. In order to facilitate the reaction, a relatively low temperature has been set, around 30 °C. The experiment was carried out at atmospheric pressure, the load capacity, expressed in mol CO₂/mol MEA, is reported as a function of time in Figure 5.1.

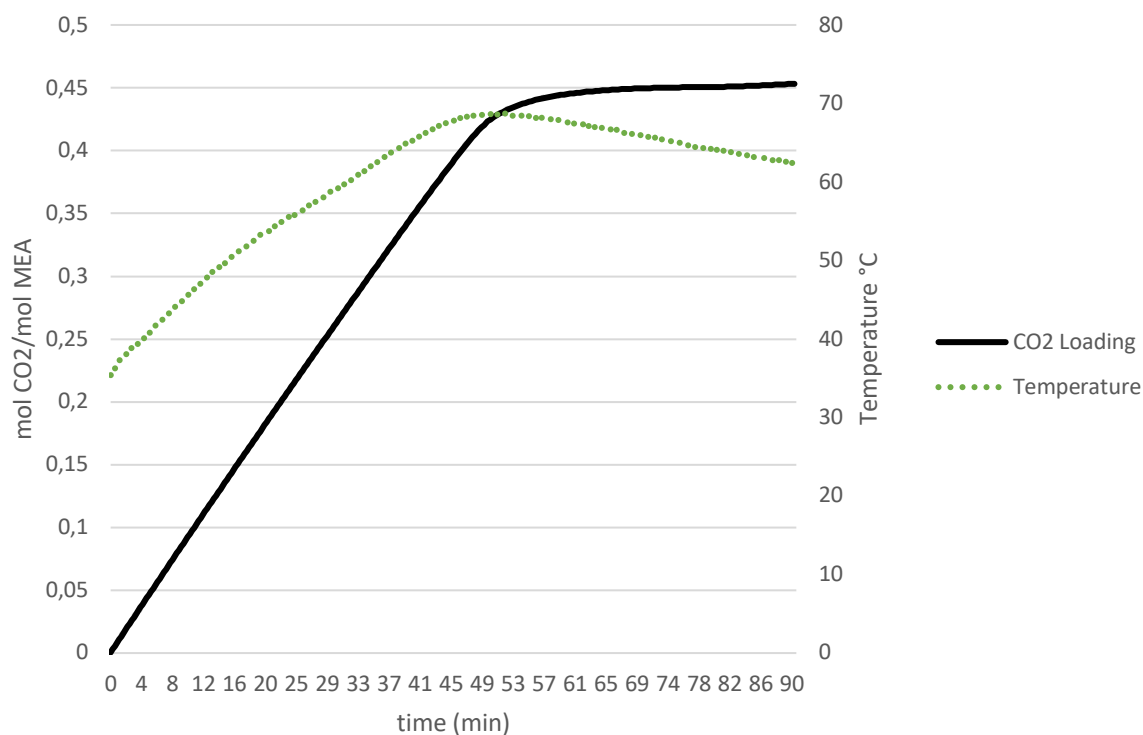


Figure 5.7 The CO₂ loading in the pure solution of 30% wt/wt MEA in function of time (starting absorption temperature: 303 K, gas flow: 78 Nl/h, CO₂ concentration: 100%, solution volume: 1,00 l).

After 90 minutes, no more CO₂ is absorbed by the solution. The result is in good agreement with the literature ⁶³, approaching the theoretical value of 0,5 mol CO₂/mol MEA. It is important to consider how the test bench does not present a heat sink at the absorption column, such as to remove excess heat. Therefore, due to the exothermic nature of the reaction, the temperature inside the absorption column has increased reaching a peak around 70 °C, then decrease then decrease when the absorption rate goes down, expressed in mol CO₂/m²/min, as shown in *Figure 5.2*.

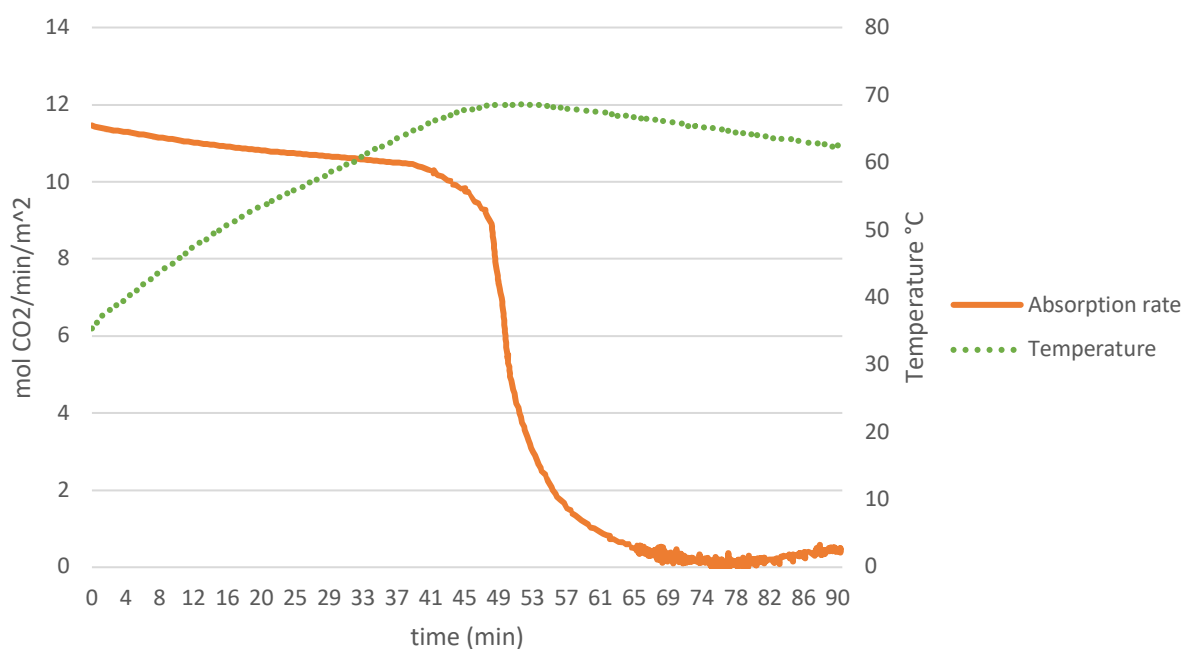


Figure 5.8 Absorption rate of CO₂ into aqueous solution of MEA, in function of temperature time (starting absorption temperature: 303 K, gas flow: 78 NL/h, CO₂ concentration: 100%, solution volume: 1,00 l).

The rate of absorption settles around an almost constant value for about 40 minutes, and then drop to zero, for which no more absorption reaction occurs. The slight increase in the absorption rate at a temperature reduction indicate how the temperature variation during the test hindered the absorption reaction, preventing the effective saturation of the solution.

In order to assess the influence of temperature on the CO₂ loading capacity, the test was repeated for three different initial temperatures, and the results are presented in *Figure 5.3*. Although the absence of a heat sink prevents testing at a constant temperature, the effect of temperature on the absorption performance of the aqueous solution of MEA is evident. There is a marked reduction of the capacity loading of the CO₂ to 40 and 50 °C against a relatively low temperature, as well as there is a progressive decrease of the percentage of CO₂ absorbed, compared to that sent in the absorption column. A more homogeneous variation, compared to the three temperatures, occurs in comparison to the trendlines of saturation curves. In which 0% indicates that all the CO₂ sent is absorbed by the solution, and 100% represents the saturation condition of the mixture at that given temperature and pressure.

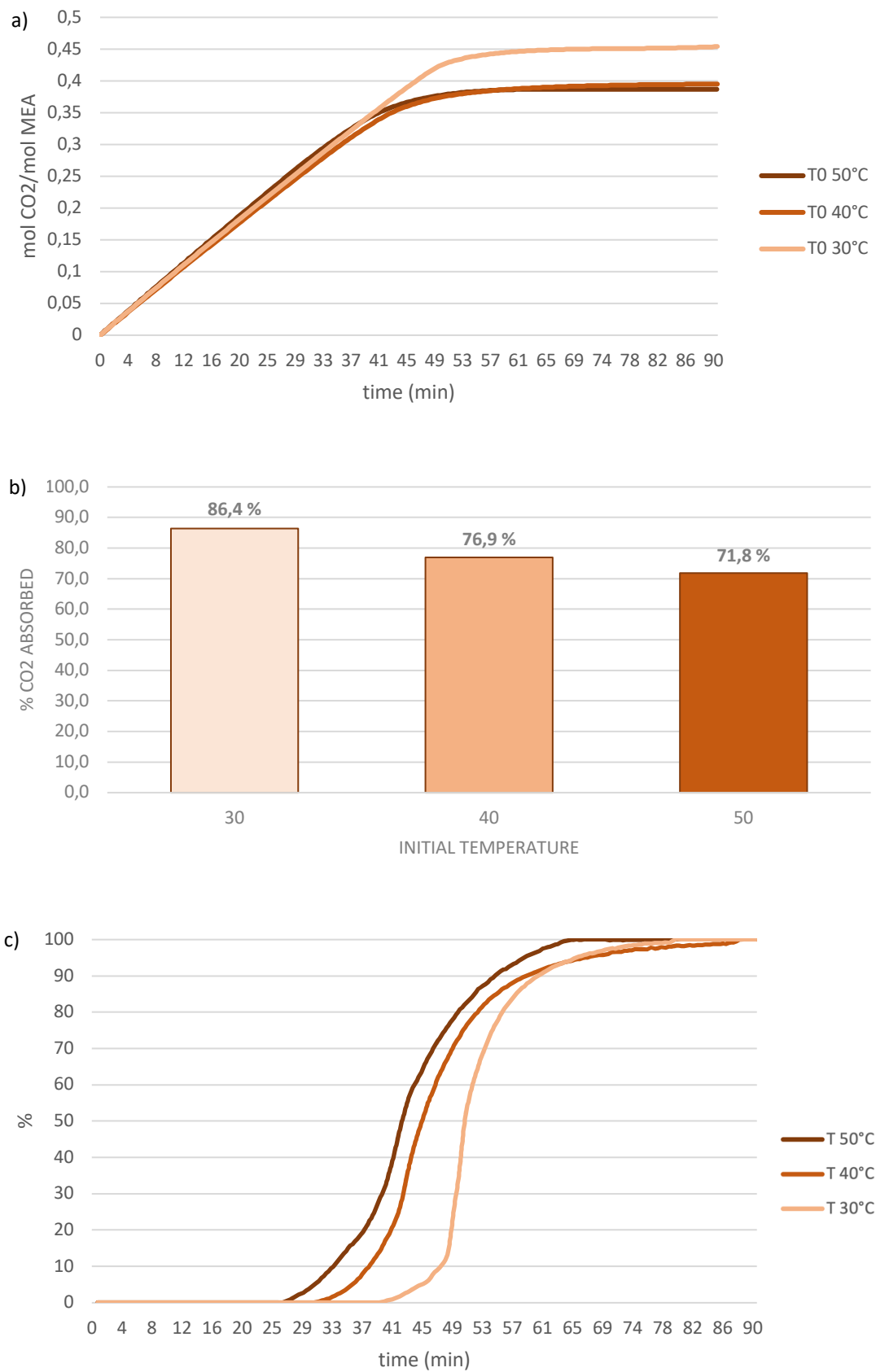


Figure 5.9 Absorption of CO₂ into an aqueous solution of MEA at different temperatures. a) CO₂ loading, b) CO₂ uptake after 60 minutes, c) trendlines of saturation curves (absorption pressure: 1 bar, gas flow: 78 NI/h, CO₂ concentration: 100%, solution volume: 1,00 l).

5.2 Absorption of CO₂ with a solution of [Cho][Pro] in DMSO

The absorption capacity of the CO₂ for a fresh [Cho][Pro] solution in DMSO is measured for 90 minutes, bubbling a constant gas flow rate (9 NL/h) of pure CO₂ at atmospheric pressure. To compare the absorption performance with that of MEA and have a match to the results in the literature, was chosen the temperature of 30 °C. The results are presented in *Figure 5.4*.

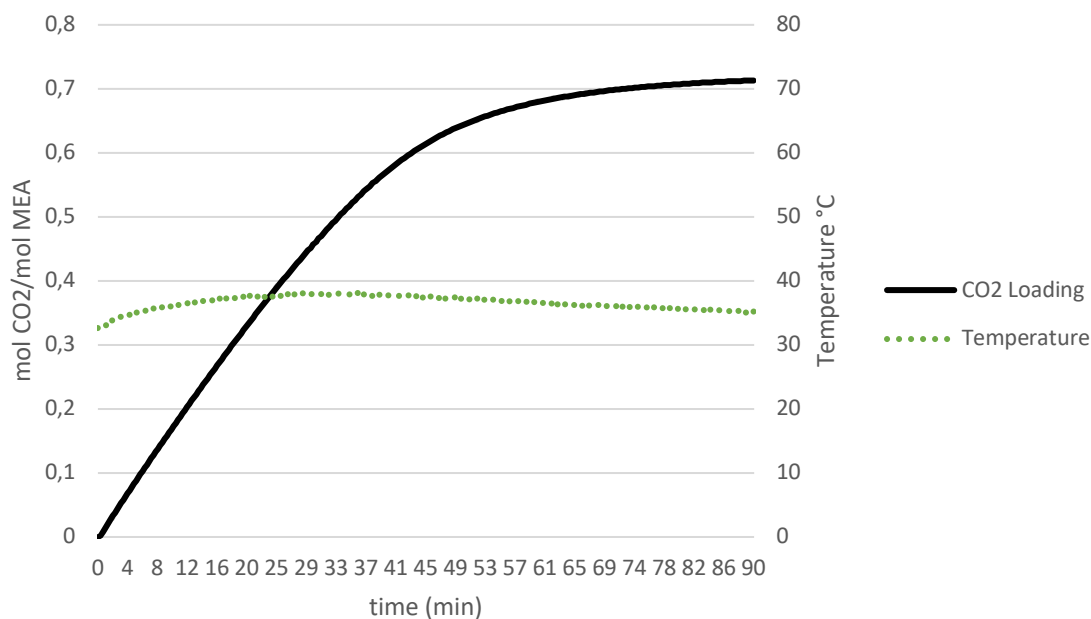


Figure 5.10 The CO₂ loading in the fresh solution of 12,5% wt/wt [Cho][Pro] in DMSO in function of time (starting absorption temperature: 303 K, gas flow: 9 NL/h, CO₂ concentration: 100%, solution volume: 0,50 l).

In contrast to the MEA, the operating temperature during the test remained almost constant, despite the lack of a heat sink. This provides a clear indication of the lower exothermicity of IL, which results in lower consumption due to the need for heat removal in order to improve the CO₂ absorption performance.

In addition, the figure shows how the loading capacity of [Cho][Pro] exceeds the value of 0,5 mol CO₂/mol IL. In fact, according to the literature ⁵⁴, the heterocyclic ring of proline should favour the stoichiometric reaction 1:1, compared to the reaction mechanism 1:2, with the formation of carbamic acid.

The CO₂ absorption capacity for [Cho][Pro] was compared to the results obtained by *Shengjuan Yuan et al.* ⁶⁴, for the same [AA] in a 5 to 30% wt/wt solution in water. Such results showed a good agreement with respect to the same IL solution in water (\approx 10% wt/wt) at a temperature of 30 °C.

In addition, the results indicate that it is possible to approximate and exceed the theoretical value of $1 \text{ mol CO}_2/\text{mol IL}$, but using greater concentrations of IL and operating pressures of up to 15 bar. Infected, the increase in the partial pressure of CO_2 corresponds to an increase in the driving force that regulates the concentration gradient of CO_2 between the gaseous and liquid phases. This favours the process of diffusion of the molecules of CO_2 inside of the bulk of the liquid phase, favouring the chemical reaction.

5.2.1 Effect of absorption/desorption cycle on regeneration efficiency

Besides the absorption performance, the feasibility of solvent regeneration is also an important factor in practical applications. The regeneration of the [Cho][Pro] solution in DMSO was investigated during four cycles of absorption/desorption with a duration of 90 minutes per process. The desorption process was studied by using an inert gas (N_2) with a flow rate of 18 NL/h . During the process, the system was heated up to 80°C , with a rate of $3,9^\circ\text{C}/\text{min}$, at atmospheric pressure. The results of this experiment are presented in Figure 5.5, showing CO_2 loading capacity variation during the absorption/desorption cycles.

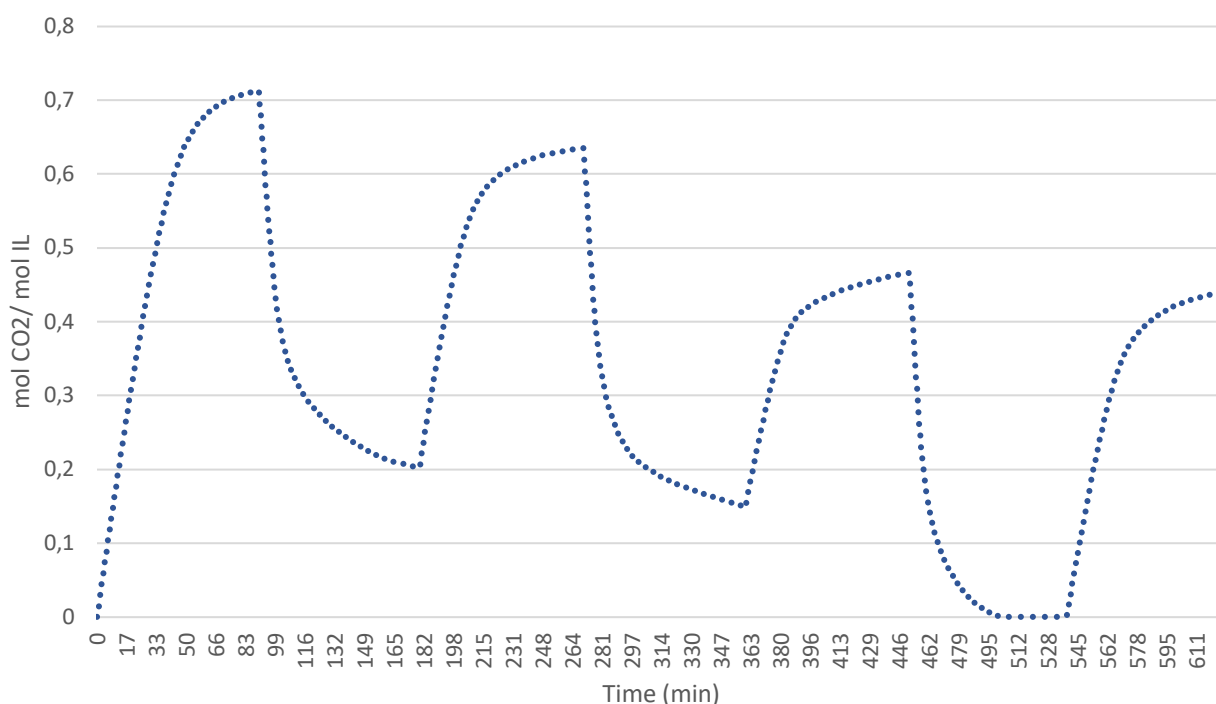


Figure 5.11 Four consecutive cycle of CO_2 absorption (absorption temperature: 30°C , CO_2 flow: 9 NL/h , N_2 flow: 18 NL/h , solvent volume: $0,5 \text{ l}$, regeneration temperature: 80°C , absorption time: 90 min , desorption time: 90 min)

The absorption performance of the [Cho][Pro] decreasing progressively from the first cycle, which has a CO_2 loading above $0,7 \text{ mol CO}_2/\text{mol IL}$, and then stand at a steady-state value of $\approx 0,45 \text{ mol CO}_2/\text{mol IL}$ for the third and fourth cycles of absorption.

The regeneration efficiency, with respect to the first cycle, in turn, was 89,1%, 65,4%, 61,8% for the second, the third and the fourth cycle respectively, as shown in *Figure 5.6*.

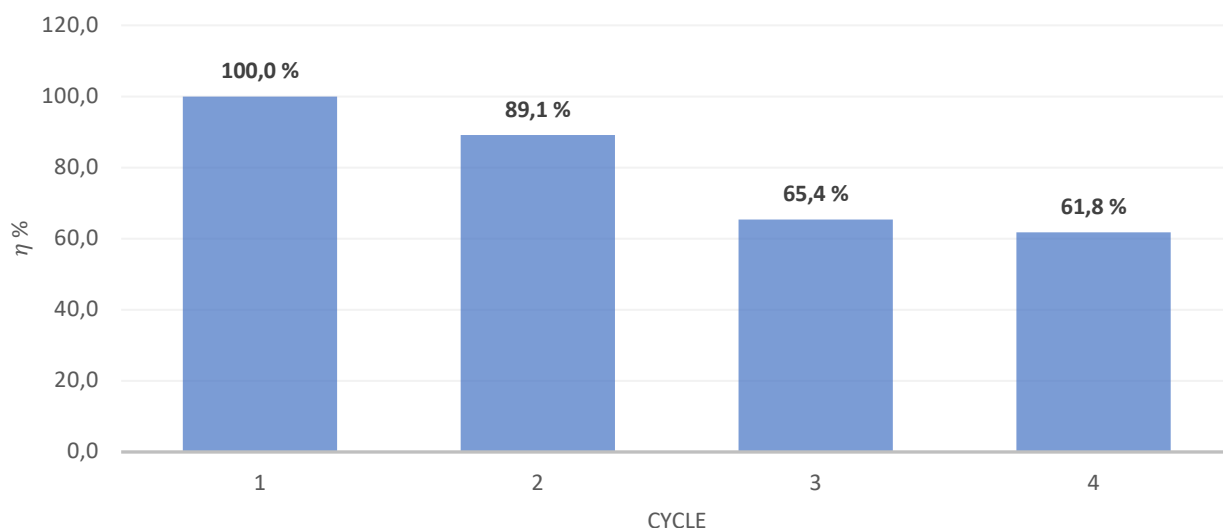


Figure 5.12 Regeneration efficiency related to the four absorption/desorption cycles (absorption temperature: 30 °C, CO₂ flow: 9 NL/h, N₂ flow: 18 NL/h, solvent volume: 0,5 l, regeneration temperature: 80 °C, absorption time: 90 min, desorption time: 90 min)

However, this IL-DMSO solution revealed competitive performances as its regeneration efficiency reported a few reductions (<4% variation) during the last two cycles and its absorption capacity was compared to such of the fresh aqueous MEA (i.e., between 0,44 and 0,45 mol CO₂/mol IL), although the aqueous MEA is recognized as very efficient absorbent.

The normalized CO₂ absorbed (Ads) and desorbed (Des) amounts from [Cho][Pro] solution during the four cycles is indicated in *Table 5.1* in terms of mol CO₂/ mol IL.

Table 5.1 Absorption/Desorption capacity of [Cho][Pro] solution through the four cycles

Absorption/Desorption capacity (mol CO ₂ /mol IL)						
Cycle 1		Cycle 2		Cycle 3		Cycle 4
Ads	Des	Ads	Des	Ads	Des	Ads
0,713	0,510	0,432	0,486	0,317	0,466	0,441

It is important to note that the amount of desorbed CO₂ does not change for the different cycles, this indicates how the desorption performance at 80 °C is around values of 0,44 and 0,45 mol CO₂/mol IL. Complete desorption would be possible by increasing the regeneration time or increasing the temperature, allowing the release of the carbamate species, which have high thermal stability. From this point of view, the lack of complete solubility of Proline, at such desorption temperatures, can be considered the cause of the loss of absorption capacity, an effect that can be removed with an increase in temperature.

5.2.2 Effect of temperature on the absorption

Based on the results of the regeneration efficiency study, it can be stated that absorption performance, under the same operating conditions, remains almost constant from the third uptake/desorption cycle. Therefore, from a fully regenerated solution, the CO₂ loading capacity of a [Cho][Pro] solution in DMSO at different temperatures was assessed. The results are shown in *Figure 5.7*.

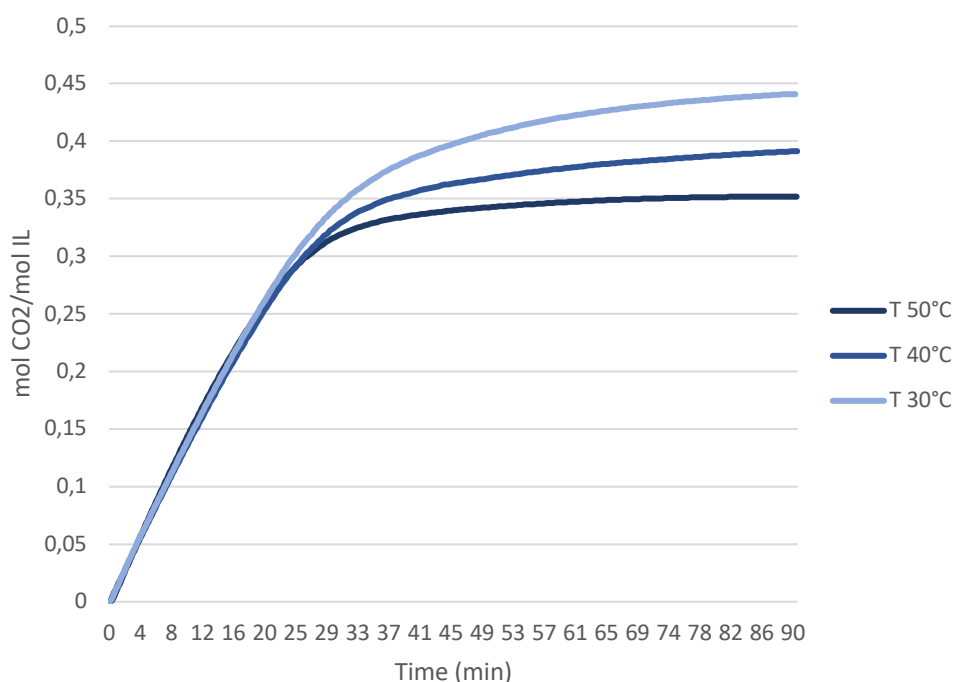


Figure 5.13 Absorption loading into 12,5% wt/wt [Cho][Pro] solution in DMSO at different temperature (gas flow: 9 NL/h, CO₂ concentration: 100%, solution volume: 0,50 l).

Due to the lower exothermic reaction of IL, the effect of temperature on absorption loading is more marked. Showing how low temperatures favor the CO₂ absorption process.

5.3 Effect of temperature on desorption process

In addition to absorption, the desorption process at different temperatures was subsequently analysed. The CO₂ release experiment was carried out in the presence of an inert gas (N₂) at 18 NL/h. The entire process of absorption and desorption in solution at 12,5% wt/wt [Cho][Pro] in DMSO is represented in *Figure 5.8*, where the percentage of CO₂ absorbed and desorbed (black line) and the variation of temperature during the test (green line) is reported.

The absorption process is carried out at an almost constant temperature of 30 °C, under the presence of a gas flow of 9 NL/h of pure CO₂, until saturation occurs.

The desorption process was carried out by exposing the solution to a constant flow of 18 *Nl/h* of N₂ and divided into several steps. Initially, the solution was heated to a temperature of 70 °C, and left unchanged until no more CO₂ was released, for a total of 80 minutes. Subsequently, the temperature has been increased to 80 °C to assess the desorption performance under these conditions. The process has been repeated several times with a gradual temperature increase of 10 °C per step, up to 110 °C.

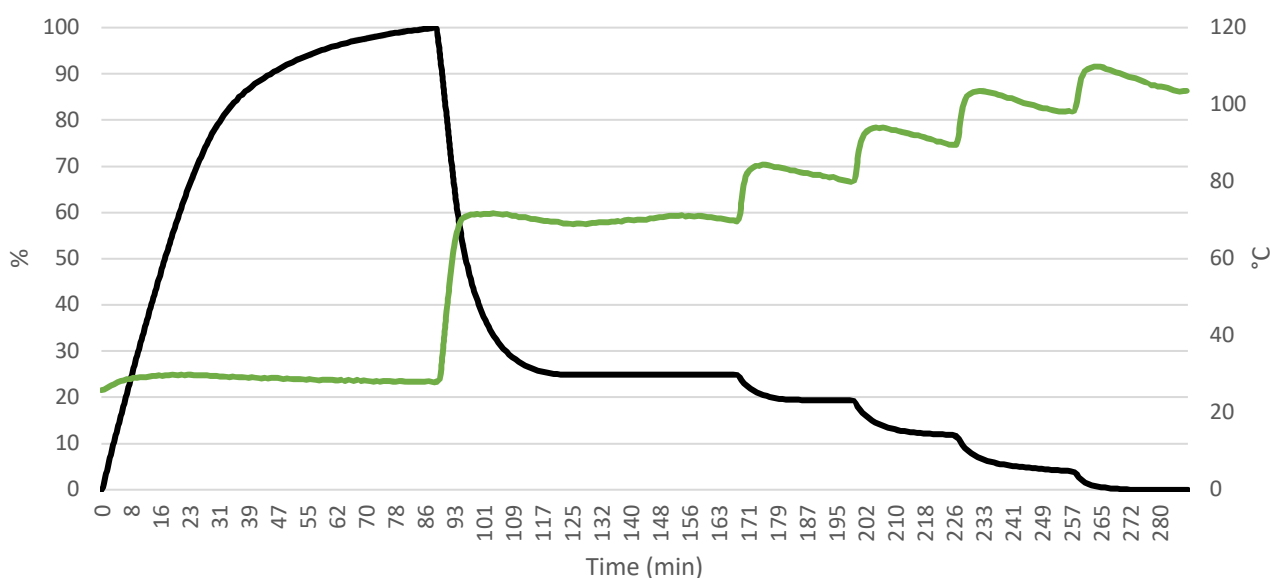


Figure 5.14 Variation of CO₂ concentration into 12,5% wt/wt [Cho][Pro] in DMSO (absorption temperature: 303 K, operating pressure: 1 bar, CO₂ gas flow: 9 *Nl/h*, N₂ gas flow: 18 *Nl/h*, solution volume: 0,50 l).

As can be seen from the figure, in the first minutes of the desorption process the CO₂ is released even at low temperatures, this is due to the reduction of the partial pressure of the CO₂ in the presence of a constant flow of nitrogen. In addition, CO₂ is released by the decomposition of the carbonic acid species, whose formation reaction is reversible at room temperature. Subsequently, the rate of desorption of CO₂ decreases, until it reaches a plateau after about 25-30 minutes from the beginning of the desorption process. Therefore, the desorption process is accelerated again only in the presence of an increase in temperature, such as to allow the release of CO₂ from the carbamate species, which have greater thermal stability. For this experiment, the complete desorption of the released CO₂ occurs in the vicinity of 110 °C.

To assess the influence of the initial desorption temperature, the process was subsequently repeated to assess the variation of the CO₂ concentration in solution for an initial desorption temperature of 80 and 90 °C. The two desorption processes were carried out starting from the absorption tests at 40 and 50 °C (Figure 5.9), completing the CO₂ capture bringing the mixture around 30 °C, and continuing the absorption step until saturation.

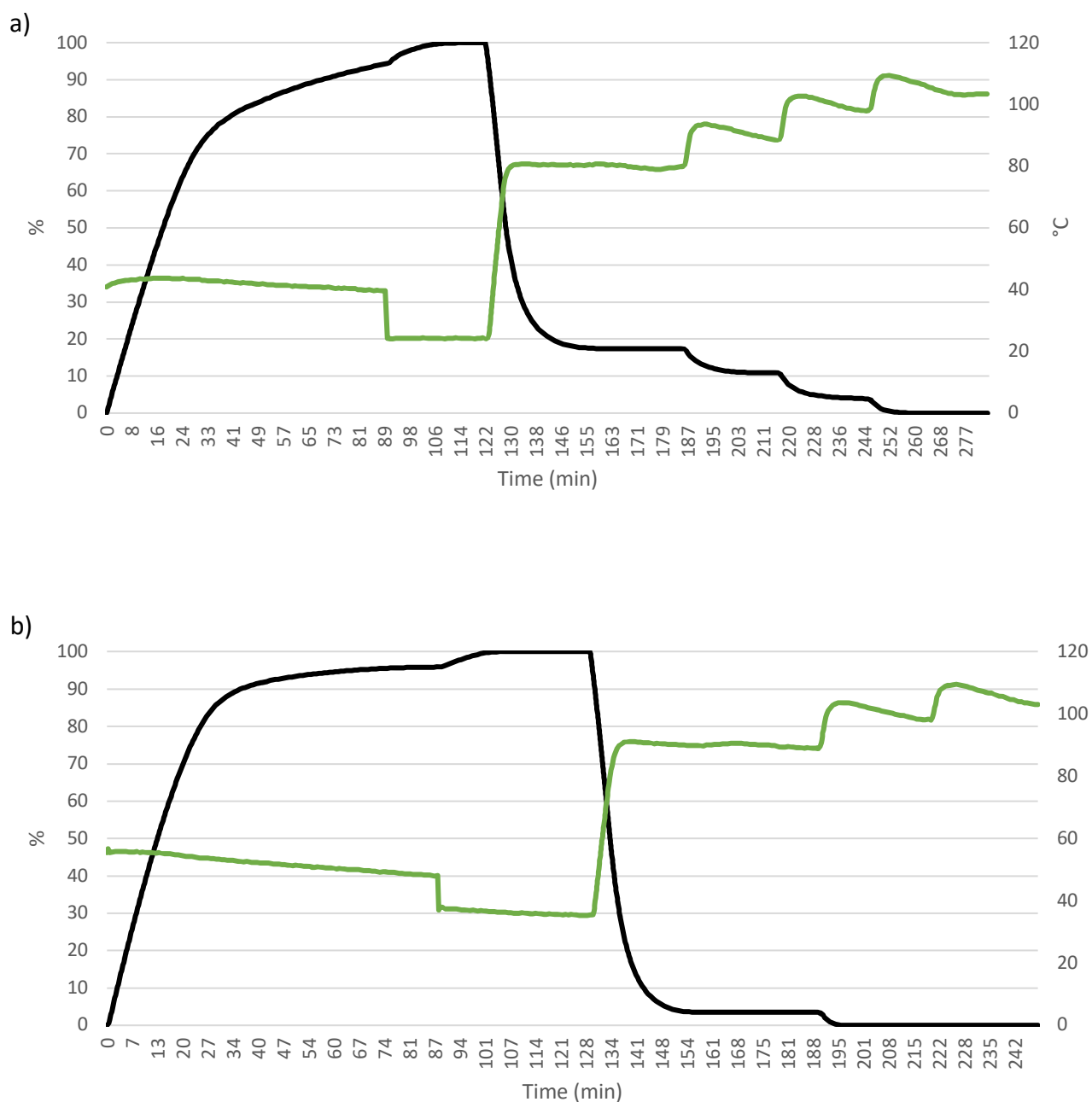


Figure 5.15 Variation of CO₂ concentration into 12,5% wt/wt [Cho][Pro] in DMSO. a) Starting absorption temperature: 40 °C, starting desorption temperature: 80 °C, b) Starting absorption temperature: 50 °C, starting desorption temperature: 90 °C (operating pressure: 1 bar, CO₂ gas flow: 9 NL/h, N₂ gas flow: 18 NL/h, solution volume: 0,50 l).

As expected, an increase in the initial desorption temperature results in a higher regeneration performance. The higher the temperature, the greater the amount of CO₂ released during the first desorption step. Completion of uptake has a greater impact for the absorption test a lower temperature, resulting in an increase of CO₂ loading of 5 and 3,5 % for the absorption test at 40 and 50 °C, respectively. The variation in the percentage of CO₂ released as the initial desorption temperature changes is shown in *Figure 5.10*.

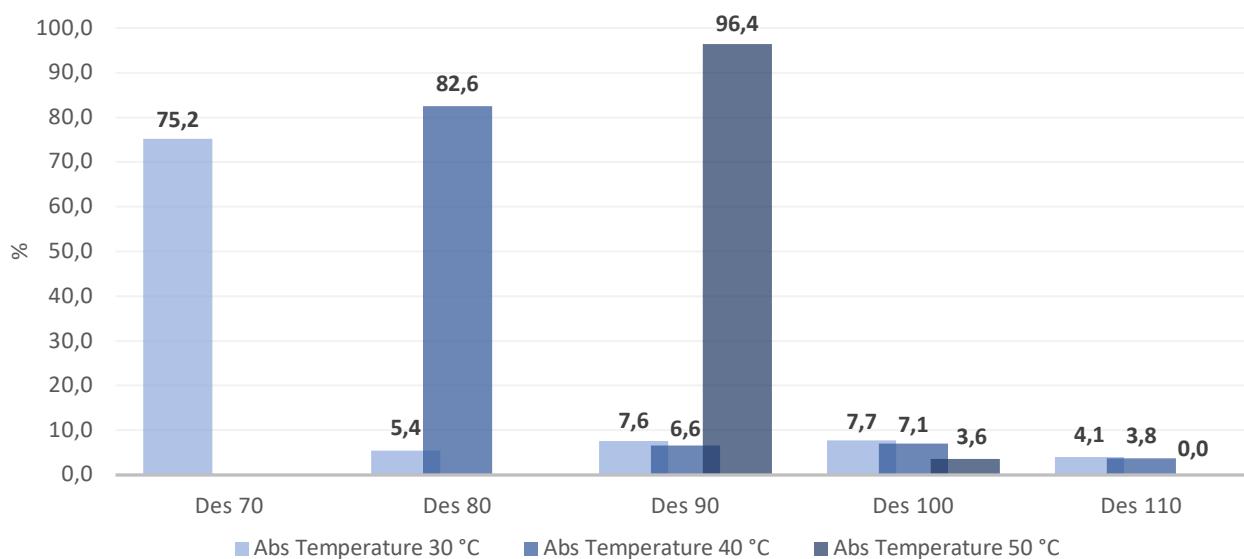


Figure 5.16 Variation in the percentage of desorbed CO₂ for the three desorption tests, as temperature changes

This experiment shows that, even if for total regeneration of the solvent it is necessary to go up to high temperatures (up to 100 °C for an initial desorption temperature of 90 °C), good regeneration performance also occurs at relatively low temperatures (over 75 % of CO₂ released at 70 °C). It is worth that the classic aqueous solutions of amine, such as MEA, require temperatures of around 120 °C to approach regeneration. In addition, tests carried out on the 30% wt/wt aqueous solution of MEA showed that no desorption was detected for temperatures below 100 °C.

Finally, it has been shown that the absorption reaction by [Cho][Pro] is actually reversible, although relatively high temperatures are needed to achieve complete regeneration. Based on, it can be stated how it is possible to improve the regeneration efficiency by performing absorption/desorption cycles at 30 and 90 °C. However, it must be taken into account how an increase in T between the absorption column and the desorption column leads to higher energy expenditure in terms of the demand for sensible heat to heat the rich solvent mixture.

5.4 Comparison with 30% aqueous MEA solution

For a comparison purpose, CO₂ uptake at 30 °C was analyzed by two fresh solutions at 30% wt/wt MEA in water, and 12.5% wt/wt of [Cho][Pro] in DMSO. In addition, to assess the effect of the variation of the partial pressure of CO₂ on performance, the % of CO₂ in the gas flow sent within the absorption column has been varied.

In particular, the percentage of CO₂ in the gas mixtures accounts for the average CO₂ content of biogas from biomass waste (i.e., about 65% CH₄, 35% CO₂)¹⁴. The results are illustrated in *Figure 5.8*.

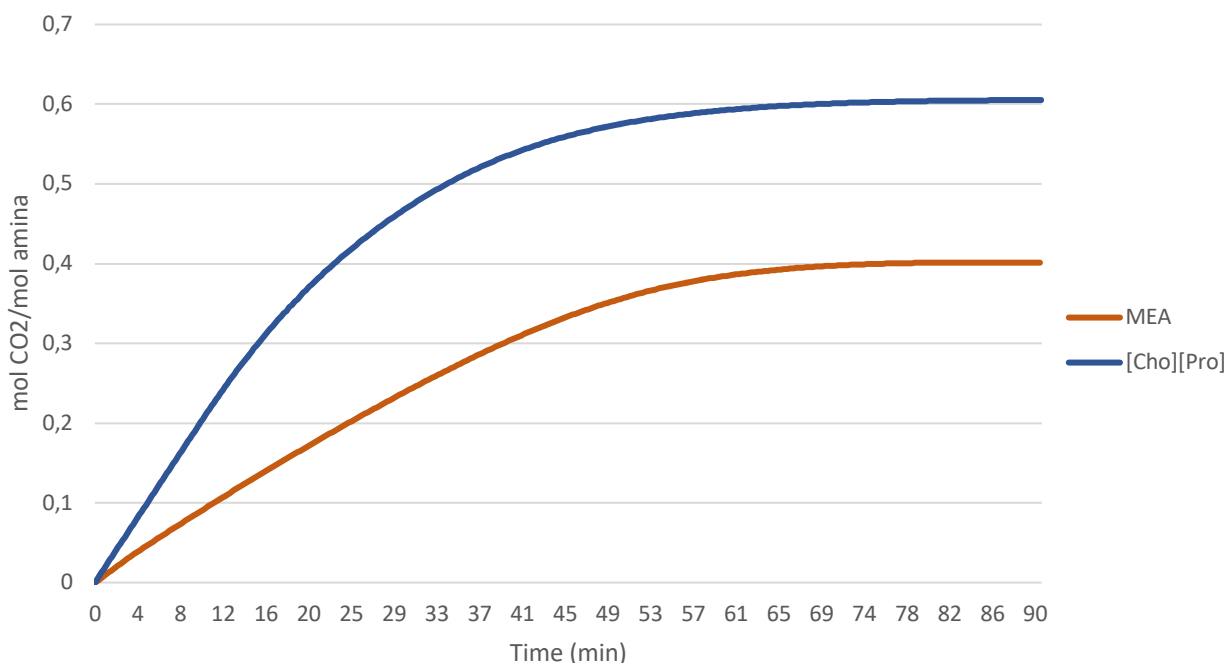


Figure 5.17 Absorption loading of CO₂ into two different absorbents (absorption temperature: 303 K, operating pressure: 1 bar, CO₂ concentration: 35%, solution volume: 0,50 l).

As expected, the absorption performance is reduced compared to the same tests carried out with pure CO₂ (i.e., 0,6 against 0,7 mol/mol IL and 0,4 against 0,5 mol/mol MEA). By reducing the partial pressure of CO₂, the driving force is reduced, and the diffusion process is disadvantaged.

In order to obtain a better comparison between the absorption performance of [Cho][Pro] and MEA, as well as the load capacity expressed in terms of captured CO₂ mol/mol amine, it was decided to derive the CO₂ absorption capacity expressed in terms of CO₂ mol/kg absorbent, normalized for the gas flow rate sent. This will also take into account 70% water and 87,5% DMSO by weight in the two solutions, which need to be circulated and heated throughout the entire process. The results are reported in *Table 5.2*.

The results show that the [Cho][Pro] has higher loading capacities (mol CO₂/mol amine), due to the different stoichiometric that characterize the two solvents. In contrast, by assessing the solubility of CO₂ in terms of mol per mass of solvent, the results obtained for IL are similar to those obtained for an aqueous solution of MEA.

Table 5.2 Absorption loading expressed in terms of mol CO₂/mol amine and mol CO₂/kg absorbent of MEA and [Cho][Pro]

Solvent	vol (dm ³)	mass (kg)	mol amine	gas composition	<i>m</i> (mol _{CO₂} /mol amine)	<i>α</i> (mol _{CO₂} /kg absorbent)
30% MEA	1,00	1,06	5,21	CO ₂	0,454	0,030
	0,55	0,59	2,88	CO ₂ /CH ₄	0,402	0,016
12,5% [Cho][Pro]	0,49	0,55	0,31	CO ₂	0,713	0,045
	0,46	0,52	0,29	CO ₂ /CH ₄	0,605	0,014

One of the main disadvantages of using the MEA is the presence of water in the solution, which results in a significant increase in the energy consumption of the process compared to using the IL. The energy required for the regeneration of the conventional aqueous solution, which is the main contribution to the overall energy expenditure, includes the demand for sensitive and latent heat, as well as the enthalpic energy necessary to occur the opposite reaction and to decompose the carbamate and carbamic acid moieties. Although the enthalpy of reaction of [Cho][Pro] and MEA has not been evaluated, some qualitative considerations can be made on the remaining two contributions. The demand for sensitive heat is necessary to heat the solvent up to the operating temperature of the desorption step, while latent heat is needed to generate steam within the stripping column such as to dilute the CO₂ released and facilitate the regeneration process. This latter contribution is absent for the [Cho][Pro] since it does not need any steam production for solvent regeneration. Moreover, the sensitive heat decreases as the specific heat of IL-based solvents is lower than the conventional solution at 30% MEA, which is greatly influenced by the high specific heat of the water.

Conclusion

The initial purpose of this work was to evaluate the reliability of the bench, performing absorption tests with an aqueous monoethanolamine solution (MEA, 30% by weight) and comparing the results with the literature. Furthermore, the alternative of chemical absorption with Choline-based AAILs solution, which shows promising physicochemical and thermal properties, has been investigated. The drawbacks related to the high viscosity and high IL cost were reduced by applying DMSO as IL solvent, using a 12,5% wt/wt [Cho][AA] solution in DMSO. Proline has been used as an amino acid, as the heterocyclic ring should favour its solubility in DMSO, favoring the regeneration of the solvent.

The results obtained from the absorption tests with the aqueous solution of MEA showed a good correspondence with the literature, approaching the theoretical loading value of 0,5 mol CO₂/mol MEA. Tests carried out at different temperatures have also confirmed that the absorption reaction is favoured at relatively low temperatures (around 30 °C). The absorption tests carried out for a fresh solution of [Cho][Pro] in DMSO found values of loading capacity around 0,7 mol CO₂/mol IL, for an operating pressure of 1 bar. It is necessary for the future to work at higher pressure, to verify how more favourable absorption conditions involve a better loading value, approaching 1 mol CO₂ captured/ mol IL in solution. In addition, the regeneration efficiency for the [Cho][Pro] has been evaluated by means of 4 consecutive absorption/desorption cycles, carried out at 30 and 80 °C. The results obtained show a loss of absorption performance, which stabilize from the third cycle (89,1%, 65,4%, 61,8% for the second, third, and fourth cycles, respectively). In contrast, desorption performance remains constant, showing that at 80 °C the solution is able to desorb around 0,5 mol CO₂/mol IL. Based on the results obtained from the influence of temperature on solvent regeneration, it can be said that absorption/desorption cycles at 30 and 90 °C can improve regeneration efficiency, decreasing the loss of absorption performance. Assumptions that need to be verified by means of additional tests.

Based on the comparison made between the aqueous solution of MEA and the solution of [Cho][Pro] in DMSO, it can be established that the potential benefits of using IL include: (i) lower consumption due to the need to dissipate heat during the absorption process, linked to the minor exothermicity of IL; (ii) a zero contribution of latent heat on the energy demand for solvent regeneration; (iii) a reduced latent energy demand due to the absence of water in the solution and a reduced temperature difference between the absorption and desorption process. Finally, the use of a TSIL solution from renewable biomaterials provides additional benefits such as low costs, low environmental impacts, low viscosity values. These features make the solutions based on [Cho][Pro] an optimal absorbent and competitive at the state-of-the-art for industrial flue gas treatment, which would allow the CO₂ capture or its subsequent use as raw material with high purity.

References

1. IPCC Panel. Climate Change 2014: Synthesis Report. 1–151 (2014).
2. Maddison. Annual production-based emissions of carbon dioxide (CO₂), measured in tonnes per year. *Our World in Data based on Global Carbon Project* <https://ourworldindata.org/co2-and-other-greenhouse-gas-emissions>.
3. Kaya, Y. The role of CO₂ removal and disposal. *Energy Convers. Manag.* **36**, 375–380 (1995).
4. Mathieu, P. *The IPCC special report on carbon dioxide capture and storage. ECOS 2006 - Proceedings of the 19th International Conference on Efficiency, Cost, Optimization, Simulation and Environmental Impact of Energy Systems* (2006).
5. International Energy Agency (IEA). Energy Technology Perspectives (ETP) - Catalysing Energy Technology Transformations, Paris, France, 2017. (2017).
6. UNFCCC. Adoption of the Paris Agreement. *United Nations Framework Convention on Climate Change (UNFCCC), Paris, France*, <https://unfccc.int/process-and-meetings/the-paris-agreement/the-paris-agreement> (2015).
7. Benson, S. M. & Orr, F. M. Carbon dioxide capture and storage. *MRS Bull.* **33**, 303–305 (2008).
8. Koelbl, B. S., van den Broek, M. A., Faaij, A. P. C. & van Vuuren, D. P. Uncertainty in Carbon Capture and Storage (CCS) deployment projections: A cross-model comparison exercise. *Clim. Change* **123**, 461–476 (2014).
9. Bui, M. *et al.* Carbon capture and storage (CCS): The way forward. *Energy Environ. Sci.* **11**, 1062–1176 (2018).
10. Adger, N. & Coauthors including Fischlin, A. Summary for policymakers. *Clim. Chang. 2007 Impacts, Adapt. vulnerability. Contrib. Work. Gr. II to Fourth Assess. Rep. Intergov. Panel Clim. Chang.* 7–22 (2007) [doi:http://www.ipcc.ch/publications_and_data/ar4/wg2/en/spm.html](http://www.ipcc.ch/publications_and_data/ar4/wg2/en/spm.html).
11. Riahi, K. *et al.* Locked into Copenhagen pledges - Implications of short-term emission targets for the cost and feasibility of long-term climate goals. *Technol. Forecast. Soc. Change* **90**, 8–23 (2015).
12. Bui, M., Fajardy, M. & Mac Dowell, N. Bio-energy with carbon capture and storage (BECCS): Opportunities for performance improvement. *Fuel* **213**, 164–175 (2018).
13. Rasi, S., Lehtinen, J. & Rintala, J. Determination of organic silicon compounds in biogas from wastewater treatments plants, landfills, and co-digestion plants. *Renew. Energy* **35**, 2666–2673 (2010).
14. Nguyen, L. N. *et al.* Biomethane production from anaerobic co-digestion at wastewater treatment plants: A critical review on development and innovations in biogas upgrading techniques. *Sci. Total Environ.* **765**, 142753 (2021).

15. Gibbins, J. & Chalmers, H. Carbon capture and storage. *Energy Policy* **36**, 4317–4322 (2008).
16. International Energy Agency. CO₂ Capture As a Factor in Power Station Investment. *Energy* **19**, (2006).
17. Hu, Y. *CO₂ capture from oxy-fuel combustion power plants*. (2011).
18. Boot-Handford, M. E. *et al.* Carbon capture and storage update. *Energy Environ. Sci.* **7**, 130–189 (2014).
19. DOE. Petra Nova. *W.A. Parish Project, Office of Fossil Energy, U.S. Department of Energy (DOE)* <https://www.energy.gov/fe/petra-nova-wa-parish-project>.
20. D. Wagman. The three factors that doomed Kemper County IGCC. *IEEE Spectrum* <https://spectrum.ieee.org/energywise/energy/fossil-fuels/the-three-factors-that-doomed-kemper-county-igcc> (2017).
21. GCCSI. Large-scale CCS projects. *Global CCS Institute* <https://www.globalccsinstitute.com/news-media/press-room/media-releases/new-wave-of-ccs-activity-ten-large-scale-projects-announced/>.
22. Feron, P. H. M. 1 - Introduction. in (ed. Feron, P. H. M. B. T.-A.-B. P. C. of C. D.) 3–12 (Woodhead Publishing, 2016). doi:<https://doi.org/10.1016/B978-0-08-100514-9.00001-9>.
23. Puxty, G. & Maeder, M. 2 - The fundamentals of post-combustion capture. in (ed. Feron, P. H. M. B. T.-A.-B. P. C. of C. D.) 13–33 (Woodhead Publishing, 2016). doi:<https://doi.org/10.1016/B978-0-08-100514-9.00002-0>.
24. Crovetto, R. Evaluation of Solubility Data of the System CO₂–H₂O from 273 K to the Critical Point of Water. *J. Phys. Chem. Ref. Data* **20**, 575–589 (1991).
25. Wilke, C. R. & Chang, P. Correlation of diffusion coefficients in dilute solutions. *AIChE J.* **1**, 264–270 (1955).
26. Jeon, S. Bin *et al.* Effect of adding ammonia to amine solutions for CO₂ capture and mass transfer performance: AMP-NH₃ and MDEA-NH₃. *J. Taiwan Inst. Chem. Eng.* **44**, 1003–1009 (2013).
27. Krupiczka, R., Rotkegel, A. & Ziobrowski, Z. Comparative study of CO₂ absorption in packed column using imidazolium based ionic liquids and MEA solution. *Sep. Purif. Technol.* **149**, 228–236 (2015).
28. Rochelle, G. T. 3 - Conventional amine scrubbing for CO₂ capture. in (ed. Feron, P. H. M. B. T.-A.-B. P. C. of C. D.) 35–67 (Woodhead Publishing, 2016). doi:<https://doi.org/10.1016/B978-0-08-100514-9.00003-2>.
29. Notz, R., Mangalapally, H. P. & Hasse, H. Post combustion CO₂ capture by reactive absorption: Pilot plant description and results of systematic studies with MEA. *Int. J. Greenh. Gas Control* **6**, 84–112 (2012).
30. Gonzalez-Salazar, M. A. *et al.* Comparison of current and advanced post-combustion CO₂ capture technologies for power plant applications. *Energy Procedia* **23**, 3–14 (2012).
31. Rochelle, A. G. T. *et al.* CO₂ Capture by Absorption with Potassium Carbonate Third Quarterly Report 2006. *Corrosion* 1–55 (2006).
32. Dugas, R. E. Carbon Dioxide Absorption , Desorption , and Diffusion in

Aqueous Piperazine and Monoethanolamine. *Dr. thesis Tech. Univ. Texas Austin* 282 (2009).

33. Sachde, D. & Rochelle, G. T. Absorber intercooling configurations using aqueous piperazine for capture from sources with 4 to 27% CO₂. *Energy Procedia* **63**, 1637–1656 (2014).
34. Lin, Y. J. & Rochelle, G. T. Optimization of advanced flash stripper for CO₂ capture using piperazine. *Energy Procedia* **63**, 1504–1513 (2014).
35. Li, L., Li, H., Namjoshi, O., Du, Y. & Rochelle, G. T. Absorption rates and CO₂ solubility in new piperazine blends. *Energy Procedia* **37**, 370–385 (2013).
36. Rochelle, G. T. Thermal degradation of amines for CO₂ capture. *Curr. Opin. Chem. Eng.* **1**, 183–190 (2012).
37. Davis, J. D. Thermal Degradation of Aqueous Amines Used for Carbon Dioxide Capture. PhD Thesis. *Univ. Texas Austin* **2**, S165–S170 (2009).
38. Voice, A. K., Closmann, F. & Rochelle, G. T. Oxidative degradation of amines with high-temperature cycling. *Energy Procedia* **37**, 2118–2132 (2013).
39. Fine, N. A. Nitrosamine Management in Aqueous Amines for Post-Combustion Carbon Capture. (2015).
40. Plechkova, N. V. & Seddon, K. R. Applications of ionic liquids in the chemical industry. *Chem. Soc. Rev.* **37**, 123–150 (2008).
41. Ramdin, M., De Loos, T. W. & Vlugt, T. J. H. State-of-the-art of CO₂ capture with ionic liquids. *Ind. Eng. Chem. Res.* **51**, 8149–8177 (2012).
42. Bara, J. E. 11 - Ionic liquids for post-combustion CO₂ capture. in (ed. Feron, P. H. M. B. T.-A.-B. P. C. of C. D.) 259–282 (Woodhead Publishing, 2016). doi:<https://doi.org/10.1016/B978-0-08-100514-9.00011-1>.
43. Zeng, S. *et al.* Ionic-Liquid-Based CO₂ Capture Systems: Structure, Interaction and Process. *Chem. Rev.* **117**, 9625–9673 (2017).
44. Huang, Y., Zhang, X., Zhang, X., Dong, H. & Zhang, S. Thermodynamic modeling and assessment of ionic liquid-based CO₂ capture processes. *Ind. Eng. Chem. Res.* **53**, 11805–11817 (2014).
45. Anthony, J. L., Anderson, J. L., Maginn, E. J. & Brennecke, J. F. Anion Effects on Gas Solubility in Ionic Liquids. *J. Phys. Chem. B* **109**, 6366–6374 (2005).
46. H. Davis James, J. Task-Specific Ionic Liquids. *Chem. Lett.* **33**, 1072–1077 (2004).
47. Tao, D. J. *et al.* Synthesis and thermophysical properties of biocompatible cholinium-based amino acid ionic liquids. *J. Chem. Eng. Data* **58**, 1542–1548 (2013).
48. Lei, Z. *et al.* Solubility of CO₂ in methanol, 1-octyl-3-methylimidazolium bis(trifluoromethylsulfonyl)imide, and their mixtures. *Chinese J. Chem. Eng.* **21**, 310–317 (2013).
49. Liwarska-Bizukojc, E., Maton, C. & Stevens, C. V. Biodegradation of imidazolium ionic liquids by activated sludge microorganisms. *Biodegradation* **26**, 453–463 (2015).
50. Deng, Y. *et al.* When can ionic liquids be considered readily biodegradable? Biodegradation pathways of pyridinium, pyrrolidinium and ammonium-based

- ionic liquids. *Green Chem.* **17**, 1479–1491 (2015).
51. Neumann, J., Grundmann, O., Thöming, J., Schulte, M. & Stolte, S. Anaerobic biodegradability of ionic liquid cations under denitrifying conditions. *Green Chem.* **12**, 620–62 (2010).
 52. Liu, Q. P., Hou, X. D., Li, N. & Zong, M. H. Ionic liquids from renewable biomaterials: Synthesis, characterization and application in the pretreatment of biomass. *Green Chem.* **14**, 304–307 (2012).
 53. Fukumoto, K., Yoshizawa, M. & Ohno, H. Room temperature ionic liquids from 20 natural amino acids. *J. Am. Chem. Soc.* **127**, 2398–2399 (2005).
 54. Latini, G. *et al.* Unraveling the CO₂ reaction mechanism in bio-based amino-acid ionic liquids by operando ATR-IR spectroscopy. *Catal. Today* **336**, 148–160 (2019).
 55. Davarpanah, E., Hernández, S., Latini, G., Pirri, C. F. & Bocchini, S. Enhanced CO₂ Absorption in Organic Solutions of Biobased Ionic Liquids. *Adv. Sustain. Syst.* **4**, (2020).
 56. Li, B., Chen, Y., Yang, Z., Ji, X. & Lu, X. Thermodynamic study on carbon dioxide absorption in aqueous solutions of choline-based amino acid ionic liquids. *Sep. Purif. Technol.* **214**, 128–138 (2019).
 57. Li, X. *et al.* Absorption of CO₂ by ionic liquid/polyethylene glycol mixture and the thermodynamic parameters. *Green Chem.* **10**, 879–88 (2008).
 58. Feng, Z. *et al.* Absorption of CO₂ in the aqueous solutions of functionalized ionic liquids and MDEA. *Chem. Eng. J.* **160**, 691–697 (2010).
 59. McDonald, J. L., Sykora, R. E., Hixon, P., Mirjafari, A. & Davis, J. H. Impact of water on CO₂ capture by amino acid ionic liquids. *Environ. Chem. Lett.* **12**, 201–208 (2014).
 60. Yin, L., Li, X., Zhang, L. & Li, J. Characteristics of carbon dioxide desorption from MEA-based organic solvent absorbents. *Int. J. Greenh. Gas Control* **104**, 103224 (2021).
 61. Gao, J. *et al.* Integration study of a hybrid solvent MEA-Methanol for post combustion carbon dioxide capture in packed bed absorption and regeneration columns. *Sep. Purif. Technol.* **167**, 17–23 (2016).
 62. Chen, Y. *et al.* Kinetics study and performance comparison of CO₂ separation using aqueous choline-amino acid solutions. *Sep. Purif. Technol.* **261**, 118284 (2021).
 63. Barzagli, F., Mani, F. & Peruzzini, M. A Comparative Study of the CO₂ Absorption in Some Solvent-Free Alkanolamines and in Aqueous Monoethanolamine (MEA). *Environ. Sci. Technol.* **50**, 7239–7246 (2016).
 64. Yuan, S., Chen, Y., Ji, X., Yang, Z. & Lu, X. Experimental study of CO₂ absorption in aqueous cholinium-based ionic liquids. *Fluid Phase Equilib.* **445**, 14–24 (2017).

*Ringrazio tutti coloro che mi hanno accompagnato in questi lunghi anni di studio,
che hanno condiviso con me gioie e delusioni.*

*Ringrazio in particolar modo la mia compagna,
per essermi stata sempre a fianco a partire dai momenti di difficoltà.*

*Ringrazio la mia famiglia,
per avermi lasciato crescere e reagire con le mie idee, senza mai imporre le loro.*

*Ringrazio i miei amici,
e lasciatemi ringraziare anche me stesso,
per aver creduto in me nel momento in cui la fiducia doveva partire da me stesso.*